Supplementary Information

Dissipative Self-Assembly, Competition and Inhibition in a Self-Reproducing Protocell Model

Elias A. J. Post and Stephen P. Fletcher*

Department of Chemistry, Chemistry Research Laboratory, University of Oxford, 12 Mansfield Road, Oxford, OX1 3TA, U.K.

Corresponding Author: stephen.fletcher@chem.ox.ac.uk

TABLE OF CONTENTS

General Information
Procedures using oxygen- and/or moisture-sensitive materials were performed with anhydrous solvents under an atmosphere of anhydrous argon in flame-dried flasks, using standard Schlenk techniques. Analytical TLC was performed on precoated aluminum-backed plates (Silica Gel 60 F254; Merck), and visualised using aqueous basic potassium permanganate, or ninhydrin stains. Flash column chromatography was carried out using Merck Geduran® Si 60 (40-63 μm) silica gel. Compound was dry-loaded on to columns with Chemtube Hydromatrix from Agilent Technologies. Pressure was applied at the column head via a flow of nitrogen with the solvent system used in parentheses.
Cooling of reaction mixtures to 0 °C was achieved using an ice-water bath. Cooling to –10 °C was achieved using a salt-ice bath. Cooling to –78 °C was achieved using a dry ice-acetone bath.

Chemicals
All chemicals were purchased from Sigma Aldrich or Fluorochem Scientific and used without further purification. Dry $CHCl_3$, THF, CH_2Cl_2, Et_2O, toluene, benzene, hexane, pentane, DMF, and acetonitrile were collected fresh from an mBraun SPS-5 solvent purification system having been passed through anhydrous alumina columns. All other solvents were used as purchased from Sigma-Aldrich, Honeywell, or Fisher Scientific.

Equipment
All NMR spectra were recorded at room temperature. ^{1}H NMR and ^{13}C NMR spectra were recorded using Bruker AVIII HD 400 (400/101 MHz) and AVIII HD 500 (500/126 MHz) spectrometers. Chemical shifts are reported in p.p.m. from the residual solvent peak. Chemical shifts (δ) are given in p.p.m. and coupling constants (J) are quoted in hertz (Hz). Resonances are described as s (singlet), d (doublet), t (triplet), q (quartet) and m (multiplet). Assignments were made with the assistance of 2D COSY and HSQC NMR experiments.

DOSY NMR measurements were performed using a Bruker AVIII HD 500 equipped with a TFI probehead at 298 K using the 2D sequence for diffusion measurement using double stimulated echo for convection compensation and longitudinal eddy current delay, using bipolar gradient pulses for diffusion, and using three spoil gradients (Bruker terminology: dstebpgp35) pulse sequence. The samples were thoroughly mixed using a Vortex Genie 2 mixer (Scientific Industries), and were then clarified using a hand centrifuge (Hettich, model 1011) and then measured. Samples containing saturated azide consequently had a small layer of neat azide above the D_2O layer; sufficient D_2O was used to ensure that the alkyne layer was not detectible by the NMR probe. Experiments were performed in two stages: initially 1D-edited DOSY experiments were used to optimize the diffusion period to Δ=100 ms. The 2D dstebpgp35 sequence was then used, based on the optimized Δ from the previous procedure and with δ=4 ms, with gradient amplitude ranging from 2 to 85% with 16 points in between. Data were analysed using the T_1T_2 module in TOPSPIN 3.2 and plots were generated using the eddosy module.

High-resolution mass spectra (EI and ESI) were recorded using a Bruker MicroTOF spectrometer by the internal service at the University of Oxford. Low-resolution mass spectra were recorded using a Walters LCT premier XE.

Infrared measurements (thin film) were carried out using a Bruker Tensor 27 FTIR with internal calibration in the range 4000-600 cm^{-1}.

Optical rotations were recorded using a Perkin-Elmer 241 polarimeter at 25 °C in a 10 cm cell in the stated solvent. $[\alpha]_D$ values are given in 10^{-1} deg·cm^2 g^{-1}, with concentration c given as g/100 mL.

Fluorimetry was performed using Edinburgh Instruments Spectrofluorometer FS5 model with Fluoracle software. The slit width for both excitation and emission was set at 1 nm.

DLS measurements were recorded using a Microtrac Nanotrac Wave W3043 (University of Twente) and Malvern Zetasizer Nano S (University of Oxford) instruments and analysed with Origin software.

TEM measurements were performed with a Philips CM300ST-FEG Transmission Electron Microscope with a GATAN Ultrascan1000 (2kx2k CCD camera), GATAN Tridiem energy filter (2kx2k CCD camera) and Noran System Six EDX analyser Nanotrace detector. The samples were deposited on a copper grid and stained with 2% uranyl acetate.

Confocal micrographs where captured with a Nikon A1plus confocal microscope (University of Twente) and Olympus FV1200 laser scanning microscope (University of Oxford) with the laser set at 488 nm. All the samples were stained with the dye Coumarin 6 by adding 1 μL of a 1 mM solution of dye in THF to 200 μL of sample giving a final concentration of 5 μM.

Image processing of all micrographs was done with Fiji ImageJ software. Segmentation and thresholding were performed by training classifiers with the Trainable Weka Segmentation plugin. Particles were counted with the analyse particles function and diameters were calculated from the counted areas.

UPLC analyses were performed using a Waters Acquity ultra performance liquid chromatography (UPLC) H-Class system with photodiode array (PDA) detector. Instrument control and data processing were performed using Empower software. An Acquity® UPLC BEH Amide column (130 Å, 1.7 μm, 2.1 mm × 150 mm) was used. Conditions: Flow rate: 0.6 ml/min. Gradient: H_2O:MeCN:MeOH with a gradient of 0:95:5 to 30:65:5 in 0 to 2.5 min; 30:65:5 isocratically 2.5 to 4 min; 0:95:5 isocratically from 4 to 5 min. λ_{det} = 214.5 nm.

SFC (supercritical fluid chromatography) separations were conducted with a chiral non-racemic stationary phase on a Waters Acquity UPC2 system using Waters Empower software. A Chiralpak® IE column (3 μm, 150×3 mm) was used. Conditions: Flow rate: 1.5 ml/min. Gradient: CO_2:MeOH with a gradient of 99:1 to 60:40 in 0 to 5 min; gradient of 60:40 to 40:60 in 5 to 5.5 min; 40:60 isocratically from 5.5 to 7 min; 100:0 isocratically from 7 to 8 min. λ_{det} = 266.8 nm.

Experimental Procedures and Characterisation of Compounds

Representative procedure for kinetic analysis of reactions

The concentrations of all UV active reaction species in aliquots removed from reaction were monitored by UPLC using an external standard. The external standard solution was first prepared by the dissolution of ethyl benzoate (50 μL, 0.35 mmol) in MeCN (500 mL) giving an overall concentration of 0.7 μM. To monitor the reactions a small volume (±25 μL) of the reaction mixture was withdrawn at specified time points by plastic syringe. A 20 μL aliquot of this withdrawn solution was then measured by microsyringe and injected into 500 μL of the standard solution in an MS vial. Five microliter of the resultant solution was the standard injection volume for analysis by UPLC. Concentration of compounds were calculated from the peak area using the UPLC calibration curves reported in this Supplemental Information.

Representative procedure for setup of kinetic experiments (Figure 2b)

A solution of alkyne **2** (23.5 mg, 0.10 mmol, 1 eq, 1 mL of 100 mM standard solution in H_2O), $CuSO_4 \cdot 5H_2O$ (2.5 mg, 0.01 mmol, 0.1 eq, 250 μL of 40 mM standard solution in H_2O) (and surfactant **3** (17.6 mg, 0.02 mmol, 0.2 eq) for the seeded reactions) were added to H_2O (3.75 mL) to give a total volume of 5 mL in a round bottom flask (25 mL) with a stirrer bar of an identical size (4.5 mm diameter and 12 mm length) for each experiment. Subsequently TBTA (5.3 mg, 0.01 mmol, 0.1 eq), azide **1** (100 μL, 0.156 mmol, 1.56 eq) were added and the flask was capped with a septum and the solution was degassed by bubbling argon through it for 30 minutes. Afterwards sodium ascorbate (6.0 mg, 0.03 mmol, 0.3 eq) was added to initiate the reaction. The reaction mixture was stirred at 1000 rpm under a continuous flow of argon.

Note: For the thin film seeded reaction surfactant **3** (17.6 mg, 0.04 mmol, 0.4 eq) was first dissolved in a minimum of MeOH and then concentrated *in vacuo* to generate a thin film of the compound on the flask. This was hydrated in H_2O (3 mL) before addition of the other reagents.
Note 2: For figure 4b, azide **1** (100 μL, 0.156 mmol, 1.56 eq) and azide **6** (45 μL, 0.156 mmol, 1.56 eq) were added to the reaction mixture. The reaction was stirred at 1000 rpm.
Note 3: These reactions are very sensitive to physical parameters, so changing the flask size, stirrer bar or adding compounds at different time points during the degassing process might affect the overall kinetics of the reaction.

Representative procedure for setup of hydrolysis experiments (Figure S38)

A solution of alkyne **2** (23.5 mg, 0.10 mmol, 1 eq, 1 mL of 100 mM standard solution in H_2O) and of $CuSO_4 \cdot 5H_2O$ (10 mg, 0.04 mmol, 0.4 eq, 1 mL of 40 mM standard solution in H_2O) were added to H_2O (2.5 mL) in a round bottom flask (25 mL) with a stirrer bar of an identical size (4.5 mm diameter and 12 mm length) for each experiment. Subsequently TBTA (21 mg, 0.04 mmol, 0.1 eq), azide **1** (100 μL, 0.156 mmol, 1.56 eq) were added and the flask was capped with a septum and the solution was degassed by bubbling argon through it for 30 minutes. Subsequently, 0.5 mL of a degassed, aqueous NaOH (500 mM) solution was added to give a final reaction volume of 5 mL with 50 mM of NaOH. Afterwards sodium ascorbate (24.0 mg, 0.12 mmol, 1.2 eq) was added to initiate the reaction. The reaction mixture was stirred at 1000 rpm under a continuous flow of argon.

Note: For figure 4c, azide **1** (100 μL, 0.156 mmol, 1.56 eq) and azide **6** (45 μL, 0.156 mmol, 1.56 eq) were added to the reaction mixture.

Representative procedure for setup of hydrolysis experiments in a continuously stirred tank reactor (Figure 3c)

A solution of alkyne **2** (70.5 mg, 0.30 mmol, 1 eq, 3 mL of 100 mM standard solution in H_2O) and of $CuSO_4 \cdot 5H_2O$ (30 mg, 0.12 mmol, 0.4 eq, 3 mL of 40 mM standard solution in H_2O) were added to H_2O (6 mL) in a round bottom flask (25 mL) with a stirrer bar of an identical size (4.5 mm diameter and 12 mm length) for each experiment. Subsequently TBTA (63 mg, 0.12 mmol, 0.1 eq) was added and the flask was capped with a septum and the solution was degassed by bubbling argon through it for 30 minutes. Afterwards 3 mL of a degassed, aqueous NaOH (500 mM) solution and sodium ascorbate (72.0 mg, 0.36 mmol, 1.2 eq) were added to give a final reaction volume of 15 mL with 100 mM of NaOH. Of this solution 10 mL was withdrawn into a 10 mL syringe which was subsequently installed into a syringe pump set at a flow of 200 μL/h. In a second syringe pump a 1 mL syringe with 200 μL of azide **1** was installed with a flow rate of 4 μL/h. A third syringe pump had an empty 10 mL syringe installed and was set at withdrawal rate of 204 μL/h. Azide **1** (100 μL, 0.156 mmol, 1.56 eq) was added to the reaction mixture and the pumps were turned on to initiate the reaction. The reaction mixture was stirred at 1000 rpm under a continuous flow of argon.

Note: During the periods that the reaction was monitored the withdrawal rate was lowered to 180 μL/h to compensate for the amount of reaction mixture removed by taking aliquots.
Note 2: For figure 4d, a syringe with a mixture of azide **1** (100 μL, 0.156 mmol, 1.56 eq) and azide **6** (45 μL, 0.156 mmol, 1.56 eq) was installed in syringe pump 2 which was set at 5.8 μL/h. The withdrawal pump was set at of 205.8 μL/h. A mixture of azide **1** (100 μL, 0.156 mmol, 1.56 eq) and azide **6** (45 μL, 0.156 mmol, 1.56 eq) was added to the reaction mixture to initiate the reaction.

Representative procedure for setup of enantioselective aldol reaction in a self-replicating protocell (Figure 5d, entry 7)

A solution of alkyne **2** (23.5 mg, 0.10 mmol, 1 eq, 1 mL of 100 mM standard solution in H_2O), $CuSO_4 \cdot 5H_2O$ (10 mg, 0.04 mmol, 0.4 eq, 1 mL of 40 mM standard solution in H_2O) were added to H_2O (3 mL) to give a total volume of 5 mL in a round bottom flask (25 mL) with a stirrer bar of an identical size (4.5 mm diameter and 12 mm length) for each experiment. Subsequently TBTA (21 mg, 0.04 mmol, 0.4 eq), azide **1** (100 μL, 0.156 mmol, 1.56 eq) were added and the flask was capped with a septum and the solution was degassed by bubbling argon through it for 30 minutes. Afterwards sodium ascorbate (24 mg, 0.12 mmol, 1.2 eq), precatalyst **9** (3.4 mg, 0.02 mmol, 0.2 eq), nitrobenzaldehyde **11** (10 mg, 0.066 mmol, 0.66 eq) and cyclohexanone **12** (34 μL, 0.33 mmol, 3.3 eq) were added to initiate the reaction. The reaction mixture was stirred at 1000 rpm under a continuous flow of argon.

Note: Entry 3 was performed in an identical manner however alkyne **2** was not added.
Note 2: Entry 1, 2, 4, 5 and 6 were performed by simply stirring the reported substrates at the reported concentrations in 1 mL of H_2O. Compounds **3** and **10** were first dissolved in a minimum of MeOH and then concentrated *in vacuo* to generate a thin film of the compound on the flask. This was hydrated in H_2O (1 mL) before addition of the other reagents.

2-Oxopropane-1,3-diyl dioleate (14)

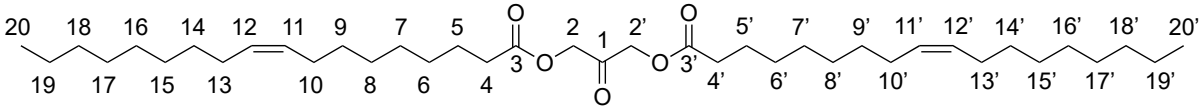

Chemical Formula: $C_{39}H_{70}O_5$
Molecular Weight: 618.9840

Synthesised according to procedure adapted from Li *et al.*[1] To a solution of 1,3-dihydroxylacetone (7.2 g, 79.74 mmol, 1 eq) in $CHCl_3$ (300 mL), oleoyl chloride (60 ml, 159.48 mmol, 2 eq, 89% pure) was added, followed by dropwise addition of pyridine (14.4 mL, 178.77 mmol, 2.2 eq). The reaction mixture was stirred at room temperature overnight and was subsequently washed with 5% aqueous HCl (300 mL), saturated aqueous $NaHCO_3$ (300 mL), and brine (300 mL). The organic layer was dried (Na_2SO_4) and concentrated *in vacuo*. The crude product was recrystallized from hot 2-propanol (25 mL/g). The crystals were collected by filtration and purified by flash column chromatography (10% EtOAc in hexane) to yield diester **14** (41.76 g, 67.47 mmol, 85%) as a white, waxy solid.

^{1}H NMR (400 MHz, $CDCl_3$) δ 5.39 – 5.29 (m, 4H, C<u>H</u>-11;C<u>H</u>-11';C<u>H</u>-12;C<u>H</u>-12'), 4.75 (s, 4H, C<u>H</u>$_2$-2;C<u>H</u>$_2$-2'), 2.42 (t, J = 7.6 Hz, 4H, C<u>H</u>$_2$-4;C<u>H</u>$_2$-4'), 2.08 – 1.95 (m, 8H, C<u>H</u>$_2$-10;C<u>H</u>$_2$-10';C<u>H</u>$_2$-13;C<u>H</u>$_2$-13'), 1.66 (p, J = 7.4 Hz, 4H, C<u>H</u>$_2$-5;C<u>H</u>$_2$-5'), 1.39 – 1.20 (m, 40H, (C<u>H</u>$_2$)$_4$-6-9;(C<u>H</u>$_2$)$_4$-6'-9';(C<u>H</u>$_2$)$_6$-14-19;(C<u>H</u>$_2$)$_6$-14'-19'), 0.92 – 0.83 (m, 6H, C<u>H</u>$_3$-20;C<u>H</u>$_3$-20').

^{13}C NMR (101 MHz, $CDCl_3$) δ 198.3, 173.1 (2C), 130.2 (2C), 129.9 (2C), 66.3 (2C), 33.9 (2C), 32.1 (2C), 29.9 (2C), 29.8 (2C), 29.7 (2C), 29.5 (4C), 29.3 (2C), 29.2 (2C), 29.2 (2C), 27.4 (2C), 27.3 (2C), 25.0 (2C), 22.8 (2C), 14.3 (2C).

HRMS (ESI) *m/z* calcd for $C_{39}H_{70}O_5Na$ $[M+Na]^+$: 641.5116, found: 641.5114.
Consistent with reported literature values.[1]

2-Hydroxypropane-1,3-diyl dioleate (15)

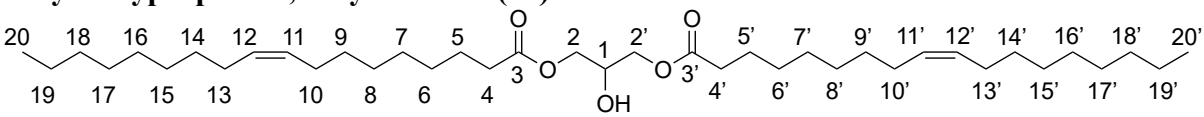

Chemical Formula: $C_{39}H_{72}O_5$
Molecular Weight: 621.0000

Synthesised according to procedure adapted from Li *et al.*[1] $NaBH_4$ (2.77 g, 73.22 mmol, 1.5 eq) in water (a minimum quantity) was slowly added to a solution of diester **14** (30.22 g, 48.82, 1 eq) in THF (500 mL) at 0 °C. The reaction mixture was stirred at 0 °C for 30 min and quenched by addition of 5% HCl (10 mL). H_2O (300 mL) was added, and the mixture was extracted with $CHCl_3$ (600 mL). The organic layer was washed sequentially with H_2O (400 mL), saturated aqueous $NaHCO_3$ (300 mL), and brine (400 mL). The organic layer was dried (Na_2SO_4), concentrated *in vacuo* and purified by flash column chromatography (5% EtOAc in hexane) to yield alcohol **15** (27.29 g, 43.95 mmol, 89%) as a transparent oil. Some of the regioisomer is formed during the reaction due to transesterifaction.

^{1}H NMR (400 MHz, $CDCl_3$) δ 5.45 – 5.26 (m, 4H, C<u>H</u>-11;C<u>H</u>-11';C<u>H</u>-12;C<u>H</u>-12'), 4.21 – 4.04 (m, 5H, C<u>H</u>-1;C<u>H</u>$_2$-2;C<u>H</u>$_2$-2'), 2.43 (d, J = 4.8 Hz, 1H, CH-O<u>H</u>-1), 2.34 (t, J = 7.6 Hz, 4H, C<u>H</u>$_2$-4;C<u>H</u>$_2$-4'), 2.07 – 1.94 (m, 8H, C<u>H</u>$_2$-10;C<u>H</u>$_2$-10';C<u>H</u>$_2$-13;C<u>H</u>$_2$-13'), 1.62 (p, J = 7.2 Hz, 4H, C<u>H</u>$_2$-5;C<u>H</u>$_2$-5'), 1.39 – 1.19 (m, 40H, (C<u>H</u>$_2$)$_4$-6-9;(C<u>H</u>$_2$)$_4$-6'-9';(C<u>H</u>$_2$)$_6$-14-19;(C<u>H</u>$_2$)$_6$-14'-19'), 0.94 – 0.83 (m, 6H, C<u>H</u>$_3$-20;C<u>H</u>$_3$-20').

^{13}C NMR (101 MHz, $CDCl_3$) δ 174.0 (2C), 130.2 (2C), 129.9 (2C), 68.6, 65.2 (2C), 34.2 (2C), 32.1 (2C), 29.9 (2C), 29.8 (2C), 29.7 (2C), 29.5 (4C), 29.3 (2C), 29.2 (4C), 27.4 (2C), 27.3 (2C), 25.0 (2C), 22.8 (2C), 14.3 (2C).

HRMS (ESI) *m/z* calcd for $C_{39}H_{72}O_5Na$ $[M+Na]^+$: 643.5272, found: 643.5274.
Consistent with reported literature values.[1]

2-((Methylsulfonyl)oxy)propane-1,3-diyl dioleate (16)

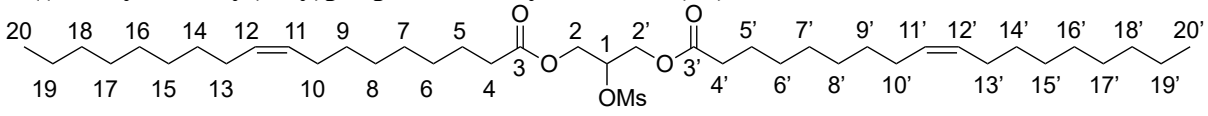

21
Chemical Formula: $C_{40}H_{74}O_7S$
Molecular Weight: 699.0850

To a solution of alcohol **15** (27.29 g, 43.95 mmol, 1 eq) and triethylamine (9.19 mL, 65.93 mmol, 1.5 eq) in anhydrous CH_2Cl_2 (200 mL) was added methanesulfonyl chloride (3.74 mL, 48.35, 1.1 eq) at 0 °C under argon atmosphere. After 2 hours the reaction mixture was washed with 5% aqueous HCl (200 mL), saturated aqueous $NaHCO_3$ (200 mL), and brine (200 mL). The organic layer was dried (Na_2SO_4), concentrated *in vacuo* and purified by flash column chromatography (2.5% EtOAc in hexane) to afford mesylate **16** (20.92 g, 29.93 mmol, 68%) as a transparent oil.

^{1}H NMR (400 MHz, $CDCl_3$) δ 5.40 – 5.29 (m, 4H, C$\underline{H}$-11;C$\underline{H}$-11';C$\underline{H}$-12;C$\underline{H}$-12'), 5.02 (tt, *J* = 6.4, 3.8 Hz, 1H, C$\underline{H}$-1), 4.36 (dd, *J* = 12.3, 3.9 Hz, 2H, C$\underline{H}_a$H$_b$-2;C$\underline{H}_a$H$_b$-2'), 4.22 (dd, *J* = 12.3, 6.5 Hz, 2H, CH$_a\underline{H}_b$-2;CH$_a\underline{H}_b$-2'), 3.08 (s, 3H, $SO_2C\underline{H}_3$-21), 2.35 (t, *J* = 7.6 Hz, 4H, C$\underline{H}_2$-4;C$\underline{H}_2$-4'), 2.05 – 1.94 (m, 8H, C$\underline{H}_2$-10;C$\underline{H}_2$-10';C$\underline{H}_2$-13;C$\underline{H}_2$-13'), 1.67 – 1.59 (m, 4H, C$\underline{H}_2$-5;C$\underline{H}_2$-5'), 1.38 – 1.21 (m, 40H, (C$\underline{H}_2$)$_4$-6-9;(C$\underline{H}_2$)$_4$-6'-9';(C$\underline{H}_2$)$_6$-14-19;(C$\underline{H}_2$)$_6$-14'-19'), 0.90 – 0.85 (m, 6H, C$\underline{H}_3$-20;C$\underline{H}_3$-20').

^{13}C NMR (101 MHz, $CDCl_3$) δ 173.2 (2C), 130.2 (2C), 129.8 (2C), 76.8, 62.4 (2C), 38.8, 34.1 (2C), 32.0 (2C), 29.9 (2C), 29.8 (2C), 29.7 (2C), 29.5 (4C), 29.3 (2C), 29.2 (2C), 29.2 (2C), 27.4 (2C), 27.3 (2C), 24.9 (2C), 22.8 (2C), 14.3 (2C).

HRMS (ESI) *m/z* calcd for $C_{40}H_{74}O_7NaS$ $[M+Na]^+$: 721.5048, found: 721.5045.

2-Azidopropane-1,3-diyl dioleate (1)

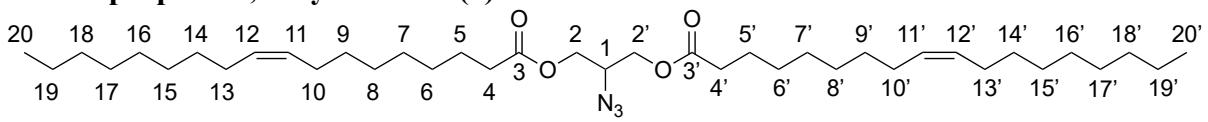

Chemical Formula: $C_{39}H_{71}N_3O_4$
Molecular Weight: 646.0140

To a solution of mesylate **16** (15.43 g, 22.08 mmol, 1 eq) in DMF (100 mL) was added sodium azide (5.73 g, 88.15 mmol, 4 eq). The reaction mixture was heated to 90 °C for 18 hours and was then concentrated *in vacuo* to remove the majority of DMF. The crude was dissolved in CH_2Cl_2 (100 mL) and washed with saturated aqueous $NaHCO_3$ (3x 100 mL). The organic layer was dried (Na_2SO_4), concentrated *in vacuo* and purified by flash column chromatography (10% EtOAc in hexane) to afford azide **1** (9.81 g, 15.18 mmol, 69%) as a transparent oil.

^{1}H NMR (400 MHz, $CDCl_3$) δ 5.40 – 5.28 (m, 4H, C$\underline{H}$-11;C$\underline{H}$-11';C$\underline{H}$-12;C$\underline{H}$-12'), 4.23 (dd, *J* = 11.6, 4.6 Hz, 2H, C$\underline{H}_a$H$_b$-2;C$\underline{H}_a$H$_b$-2'), 4.14 (dd, *J* = 11.6, 6.8 Hz, 2H, CH$_a\underline{H}_b$-2;CH$_a\underline{H}_b$-2'), 3.87 (tt, *J* = 6.8, 4.6 Hz, 1H, C$\underline{H}$-1), 2.35 (t, *J* = 7.5 Hz, 4H, C$\underline{H}_2$-4;C$\underline{H}_2$-4'), 2.07 – 1.97

(m, 8H, C$\underline{H}_2$-10;C$\underline{H}_2$-10';C$\underline{H}_2$-13;C$\underline{H}_2$-13'), 1.69 – 1.57 (m, 4H, C$\underline{H}_2$-5;C$\underline{H}_2$-5'), 1.38 – 1.20 (m, 40H, (C$\underline{H}_2$)$_4$-6-9;(C$\underline{H}_2$)$_4$-6'-9';(C$\underline{H}_2$)$_6$-14-19;(C$\underline{H}_2$)$_6$-14'-19'), 0.94 – 0.80 (m, 6H, C$\underline{H}_3$-20;C$\underline{H}_3$-20').

^{13}C NMR (101 MHz, $CDCl_3$) δ 173.4 (2C), 130.2 (2C), 129.9 (2C), 63.2 (2C), 58.8, 34.1 (2C), 32.1 (2C), 29.9 (2C), 29.8 (2C), 29.7 (2C), 29.5 (4C), 29.3 (2C), 29.2 (4C), 27.4 (2C), 27.3 (2C), 24.9 (2C), 22.8 (2C), 14.3 (2C).

HRMS (ESI) *m/z* calcd for $C_{39}H_{71}O_4N_3Na$ $[M+Na]^+$: 668.5337, found: 668.5332.

IR (ATR) ν (cm^{-1}) thin film, CH_2Cl_2: 2923 (s), 2858 (s), 2122 (w), 1745 (s), 1463 (w), 1240 (w), 1161 (m), 723 (w).

2-(But-3-yn-1-yloxy)-1,3,2-dioxaphospholane 2-oxide (17)

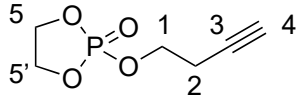

Chemical Formula: $C_6H_9O_4P$
Molecular Weight: 176.1078

Synthesised according to adapted procedure from Emrick *et al*.[2] To a solution of 3-butyn-1-ol (1.06 mL, 14.0 mmol, 1 eq) in anhydrous THF (20 mL) was added triethylamine (2.15 mL, 15.4 mmol, 1.1 eq) at 0 °C under argon atmosphere. After slow addition of 2-chloro-2-oxo-1,3,2-dioxaphospholane (1.29 mL, 14.0 mmol, 1 eq), the mixture was warmed to room temperature and stirred for 2 hours. The white suspension was filtered over a sintered funnel, and the filtrate was concentrated by rotary evaporation and dried in vacuo to give phospholane **17** (2.30 g, 13.1 mmol, 93%) as a yellow oil. This was used without further purification due to decomposition of **17** on silica.

^{1}H NMR (400 MHz, $CDCl_3$) δ 4.50 – 4.32 (m, 4H, C$\underline{H}_2$-5;C$\underline{H}_2$-5'), 4.24 (dt, J = 9.5, 6.8 Hz, 2H, C$\underline{H}_2$-1), 2.62 (td, J = 6.8, 2.7 Hz, 2H, C$\underline{H}_2$-2), 2.04 (t, J = 2.7 Hz, 1H, C$\underline{H}$-4).

^{13}C NMR (101 MHz, $CDCl_3$) δ 79.2, 70.6, 66.4 (d, J_{CP} = 5.7 Hz), 66.2 (d, J_{CP} = 3.1 Hz, 2C), 20.9 (d, J_{CP} = 6.6 Hz).

^{31}P NMR (162 MHz, $CDCl_3$) δ 17.38.

Consistent with reported literature values.[3]

But-3-yn-1-yl (2-(trimethylammonio)ethyl) phosphate (2)

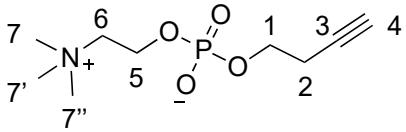

Chemical Formula: $C_9H_{18}NO_4P$
Molecular Weight: 235.2198

Synthesized according to adapted procedure from Choi *et al*.[4] Crude phospholane **20** (2.30 g, 13.1 mmol) was dissolved in dry MeCN (20 mL) in a 100 mL flame dried flask under argon. After trimethylamine (21 mL, 21 mmol, 1.6 eq, 1 M in THF) was added, the flask was closed and heated to 70 °C for 48 h. The crude mixture was concentrated *in vacuo* and purified by flash column chromatography (10% H_2O and 40% MeOH in CH_2Cl_2) to yield phosphocholine **2** (2.42 g, 10.3 mmol, 79%) as a transparent oil that crystallizes in the freezer.

^{1}H NMR (400 MHz, CD_3OD) δ 4.34 – 4.24 (m, 2H, C$\underline{H}_2$-5), 3.96 (q, J = 7.0 Hz, 2H, C$\underline{H}_2$-1), 3.66 – 3.60 (m, 2H, C$\underline{H}_2$-6), 3.23 (s, 9H, C$\underline{H}_3$-7;C$\underline{H}_3$-7';C$\underline{H}_3$-7''), 2.53 (td, J = 6.8, 2.7 Hz, 2H, C$\underline{H}_2$-2), 2.31 (t, J = 2.7 Hz, 1H, C$\underline{H}_2$-4).

^{13}C NMR (101 MHz, CD_3OD) δ 81.8, 71.0, 67.5 – 67.3 (m, J_{CN}^{+} and J_{CP}), 65.0 (d, J_{CP} = 5.6 Hz), 60.4 (d, J_{CN}^{+} = 4.9 Hz), 54.8 – 54.6 (m, J_{CN}^{+}, 3C), 49.8, 30.7, 24.2, 21.6 (d, J_{CP} = 7.9 Hz).

^{31}P NMR (162 MHz, CD_3OD) δ -0.55.

HRMS (ESI) *m/z* calcd for $C_9H_{19}NO_4P$ $[M+H]^+$: 236.1046, found: 236.1045.

IR (ATR) ν (cm^{-1}) thin film, MeOH: 3273 (broad m), 2361 (w), 1654 (w), 1479 (w) 1229 (m), 1083 (s), 1051 (s), 970 (w), 926 (w).

2-(1-(1,3-Bis(oleoyloxy)propan-2-yl)-1*H*-1,2,3-triazol-4-yl)ethyl (2-(trimethylammonio)ethyl) phosphate (3)

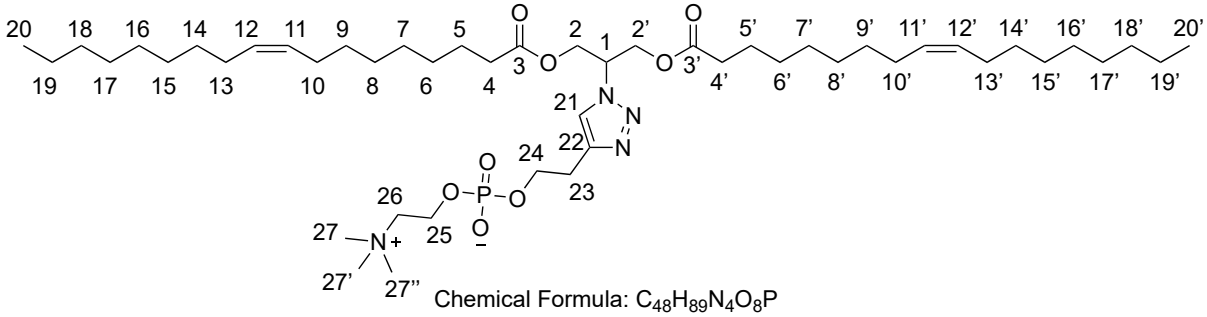

Chemical Formula: $C_{48}H_{89}N_4O_8P$
Molecular Weight: 881.2338

To a solution of alkyne **2** (203 mg, 0.863 mmol, 1 eq), $CuSO_4 \cdot 5H_2O$ (20 mg, 0.08 mmol, 0.09 eq) in Milli-Q H_2O (2.5 mL) and *t*-BuOH (2.5 mL) was added TBTA (42 mg, 0.08 mmol, 0.09 eq), azide **1** (600 μL, 0.938 mmol, 1.09 eq) were added and the flask was capped with a septum. The solution was degassed by bubbling argon through it for 30 minutes. Afterwards sodium ascorbate (48 mg, 0.246 mmol, 0.27 eq) was added to initiate the reaction. The reaction mixture was stirred at 1000 rpm under a continuous flow of argon. The crude mixture was concentrated *in vacuo* and purified by flash column chromatography (2% H_2O and 48% MeOH in CH_2Cl_2). The obtained compound was dissolved in a minimum of MeOH and filtered through a PTFE syringe filter to remove any silica particles and concentrated *in vacuo* to yield surfactant **3** (584 mg, 0.662 mmol, 77%) as a transparent viscous oil.

^{1}H NMR (400 MHz, CD_3OD) δ 7.95 (s, 1H, C$\underline{H}$-21), 5.34 – 5.23 (m, 4H, C$\underline{H}$-11;C$\underline{H}$-11';C$\underline{H}$-12;C$\underline{H}$-12'), 5.10 (p, J = 6.1 Hz, 1H, C$\underline{H}$-1), 4.50 (d, J = 6.1 Hz, 4H, C$\underline{H}_2$-2;C$\underline{H}_2$-2'), 4.22 – 4.16 (m, 2H, C$\underline{H}_2$-25), 4.08 (q, J = 6.5 Hz, 2H, C$\underline{H}_2$-24), 3.60 – 3.54 (m, 2H, C$\underline{H}_2$-26), 3.17 (s, 9H, C$\underline{H}_3$-27;C$\underline{H}_3$-27';C$\underline{H}_3$-27''), 3.00 (t, J = 6.4 Hz, 2H, C$\underline{H}_2$-23), 2.26 (t, J = 7.4 Hz, 4H, C$\underline{H}_2$-4;C$\underline{H}_2$-4'), 2.10 – 1.96 (m, 8H,C$\underline{H}_2$-10;C$\underline{H}_2$-10';C$\underline{H}_2$-13;C$\underline{H}_2$-13'), 1.51 (p, J = 6.6, 6.0 Hz, 4H, C$\underline{H}_2$-5;C$\underline{H}_2$-5'), 1.36 – 1.14 (m, 40H, (C$\underline{H}_2$)$_4$-6-9;(C$\underline{H}_2$)$_4$-6'-9';(C$\underline{H}_2$)$_6$-14-19;(C$\underline{H}_2$)$_6$-14'-19'), 0.90 – 0.79 (m, 6H, C$\underline{H}_3$-20;C$\underline{H}_3$-20').

^{13}C NMR (101 MHz, CD_3OD) δ 174.5 (2C), 130.9 (2C), 130.89 (2C), 124.0, 67.7 – 67.4 (m, J_{CN}^{+} and J_{CP}), 65.5 (d, J_{CP} = 5.8 Hz), 64.4, 63.59 (2C), 60.3 (d, J_{CN}^{+} = 4.8 Hz), 60.2, 55.0 – 54.5 (m, J_{CN}^{+}, 3C), 34.7 (2C), 33.1 (2C), 30.9 (2C), 30.8 (2C), 30.6 (2C), 30.5 (2C), 30.4 (2C), 30.3 (2C), 30.2 (2C), 30.1 (2C), 28.2 (d, J_{CP} = 7.7 Hz, 1C), 28.1 (4C), 25.9 (2C), 23.7 (2C), 14.5 (2C).

^{31}P NMR (162 MHz, CD_3OD) δ -0.71.

HRMS (ESI) *m/z* calcd for $C_{48}H_{90}O_8N_4P$ $[M+H]^+$: 881.6491, found: 881.6488.

IR (ATR) ν (cm^{-1}) thin film, MeOH: 3367 (broad w), 2924 (s), 2853, (m), 1741 (m), 1655 (w), 1465 (w) 1229 (m), 1086 (s), 970 (w).

2-(1-(1-Hydroxy-3-(oleoyloxy)propan-2-yl)-1*H*-1,2,3-triazol-4-yl)ethyl (2-(trimethylammonio)ethyl) phosphate (4)

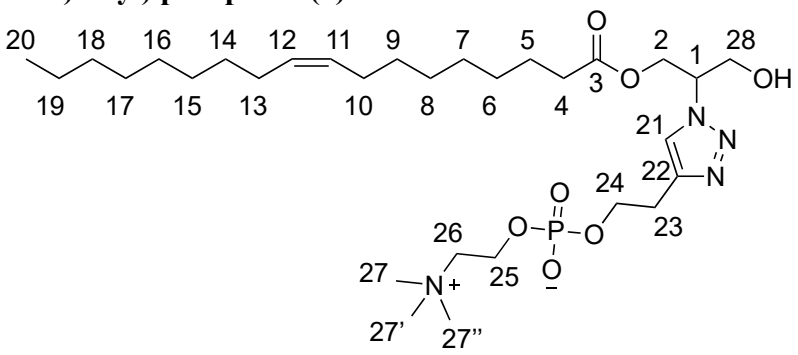

Chemical Formula: $C_{30}H_{57}N_4O_7P$
Molecular Weight: 616.7808

This compound was recovered for characterization from experiments as described in the representative procedure for setup of hydrolysis experiments. The crude reaction mixture of multiple experiments were combined, concentrated *in vacuo* and purified by flash column chromatography (5% H_2O and 45% MeOH in CH_2Cl_2). The obtained compound was dissolved in a minimum of MeOH and filtered through a PTFE syringe filter to remove any silica particles and concentrated *in vacuo* to yield compound **4** as a transparent viscous oil.

^{1}H NMR (400 MHz, CD_3OD) δ 7.92 (s, 1H, C<u>H</u>-21), 5.34 – 5.22 (m, 2H, C<u>H</u>-11;C<u>H</u>-12), 4.88 – 4.82 (m, 1H, C<u>H</u>-1), 4.46 (dt, *J* = 5.6, 2.7 Hz, 2H, C<u>H$_2$</u>-2), 4.07 (q, *J* = 6.2 Hz, 4H, C<u>H$_2$</u>-24;C<u>H$_2$</u>-25), 3.97 – 3.86 (m, 2H, C<u>H$_2$</u>-28), 3.54 – 3.48 (m, 2H, C<u>H$_2$</u>-26), 3.13 (s, 9H, C<u>H$_3$</u>-27;C<u>H$_3$</u>-27';C<u>H$_3$</u>-27''), 2.98 (t, *J* = 6.2 Hz, 2H, C<u>H$_2$</u>-23), 2.21 (t, *J* = 7.4 Hz, 2H, C<u>H$_2$</u>-4), 1.96 (q, *J* = 6.4 Hz, 4H, C<u>H$_2$</u>-10;C<u>H$_2$</u>-13), 1.46 (p, *J* = 7.2 Hz, 2H, C<u>H$_2$</u>-5), 1.41 – 1.22 (m, 20H, (C<u>H$_2$</u>)$_4$-6-9;(C<u>H$_2$</u>)$_6$-14-19), 0.87 – 0.81 (m, 3H, C<u>H$_3$</u>-20).

^{13}C NMR (101 MHz, CD_3OD) δ 174.7, 145.7, 130.9, 130.8, 124.0, 67.8 – 67.3 (m, J_{CN}^+ and J_{CP}), 65.5 (d, J_{CP} = 5.5 Hz), 63.9, 63.5, 62.1, 60.3 (d, J_{CN}^+= 5.0 Hz), 55.2 – 54.3 (m, J_{CN}^+, 3C), 34.7, 33.0, 30.8, 30.8, 30.6, 30.4, 30.3, 30.2, 30.1, 30.1, 28.3 (d, J_{CP} = 8.0 Hz), 28.1, 25.9, 23.7, 14.5.

^{31}P NMR (162 MHz, CD_3OD) δ -0.45.

HRMS (ESI) *m/z* calcd for $C_{30}H_{58}O_7N_4P$ $[M+H]^+$: 617.4039, found: 617.4038.

IR (ATR) ν (cm^{-1}) thin film, MeOH: 3352 (broad m), 2924 (m), 2854, (w), 1741 (w), 1655 (w), 1465 (w) 1229 (s), 1086 (s), 970 (w), 929 (w). 790 (w).

2-(1-(1,3-dihydroxypropan-2-yl)-1*H*-1,2,3-triazol-4-yl)ethyl (2-(trimethylammonio) ethyl phosphate (5)

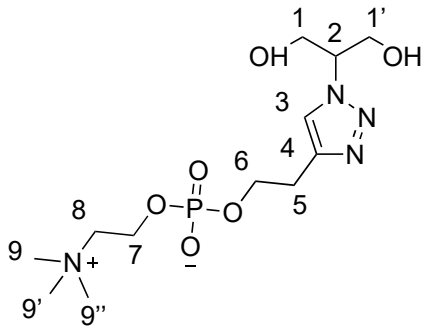

Chemical Formula: $C_{12}H_{25}N_4O_6P$
Molecular Weight: 352.3278

This compound was recovered for characterization from experiments as described in the representative procedure for setup of hydrolysis experiments. The crude reaction mixture of multiple experiments were combined, concentrated *in vacuo* and purified by flash column chromatography (10% H_2O and 40% MeOH in CH_2Cl_2). The obtained compound was dissolved in a minimum of MeOH and filtered through a PTFE syringe filter to remove any silica particles and concentrated *in vacuo* to yield compound **5** as a transparent viscous oil.

^{1}H NMR (400 MHz, CD_3OD) δ 7.89 (s, 1H, C<u>H</u>-3), 4.66 – 4.57 (m, 1H, C<u>H</u>-2), 4.07 (q, J = 6.1 Hz, 2H, C<u>H</u>$_2$-6), 4.04 – 3.98 (m, 2H, C<u>H</u>$_2$-7), 3.94 – 3.84 (m, 4H, C<u>H</u>-1;C<u>H</u>-1'), 3.51 – 3.44 (m, 2H, C<u>H</u>$_2$-8), 3.15 (d, J = 4.5 Hz, 1H, CHO<u>H</u>-1;CHO<u>H</u>-1'), 3.11 (s, 9H, C<u>H</u>$_3$-9;C<u>H</u>$_3$-9';C<u>H</u>$_3$-9''), 2.98 (t, J = 6.2 Hz, 3H, C<u>H</u>$_2$-5).

^{13}C NMR (101 MHz, CD_3OD) δ 145.6, 124.2, 67.6 – 67.3 (m, J_{CN}^+ and J_{CP}), 66.8, 65.6 (d, J_{CP} = 5.5 Hz), 62.3 (2C), 60.3 (d, J_{CN}^+ = 4.9 Hz), 55.0 – 54.6 (m, J_{CN}^+, 3C), 49.9, 28.2 (d, J_{CP} = 8.0 Hz).

^{31}P NMR (162 MHz, CD_3OD) δ -0.44.

HRMS (ESI) *m/z* calcd for $C_{12}H_{26}O_6N_4P$ $[M+H]^+$: 353.1585, found: 353.1583.

IR (ATR) ν (cm^{-1}) thin film, MeOH: 3263 (broad m), 2966 (w), 1655 (w), 1478 (w) 1224 (s), 1081 (s), 970 (m), 929 (m). 790 (m).

2-Oxopropane-1,3-diyl dihexanoate (18)

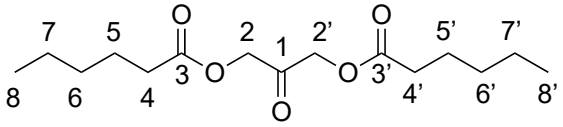

Chemical Formula: $C_{15}H_{26}O_5$
Molecular Weight: 286.3680

To a solution of 1,3-dihydroxylacetone (6.0 g, 66.45 mmol, 1 eq) in $CHCl_3$ (150 mL), hexanoyl chloride (20.5 ml, 146.67 mmol, 2.2 eq) was added, followed by dropwise addition of pyridine (12 mL, 148.98 mmol, 2.2 eq). The reaction mixture was stirred at room temperature overnight and was subsequently washed with 5% aqueous HCl (150 mL), saturated aqueous $NaHCO_3$ (150 mL), and brine (150 mL). The organic layer was dried (Na_2SO_4) and concentrated *in vacuo* and was purified by flash column chromatography (10% EtOAc in hexane) to yield diester **18** (16.3 g, 56.92 mmol, 86%) as a white waxy solid.

^{1}H NMR (400 MHz, $CDCl_3$) δ 4.75 (s, 4H, C<u>H</u>$_2$-2;C<u>H</u>$_2$-2'), 2.48 – 2.38 (m, 4H, C<u>H</u>$_2$-4;C<u>H</u>$_2$-4'), 1.73 – 1.62 (m, 4H, C<u>H</u>$_2$-5;C<u>H</u>$_2$-5'), 1.39 – 1.28 (m, 8H, C<u>H</u>$_2$-6;C<u>H</u>$_2$-6'; C<u>H</u>$_2$-7;C<u>H</u>$_2$-7'), 0.95 – 0.87 (m, 6H, C<u>H</u>$_3$-8;C<u>H</u>$_3$-8').

^{13}C NMR (101 MHz, $CDCl_3$) δ 198.3, 173.1 (2C), 66.3 (2C), 33.9 (2C), 31.3 (2C), 24.6 (2C), 22.4 (2C), 14.0 (2C).

HRMS (ESI) *m/z* calcd for $C_{15}H_{26}O_5Na$ $[M+Na]^+$: 309.1673, found: 309.1672.

2-hydroxypropane-1,3-diyl dihexanoate (19)

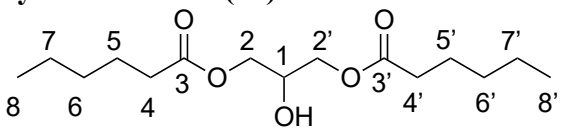

Chemical Formula: $C_{15}H_{28}O_5$
Molecular Weight: 288.3840

$NaBH_4$ (1.90 g, 50.22 mmol, 2.6 eq) in water (a small quantity) was slowly added to a solution of diester **18** (5.514 g, 19.23, 1 eq) in THF (300 mL) at 0 °C. The reaction mixture was stirred at 0 °C for 30 min and quenched by addition of 5% HCl (10 mL). H_2O (300 mL) was added, and the mixture was extracted with $CHCl_3$ (400 mL). The organic layer was washed sequentially with H_2O (300 mL), saturated aqueous $NaHCO_3$ (300 mL), and brine (300 mL). The organic layer was dried (Na_2SO_4), concentrated *in vacuo* and purified by flash column chromatography (20% EtOAc in hexane) to yield alcohol **19** (3.40 g, 11.79 mmol, 61%) as a transparent oil. A significant amount of the regioisomer is formed during the reaction due to transesterifaction.

^{1}H NMR (400 MHz, $CDCl_3$) δ 4.22 – 4.02 (m, 5H, C<u>H</u>-1;C<u>H</u>$_2$-2;C<u>H</u>$_2$-2'), 2.53 (d, J = 4.8 Hz, 1H, CHO<u>H</u>-1), 2.34 (t, J = 7.6 Hz, 4H, C<u>H</u>$_2$-4;C<u>H</u>$_2$-4'), 1.69 – 1.57 (m, 4H, C<u>H</u>$_2$-5;C<u>H</u>$_2$-5'), 1.38 – 1.22 (m, 8H, C<u>H</u>$_2$-6;C<u>H</u>$_2$-6'; C<u>H</u>$_2$-7;C<u>H</u>$_2$-7'), 0.93 – 0.85 (m, 6H, C<u>H</u>$_3$-8;C<u>H</u>$_3$-8').

^{13}C NMR (101 MHz, $CDCl_3$) δ 174.1 (2C), 68.5, 65.2 (2C), 34.2 (2C), 31.4 (2C), 24.7 (2C), 22.5 (2C), 14.1 (2C).

HRMS (ESI) *m/z* calcd for $C_{15}H_{28}O_5Na$ $[M+Na]^+$: 311.1829, found: 311.1827.
Consistent with reported literature values.[5]

2-((methylsulfonyl)oxy)propane-1,3-diyl dihexanoate (20)

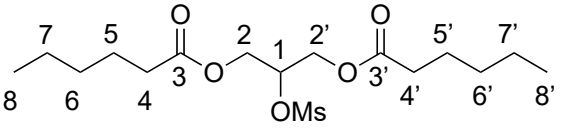

9

Chemical Formula: $C_{16}H_{30}O_7S$
Molecular Weight: 366.4690

To a solution of alcohol **19** (3.40 g, 11.79 mmol, 1 eq) and triethylamine (2.5 mL, 17.69 mmol, 1.5 eq) in anhydrous CH_2Cl_2 (50 mL) was added methanesulfonyl chloride (1.0 mL, 12.92 mmol, 1.1 eq) at 0 °C under argon atmosphere. After 2 hours the reaction mixture was washed with 5% aqueous HCl (50 mL), saturated aqueous $NaHCO_3$ (50 mL), and brine (50 mL). The organic layer was dried (Na_2SO_4), concentrated *in vacuo* and purified by flash column chromatography (10% EtOAc in hexane) to afford mesylate **20** (3.60 g, 9.82 mmol, 83%) as a transparent oil.

^{1}H NMR (400 MHz, $CDCl_3$) δ 5.02 (tt, *J* = 6.5, 3.8 Hz, 1H, C<u>H</u>-1), 4.36 (dd, *J* = 12.3, 3.8 Hz, 2H, C<u>H</u>$_a$H$_b$-2;C<u>H</u>$_a$H$_b$-2'), 4.22 (dd, *J* = 12.3, 6.5 Hz, 2H, CH$_a$<u>H</u>$_b$-2;CH$_a$<u>H</u>$_b$-2'), 3.08 (s, 3H, $SO_2C\underline{H}_3$-9), 2.35 (t, *J* = 7.6 Hz, 4H, C<u>H</u>$_2$-4;C<u>H</u>$_2$-4'), 1.69 – 1.57 (m, 4H, C<u>H</u>$_2$-5;C<u>H</u>$_2$-5'), 1.38 – 1.24 (m, *J* = 4.1, 3.7 Hz, 8H, C<u>H</u>$_2$-6;C<u>H</u>$_2$-6';C<u>H</u>$_2$-7;C<u>H</u>$_2$-7'), 0.94 – 0.84 (m, 6H, C<u>H</u>$_3$-8;C<u>H</u>$_3$-8').

^{13}C NMR (101 MHz, $CDCl_3$) δ 173.3 (2C), 76.8, 62.4 (2C), 38.9, 34.1 (2C), 31.4 (2C), 24.6 (2C), 22.5 (2C), 14.0 (2C).

HRMS (ESI) *m/z* calcd for $C_{15}H_{27}O_4$ [M-OMs]$^+$: 271.1904, found: 271.1905.

2-azidopropane-1,3-diyl dihexanoate (6)

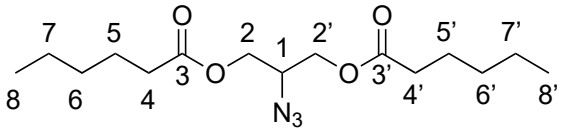

Chemical Formula: $C_{15}H_{27}N_3O_4$
Molecular Weight: 313.3980

To a solution of mesylate **20** (3.60 g, 9.82 mmol, 1 eq) in DMF (50 mL) was added sodium azide (2.78 g, 42.80 mmol, 4.4 eq). The reaction mixture was heated to 90 °C for 18 hours and was then concentrated *in vacuo* to remove the majority of DMF. The crude was dissolved in CH_2Cl_2 (50 mL) and washed with saturated aqueous $NaHCO_3$ (3x 50 mL). The organic layer was dried (Na_2SO_4), concentrated *in vacuo* and purified by flash column chromatography (10% EtOAc in hexane) to afford azide **6** (2.76 g, 8.80 mmol, 90%) as a transparent oil.

^{1}H NMR (400 MHz, $CDCl_3$) δ 4.23 (dd, *J* = 11.6, 4.7 Hz, 2H, C<u>H</u>$_a$H$_b$-2;C<u>H</u>$_a$H$_b$-2'), 4.14 (dd, *J* = 11.6, 6.8 Hz, 2H, CH$_a$<u>H</u>$_b$-2;CH$_a$<u>H</u>$_b$-2'), 3.88 (tt, *J* = 6.8, 4.6 Hz, 1H, C<u>H</u>-1), 2.35 (t, *J* = 7.6 Hz, 4H, C<u>H</u>$_2$-4;C<u>H</u>$_2$-4'), 1.68 – 1.59 (m, 4H, C<u>H</u>$_2$-5;C<u>H</u>$_2$-5'), 1.41 – 1.23 (m, 8H, C<u>H</u>$_2$-6;C<u>H</u>$_2$-6';C<u>H</u>$_2$-7;C<u>H</u>$_2$-7'), 0.95 – 0.86 (m, 6H, C<u>H</u>$_3$-8;C<u>H</u>$_3$-8').

^{13}C NMR (101 MHz, $CDCl_3$) δ 173.4 (2C), 63.1 (2C), 58.8, 34.1 (2C), 31.4 (2C), 24.6 (2C), 22.4 (2C), 14.0 (2C).

HRMS (ESI) *m/z* calcd for $C_{15}H_{27}O_4N_3Na$ [M+Na]$^+$: 336.1894, found: 336.1893.

IR (ATR) ν (cm^{-1}) thin film, CH_2Cl_2: 2957 (w), 2932 (w), 2872 (w), 2118 (w), 1741 (s), 1460 (w), 1242 (m), 1159 (s), 1099 (m), 734 (w).

2-(1-(1,3-bis(hexanoyloxy)propan-2-yl)-1*H*-1,2,3-triazol-4-yl)ethyl (2-(trimethylammonio)ethyl) phosphate (7)

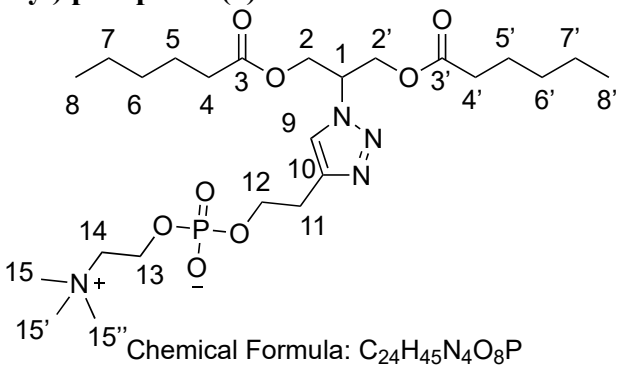

To a solution of alkyne **2** (200 mg, 0.85 mmol, 1 eq), $CuSO_4 \cdot 5H_2O$ (2.5 mg, 0.01 mmol, 0.01 eq) in Milli-Q H_2O (2.5 mL) and *t*-BuOH (2.5 mL) was added TBTA (5.2 mg, 0.01 mmol, 0.01 eq), azide **6** (300 µL, 1.00 mmol, 1.18 eq) were added and the flask was capped with a septum. The solution was degassed by bubbling argon through it for 30 minutes. Afterwards sodium ascorbate (6 mg, 0.03 mmol, 0.04 eq) was added to initiate the reaction. The reaction mixture was stirred at 1000 rpm under a continuous flow of argon. The crude mixture was concentrated *in vacuo* and purified by flash column chromatography (2% H_2O and 48% MeOH in CH_2Cl_2). The obtained compound was dissolved in a minimum of MeOH and filtered through a PTFE syringe filter to remove any silica particles and concentrated *in vacuo* to yield surfactant **7** (342 mg, 0.62 mmol, 73%) as a transparent viscous oil.

^{1}H NMR (400 MHz, CD_3OD) δ 8.02 (s, 1H, C<u>H</u>-9), 5.16 (p, *J* = 6.1 Hz, 1H, C<u>H</u>-1), 4.62 – 4.51 (m, 4H, C<u>H</u>$_2$-2;C<u>H</u>$_2$-2'), 4.22 (dt, *J* = 7.1, 3.6 Hz, 2H, C<u>H</u>$_2$-13), 4.14 (q, *J* = 6.5 Hz, 2H, C<u>H</u>$_2$-12), 3.66 – 3.59 (m, 2H, C<u>H</u>$_2$-14), 3.22 (s, 9H, C<u>H</u>$_3$-15;C<u>H</u>$_3$-15';C<u>H</u>$_3$-15''), 3.05 (t, *J* = 6.4 Hz, 2H, C<u>H</u>$_2$-11), 2.30 (t, *J* = 7.4 Hz, 4H, C<u>H</u>$_2$-4;C<u>H</u>$_2$-4'), 1.55 (p, *J* = 7.4 Hz, 4H, C<u>H</u>$_2$-5;C<u>H</u>$_2$-5'), 1.38 – 1.19 (m, 8H, C<u>H</u>$_2$-6;C<u>H</u>$_2$-6';C<u>H</u>$_2$-7;C<u>H</u>$_2$-7'), 0.90 (t, *J* = 7.1 Hz, 6H, C<u>H</u>$_3$-8;C<u>H</u>$_3$-8').

^{13}C NMR (101 MHz, CD_3OD) δ 174.5 (2C), 145.9, 124.0, 67.8 – 67.4 (m, J_{CN^+} and J_{CP}), 65.5 (d, J_{CP} = 5.3 Hz), 63.5 (2C), 60.4 – 60.3 (m, J_{CN^+}, 2C), 54.9 – 54.6 (m, J_{CN^+}, 3C), 34.6 (2C), 32.3 (2C), 28.3 (d, J_{CP} = 8.0 Hz), 25.6 (2C), 23.3 (2C), 14.2 (2C).

^{31}P NMR (162 MHz, CD_3OD) δ -0.56.

HRMS (ESI) *m/z* calcd for $C_{24}H_{46}O_8N_4P$ $[M+H]^+$: 549.3048, found: 549.3047.

IR (ATR) ν (cm^{-1}) thin film, MeOH: 3378 (broad w), 2958 (w), 2872 (w), 1742 (s), 1468 (w) 1230 (s), 1165 (m), 1086 (s), 970 (w), 786 (w).

2-(1-(1-(Hexanoyloxy)-3-hydroxypropan-2-yl)-1*H*-1,2,3-triazol-4-yl)ethyl (2-(trimethylammonio)ethyl) phosphate (8)

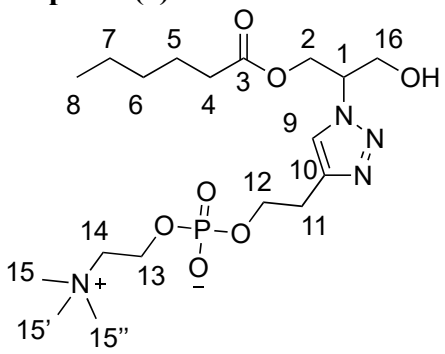

Chemical Formula: $C_{18}H_{35}N_4O_7P$
Molecular Weight: 450.4728

Compound **8** was recovered for characterization from experiments as described in the representative procedure for setup of hydrolysis experiments. The crude reaction mixture of multiple experiments were combined, concentrated *in vacuo* and purified by flash column chromatography (5% H_2O and 45% MeOH in CH_2Cl_2). The obtained compound was dissolved in a minimum of MeOH and filtered through a PTFE syringe filter to remove any silica particles and concentrated *in vacuo* to yield compound **4** as a transparent viscous oil.

^{1}H NMR (400 MHz, CD_3OD) δ 7.99 (s, 1H, C<u>H</u>-9), 4.95 – 4.89 (m, 1H, C<u>H</u>-1), 4.59 – 4.48 (m, 2H, C<u>H</u>$_2$-2), 4.13 (q, J = 6.4 Hz, 4H, C<u>H</u>$_2$-6;C<u>H</u>$_2$-7), 4.04 – 3.92 (m, 2H, C<u>H</u>$_2$-16), 3.62 – 3.53 (m, 2H, C<u>H</u>$_2$-14), 3.24 – 3.22 (m, 1H, CHO<u>H</u>-16), 3.20 (s, 9H, C<u>H</u>$_3$-15;C<u>H</u>$_3$-15';C<u>H</u>$_3$-15''), 3.05 (t, J = 6.3 Hz, 2H, C<u>H</u>$_2$-11), 2.28 (t, J = 7.4 Hz, 2H, C<u>H</u>$_2$-4), 1.53 (p, J = 7.4 Hz, 2H, C<u>H</u>$_2$-5), 1.37 – 1.16 (m, 4H, C<u>H</u>$_2$-6;C<u>H</u>$_2$-7), 0.89 (t, J = 7.1 Hz, 3H, C<u>H</u>$_3$-8).

^{13}C NMR (101 MHz, CD_3OD) δ 174.7, 124.0, 73.9, 67.8 – 67.2 (m, J_{CN}^+ and J_{CP}), 65.5 (d, J_{CP} = 5.6 Hz), 64.4, 63.9, 63.5, 62.2, 60.3 (d, J_{CN}^+ = 5.0 Hz), 54.8 – 54.7 (m, J_{CN}^+, 3C), 34.7, 32.3, 28.2 (d, J_{CP} = 7.6 Hz), 25.6, 23.3, 14.2.

^{31}P NMR (162 MHz, CD_3OD) δ -0.43.

HRMS (ESI) *m/z* calcd for $C_{18}H_{36}O_7N_4P$ $[M+H]^+$: 451.2316, found: 451.2315.

IR (ATR) ν (cm^{-1}) thin film, MeOH: 3345 (broad w), 2958 (w), 1736 (w), 1477 (w) 1225 (s), 1082 (broad s), 970 (w), 790 (w).

(2*R*,4*R*)-1-(*tert*-butoxycarbonyl)-4-(prop-2-yn-1-yloxy)pyrrolidine-2-carboxylic acid (21)

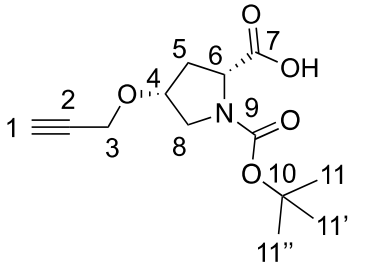

Chemical Formula: $C_{13}H_{19}NO_5$
Molecular Weight: 269.30

Synthesized according to adapted procedure from van Oers *et al*.[6] N-Boc-cis-4-hydroxy-D-proline (2.00 g, 4.32 mmol, 1.0 eq) was dissolved in anhydrous THF (20 mL) at RT. Sodium hydride (346 mg of a 60 wt. % dispersion in mineral oil, 8.65 mmol, 2.0 equiv) was added in small portions and the solution was stirred for 10 min. Next, an additional amount of THF (20 mL) was added, followed by the addition of propargyl bromide (963 μL of a 80 wt. % in toluene, 8.65 mmol, 2.0 equiv). The solution was stirred for 18 h. Afterwards, the solution was cooled to 0 °C, quenched with 5 mL water, and allowed to warm up to ambient temperature. The reaction was quenched by slow addition of H_2O (5 mL) and the mixture was acidified to pH 2 with 1 M HCl solution. The product was extracted with CH_2Cl_2 (3 × 25 mL), after which the resulting organic fractions were dried (Na_2SO_4), concentrated *in vacuo* and purified by flash column chromatography (1% AcOH and 39% EtOAc in hexane) yielded alkyne **21** (823 mg, 71%) as a white crystalline solid.

^{1}H NMR (400 MHz, CD_3OD, mixture of rotamers) δ 4.37 – 4.25 (m, 2H, C<u>H</u>-4;C<u>H</u>-6), 4.18 – 4.11 (m, 2H, C<u>H$_2$</u>-3), 3.64 (dd, *J* = 11.7, 5.5 Hz, 1H, C<u>H$_a$H$_b$</u>-8), 3.44 (ddd, *J* = 11.6, 3.0, 1.1 Hz, 1H, CH$_a$<u>H$_b$</u>-8), 2.83 (t, *J* = 2.4 Hz, 1H, C<u>H</u>-1), 2.41 (dddd, *J* = 29.7, 14.1, 9.2, 5.2 Hz, 1H, C<u>H$_a$H$_b$</u>-5), 2.32 – 2.18 (m, 1H, CH$_a$<u>H$_b$</u>-5), 1.47 (s, 3H, C<u>H$_3$</u>-11;C<u>H$_3$</u>-11';C<u>H$_3$</u>-11''), 1.43 (s, 6H, C<u>H$_3$</u>-11;C<u>H$_3$</u>-11';C<u>H$_3$</u>-11'').

^{13}C NMR (101 MHz, CD_3OD, mixture of rotamers) δ 175.7, 155.9, 81.6, 80.4, 77.7 (rotamer), 76.8, 76.0, 76.0 (rotamer), 59.0, 58.6 (rotamer), 57.0, 56.9 (rotamer), 53.1 (rotamer), 52.5, 36.7, 35.8 (rotamer), 28.7 (C3, rotamer), 28.5 (C3).

HRMS (ESI) *m/z* calcd for $C_{13}H_{19}O_5NNa$ $[M+Na]^+$: 292.1155, found: 292.1155.

IR (ATR) ν (cm^{-1}) thin film, $CHCl_3$: 3267 (w), 2978 (w), 1697 (broad s), 1407 (board strong), 1368 (m), 1164 (s), 1090 (s), 900 (w), 770 (w), 670 (w).

[α]$^{25}_D$ = +61.0 (c = 1.00, $CHCl_3$).
Consistent with reported literature values.[7]

(2*R*,4*R*)-4-(prop-2-yn-1-yloxy)pyrrolidine-2-carboxylic acid (9)

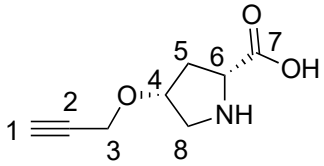

Chemical Formula: $C_8H_{11}NO_3$
Molecular Weight: 169.18

Synthesized according to adapted procedure from van Wang *et al*.[8] Alkyne **21** (500 mg, 1.86 mmol) was suspended in water and heated to reflux for 2 hours. The solution was concentrated *in vacuo* and the resultant solid was triturated with CH_2Cl_2 to yield deprotected alkyne **9** (284 mg, 1.68 mmol, 90%) as a crystalline white solid.

^{1}H NMR (400 MHz, CD_3OD) δ 4.53 – 4.44 (m, 1H, C<u>H</u>-4), 4.26 – 4.13 (m, 2H, C<u>H$_2$</u>-3), 4.05 (dd, *J* = 9.7, 4.6 Hz, 1H, C<u>H</u>-6), 3.58 (dt, *J* = 12.3, 1.7 Hz, 1H, C<u>H$_a$H$_b$</u>-8), 3.36 – 3.31 (m, 2H, CH$_a$<u>H$_b$</u>-8;N<u>H</u>), 2.91 (t, *J* = 2.4 Hz, 1H, C<u>H</u>-1), 2.48 (ddd, *J* = 12.3, 4.6, 2.3 Hz, 1H, C<u>H$_a$H$_b$</u>-5), 2.42 (ddd, *J* = 14.3, 9.8, 4.7 Hz, 1H, CH$_a$<u>H$_b$</u>-5).

^{13}C NMR (101 MHz, CD_3OD) δ 173.6, 79.9, 77.0, 76.5, 61.2, 56.7, 51.9, 35.2.

HRMS (ESI) *m/z* calcd for $C_8H_{12}O_3N$ $[M+H]^+$: 170.0812, found: 170.0812.

IR (ATR) ν (cm^{-1}) thin film, CH_3OH: 3260 (w), 3199 (w), 3099 (w), 2343 (broad w), 2111 (w), 1617 (s), 1395 (m), 1369 (m), 1307 (w), 1081 (s), 1060 (s), 1039 (m), 874 (m), 707 (w), 666 (w).

$[\alpha]^{25}_D$ = +26.2 (c = 1.00, CH_3OH).

(2*R*,4*R*)-4-((1-(1,3-bis(oleoyloxy)propan-2-yl)-1*H*-1,2,3-triazol-4-yl)methoxy)pyrrolidine-2-carboxylic acid (10)

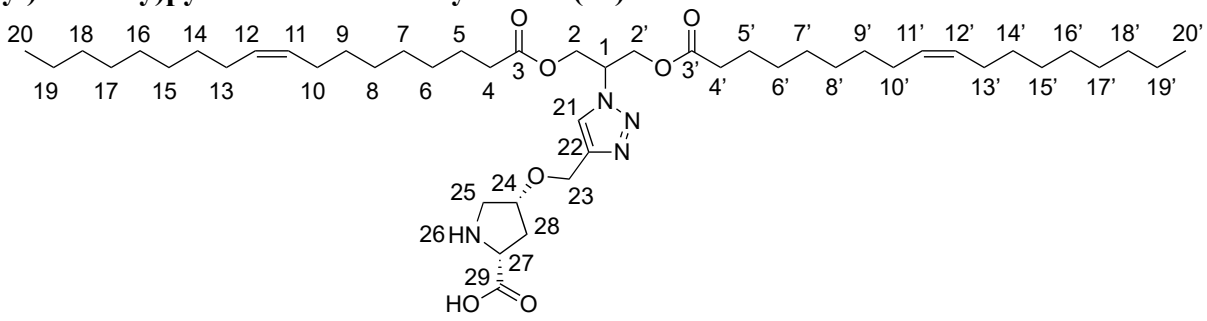

Chemical Formula: $C_{47}H_{82}N_4O_7$
Molecular Weight: 815.19

To a solution of alkyne **9** (30 mg, 0.177 mmol, 1 eq), $CuSO_4 \cdot 5H_2O$ (10 mg, 0.04 mmol, 0.23 eq) in Milli-Q H_2O (2.5 mL) and *t*-BuOH (2.5 mL) was added TBTA (21 mg, 0.04 mmol, 0.23 eq), azide **1** (130 μL, 0.203 mmol, 1.15 eq) were added and the flask was capped with a septum. The solution was degassed by bubbling argon through it for 30 minutes. Afterwards sodium ascorbate (24 mg, 0.123 mmol, 0.69 eq) was added to initiate the reaction. The reaction mixture was stirred at 1000 rpm under a continuous flow of argon. The crude mixture was concentrated *in vacuo* and purified by flash column chromatography (1→30% MeOH in CH_2Cl_2) to yield organocatalyst **10** (136 mg, 0.167 mmol, 94%) as a transparent viscous oil.

^{1}H NMR (400 MHz, CD_3OD) δ 8.11 (s, 1H, C<u>H</u>-21), 5.41 – 5.28 (m, 4H, C<u>H</u>-11;C<u>H</u>-11';C<u>H</u>-12;C<u>H</u>-12'), 5.18 (p, *J* = 6.0 Hz, 1H, C<u>H</u>-1), 4.65 – 4.59 (m, 2H, C<u>H</u>$_2$-23), 4.57 (d, *J* = 5.8 Hz, 4H, C<u>H</u>$_2$-2;C<u>H</u>$_2$-2'), 4.36 – 4.28 (m, 1H, C<u>H</u>-24), 4.09 – 4.00 (m, 1H, C<u>H</u>-27), 3.57 (d, *J* = 12.2 Hz, 1H, C<u>H</u>$_a$H$_b$-25), 3.27 (dd, *J* = 12.9, 4.6 Hz, 1H, CH$_a$<u>H</u>$_b$-25), 2.55 (d, *J* = 14.1 Hz, 1H, C<u>H</u>$_a$H$_b$-28), 2.42 – 2.34 (m, 1H, CH$_a$<u>H</u>$_b$-28), 2.30 (t, *J* = 7.4 Hz, 4H, C<u>H</u>$_2$-4;C<u>H</u>$_2$-4'), 2.03 (q, *J* = 6.4 Hz, 8H, C<u>H</u>$_2$-10;C<u>H</u>$_2$-10';C<u>H</u>$_2$-13;C<u>H</u>$_2$-13'), 1.55 (p, *J* = 7.4 Hz, 4H, C<u>H</u>$_2$-5;C<u>H</u>$_2$-5'), 1.43 – 1.22 (m, 40H, (C<u>H</u>$_2$)$_4$-6-9;(C<u>H</u>$_2$)$_4$-6'-9';(C<u>H</u>$_2$)$_6$-14-19;(C<u>H</u>$_2$)$_6$-14'-19'), 0.93 – 0.86 (m, 6H, C<u>H</u>$_3$-20;C<u>H</u>$_3$-20').

^{13}C NMR (126 MHz, CD_3OD) δ 174.4 (2C), 145.8, 130.9 (2C), 130.8 (2C), 124.9, 77.9, 63.4, 63.4, 62.8, 61.1, 60.5, 52.0, 35.4, 34.7 (2C), 33.1 (2C), 30.9 (2C), 30.8 (2C), 30.6 (2C), 30.5 (2C), 30.4 (2C), 30.3 (2C), 30.2 (2C), 30.1 (2C), 28.1 (4C), 25.9 (2C), 23.8 (2C), 14.5 (2C).

HRMS (ESI) *m/z* calcd for $C_{47}H_{83}O_7N_4$ $[M+H]^+$: 815.6256, found: 815.6254.

IR (ATR) ν (cm^{-1}) thin film, $CHCl_3$: 2924 (s), 2854 (m), 2361 (w), 1745 (s), 1604 (board m), 1457 (m), 1378 (m), 1162 (m), 1162 (m), 1084 (m), 775 (w), 695 (w).

$[\alpha]^{25}_D$ = −1.0 (c = 1.00, $CHCl_3$).

(*R*)-2-((*S*)-Hydroxy(4-nitrophenyl)methyl)cyclohexan-1-one (13)

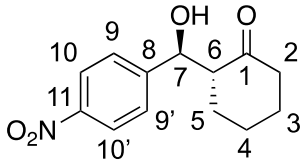

Chemical Formula: $C_{13}H_{15}NO_4$
Molecular Weight: 249.27

Enantioenriched variant of **13** was prepared according to the general procedure reported above.

The racemate of **13** was synthesised in the following manner: A solution of 4-nitrobenzaldehyde (150 mg, 0.99 mmol, 1 eq) and pyrrolidine (8 µL, 0.096 mmol, 0.1 eq) in cyclohexanone (520 µL, 5.02 mmol, 5 eq) was stirred overnight. The crude reaction mixture was purified by flash column chromatography (30% EtOAc in hexane) to yield racemic *anti* aldol product **13** (85 mg, 0.341 mmol, 34%) as an off-white solid.

^{1}H NMR (400 MHz, $CDCl_3$) δ 8.22 – 8.11 (m, 2H, C<u>H</u>-10; C<u>H</u>-10'), 7.53 – 7.44 (m, 2H, C<u>H</u>-9; C<u>H</u>-9'), 4.88 (dd, *J* = 8.3, 2.8 Hz, 1H, C<u>H</u>-7), 4.08 (d, *J* = 3.2 Hz, 1H, CHO<u>H</u>-7), 2.58 (dddd, *J* = 12.8, 8.3, 5.5, 1.2 Hz, 1H, C<u>H</u>-6), 2.50 – 2.43 (m, 1H, C<u>H$_a$</u>H$_b$-2), 2.35 (tdd, *J* = 13.6, 6.1, 1.2 Hz, 1H, CH$_a$<u>H$_b$</u>-2), 2.09 (ddt, *J* = 12.0, 5.8, 3.0 Hz, 1H, C<u>H$_a$</u>H$_b$-3), 1.85 – 1.77 (m, 1H, C<u>H$_a$</u>H$_b$-4), 1.72 – 1.51 (m, 3H, CH$_a$<u>H$_b$</u>-3;CH$_a$<u>H$_b$</u>-4;C<u>H$_a$</u>H$_b$-5), 1.42 – 1.29 (m, 1H, CH$_a$<u>H$_b$</u>-5).

^{13}C NMR (101 MHz, $CDCl_3$) δ 214.7, 148.6, 147.6, 128.0 (2C), 123.6 (2C), 74.0, 57.3, 42.7, 30.8, 27.7, 24.7.

HRMS (ESI) *m/z* calcd for $C_{13}H_{14}O_4N$ $[M-H]^-$: 248.0928, found: 248.0926.

[α]$^{25}_D$ = – 6.7 (c = 0.60, $CHCl_3$). Negative optical rotation is in agreement with the (2*R*,1'*S*) absolute stereochemistry.[9]

Enantiomeric excess was determined by SFC with a Chiralpak® IE column (3 µm, 150×3 mm). Conditions: Flow rate: 1.5 ml/min. Gradient: CO_2:MeOH with a gradient of 99:1 to 60:40 in 0 to 5 min; gradient of 60:40 to 40:60 in 5 to 5.5 min; 40:60 isocratically from 5.5 to 7 min; 100:0 isocratically from 7 to 8 min. λ_{det} = 266.8 nm. Retention time: $t_{(2S,1'R)}$ = 5.16 min (minor), $t_{(2R,1'S)}$ = 5.36 min (major).

Consistent with reported literature values.[10]

Benzyl azide (22)

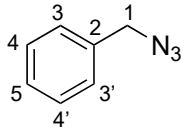

Chemical Formula: $C_7H_7N_3$
Molecular Weight: 133.15

Synthesised according to Healy *et al*.[11] Benzyl bromide (6.95 mL, 58.5 mmol, 1 eq) was added dropwise to a solution of sodium azide (7.6 g, 117 mmol, 2 eq) in (3:1 acetone/water, 100 mL) and the resulting mixture was stirred at room temperature for 1 h. The reaction was diluted with water (200 mL) and extracted with ethyl acetate (3 x 300 mL). The combined layers were washed with brine (2 x 200 mL), dried ($MgSO_4$) and concentrated *in vacuo* to give benzyl azide

22 as a crude colourless oil (7.32 g, 55.0 mmol, 94%). Due to instability **22** was immediately used in the next step.

^{1}H NMR (400 MHz, $CDCl_3$) δ 7.44 – 7.29 (m, 5H, C<u>H</u>-3;C<u>H</u>-3';C<u>H</u>-4;C<u>H</u>-4';C<u>H</u>-5), 4.35 (s, 2H, C<u>H</u>$_2$-1).

^{13}C NMR (101 MHz, $CDCl_3$) δ 128.9 (2C), 128.3, 128.2 (2C), 54.8.
Consistent with reported literature values.[11]

Tris(benzyltriazolylmethyl)amine (TBTA) (23)

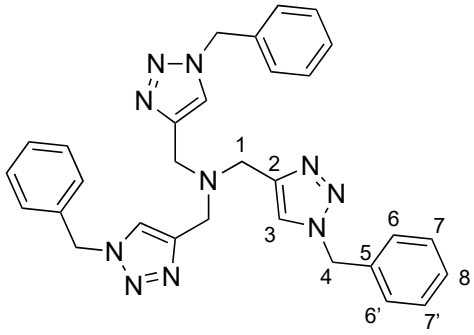

Chemical Formula: $C_{30}H_{30}N_{10}$
Molecular Weight: 530.64

Synthesised according to Zhu *et al*.[12] Benzyl azide **22** (6.87 mL, d = 1.066 g/mL, 55 mmol, 4 eq) was dissolved in *tert*-butyl alcohol (100 mL) in a 250 mL round-bottom flask equipped with a magnetic stir bar. Tripropargylamine (2.444 mL, d = 0.927 g/mL, 17.2 mmol, 1 eq) was subsequently added, and the flask was placed in a water bath at rt. $Cu(OAc)_2 \cdot H_2O$ (212 mg, 1 mmol, 0.06 eq) was added in the solid form, and the reaction flask was left uncovered while being stirred for 5 min. The flask was then closed with a rubber septum equipped with an argon balloon. The reaction mixture was allowed to stir overnight, during which time a precipitate formed. The precipitate was purified by flash column chromatography (1-3% MeOH in CH_2Cl_2) to afford a pink solid. This was then dissolved in a minimum of hot MeCN and crystallization was induced through addition of Et_2O. The crystals were collected by filtration to provide TBTA **23** (7.78 g, 14.7 mmol, 85%) as a white crystalline solid.

^{1}H NMR (400 MHz, $CDCl_3$) δ 7.65 (s, 3H, 3 × C<u>H</u>-3), 7.38 – 7.30 (m, 9H, 3 × C<u>H</u>-6;C<u>H</u>-6';C<u>H</u>-8), 7.29 – 7.22 (m, 6H, 3 × C<u>H</u>-7;C<u>H</u>-7'), 5.50 (s, 6H, 3 × C<u>H</u>$_2$-4), 3.70 (s, 6H, 3 × C<u>H</u>$_2$-1).

^{13}C NMR (101 MHz, $CDCl_3$) δ 134.7 (3C), 129.1 (6C), 128.7 (3C), 128.0 (6C), 54.2 (3C).

HRMS (ESI) *m/z* calcd for $C_{30}H_{31}N_{10}$ $[M+H]^+$: 531.2728, found: 531.2725.
Consistent with reported literature values.[12]

Fluorimetry Data

The critical micelle concentrations of the surfactants was determined with a fluorimetric procedure reported by London *et al*.[13] The fluorescent molecule 1,6-diphenyl-1,3,5-hexatriene (DPH) emits a large increase in fluorescence when present in an apolar environment such as the micellar interior when a surfactant exceeds the critical aggregation concentration. This property was used to determine the unknown CAC of surfactant compounds. Fluorescence measurements were made with an Edinburgh Instruments Spectrofluorometer FS5 model. Instrument control and data processing were performed using Fluoracle software. The excitation wavelength was 358 nm and the emission wavelength was 430 nm. The excitation and emission slits were set at bandwidths of 1 nm. In all experiments, 1 cm path length quartz cuvettes were used. The protocol for CAC determination was as follows: 3 µL of 5 mM DPH dissolved in THF was added to various amounts of surfactant dissolved in a total volume of 3 ml of aqueous solution. The intercept of two trendlines, through the data points before and after the change in fluorescence, was taken as the CAC.

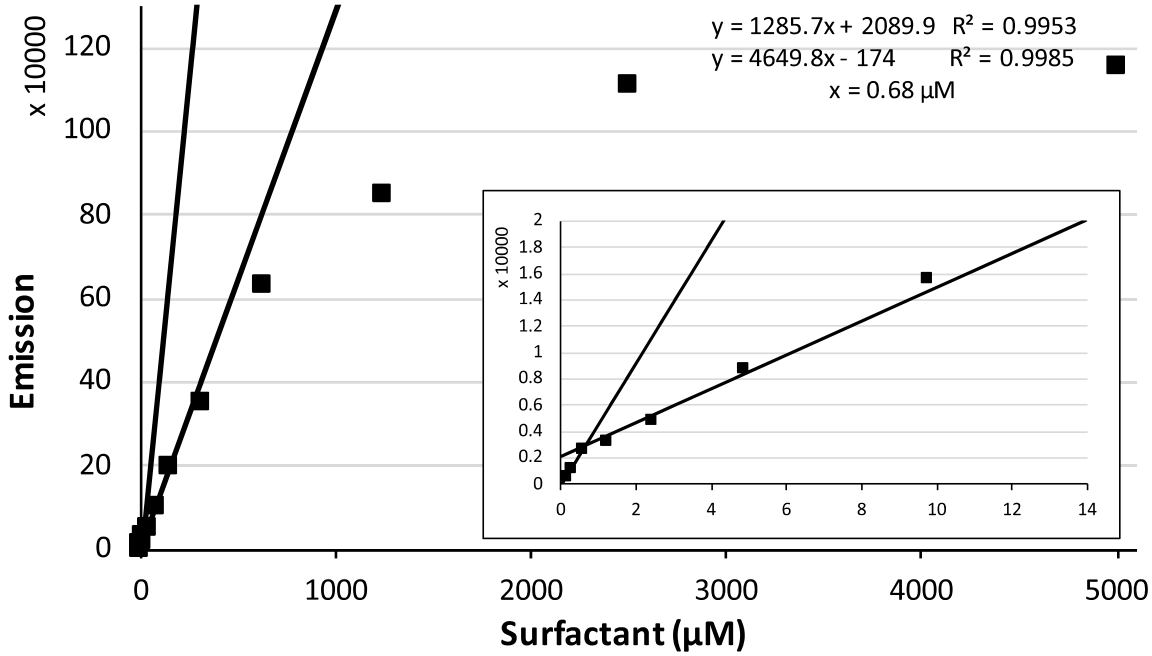

Figure S1: Determination of CAC by fluorimetry measurements. A CAC of 0.68 µM was extracted from a plot of fluorescence measurements at various concentration for surfactant **3**, related to Figure 2.

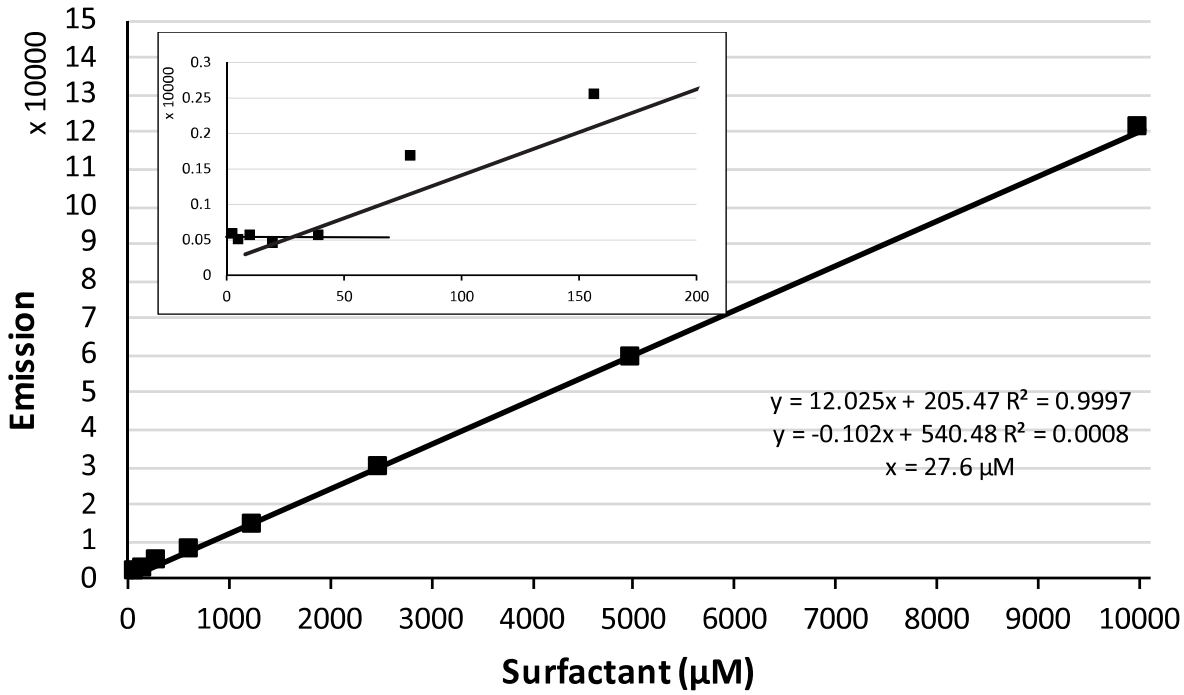

Figure S2: Determination of CMC by fluorimetry measurements. A CMC of 27.6 µM was extracted from a plot of fluorescence measurements at various concentration for surfactant **7**, related to Figure 4.

DLS Data

Samples were prepared by dissolving the surfactant in 1 mL of ultrapure Milli-Q water at the reported concentrations. In the case of reaction monitoring by DLS an aliquot was taken from the reaction mixture and this was directly measured by DLS. When the sample concentration is too low (i.e. t = 0 h), the scattering from the particles is weak and there is greater influence of noise from unwanted sources e.g. dust particles or oil droplets which gives biased results.

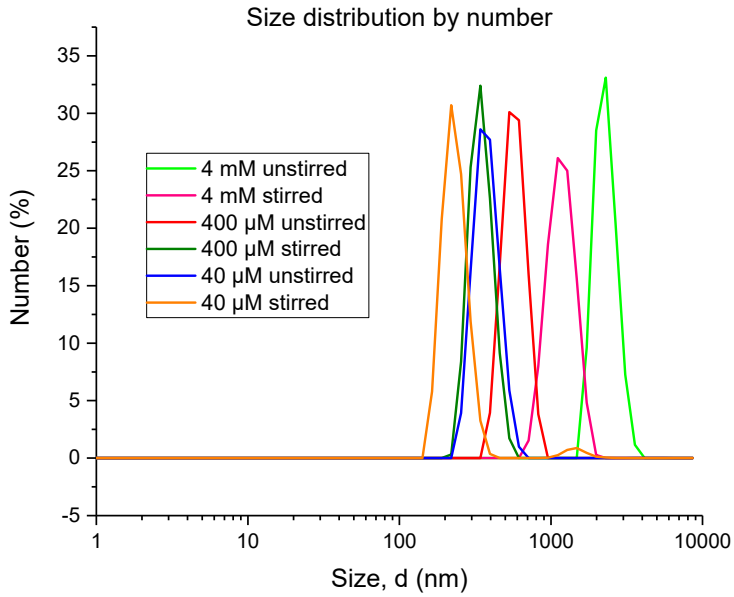

Figure S3: Determination of size and the effect of stirring on aggregates of 3. The size distribution by number of DLS measurements of surfactant **3** at 40 µM, 400 µM and 4 mM under stirred and unstirred conditions indicates a reduction in aggregate size at lower concentrations and when exposed to stirring conditions, related to Figure 2.

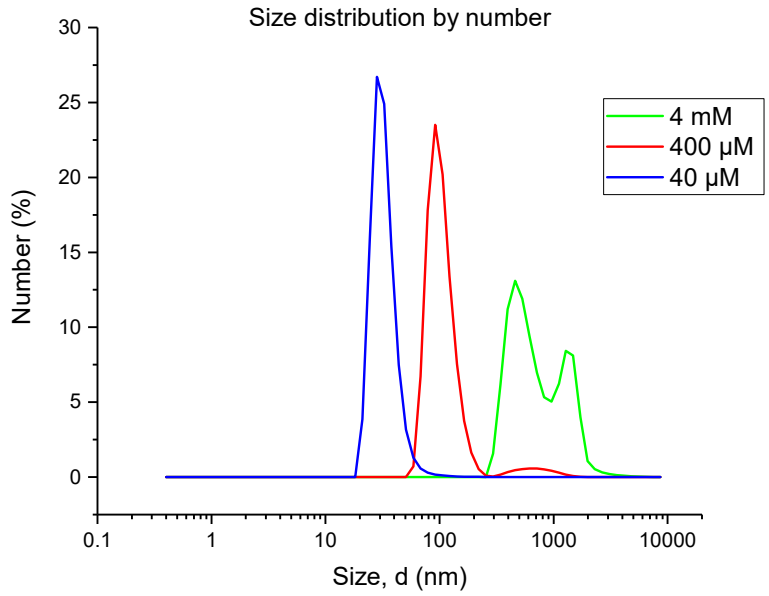

Figure S4: Determination of aggregate size of 3 by number after thin film hydration. The size distribution by number of DLS measurements of vesicles **3** at 40 µM, 400 µM and 4 mM formed through thin film hydration indicates aggregation into vesicles of smaller size than normal dissolution of **3**, related to Figure 2.

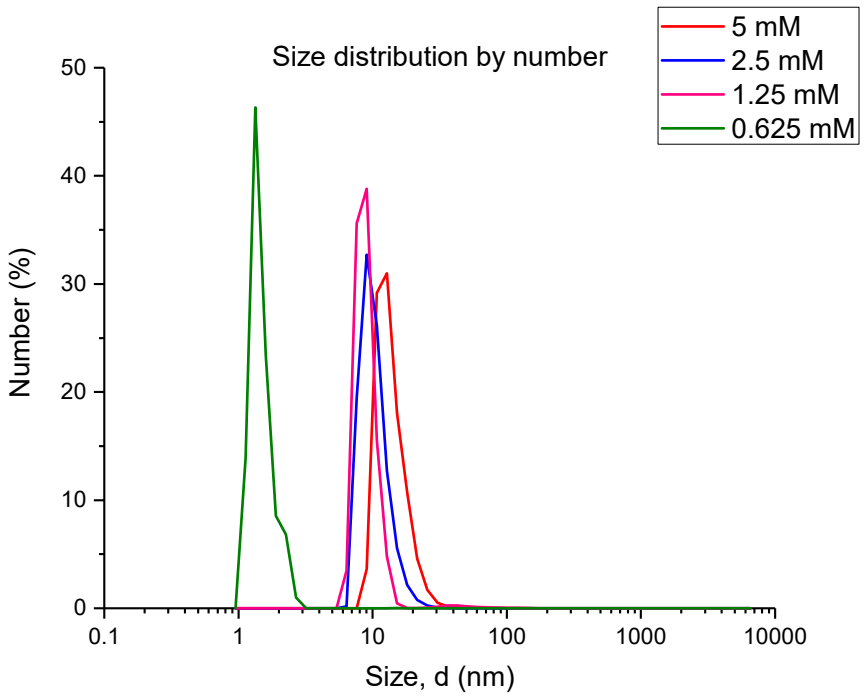

Figure S5: Determination of aggregate size of 7 by number. The size distribution by number of DLS measurements of surfactant **7** at 0.625 mM to 5 mM indicates aggregation into micelles with a consistent size around 10 nm independent of concentration, related to Figure 4.

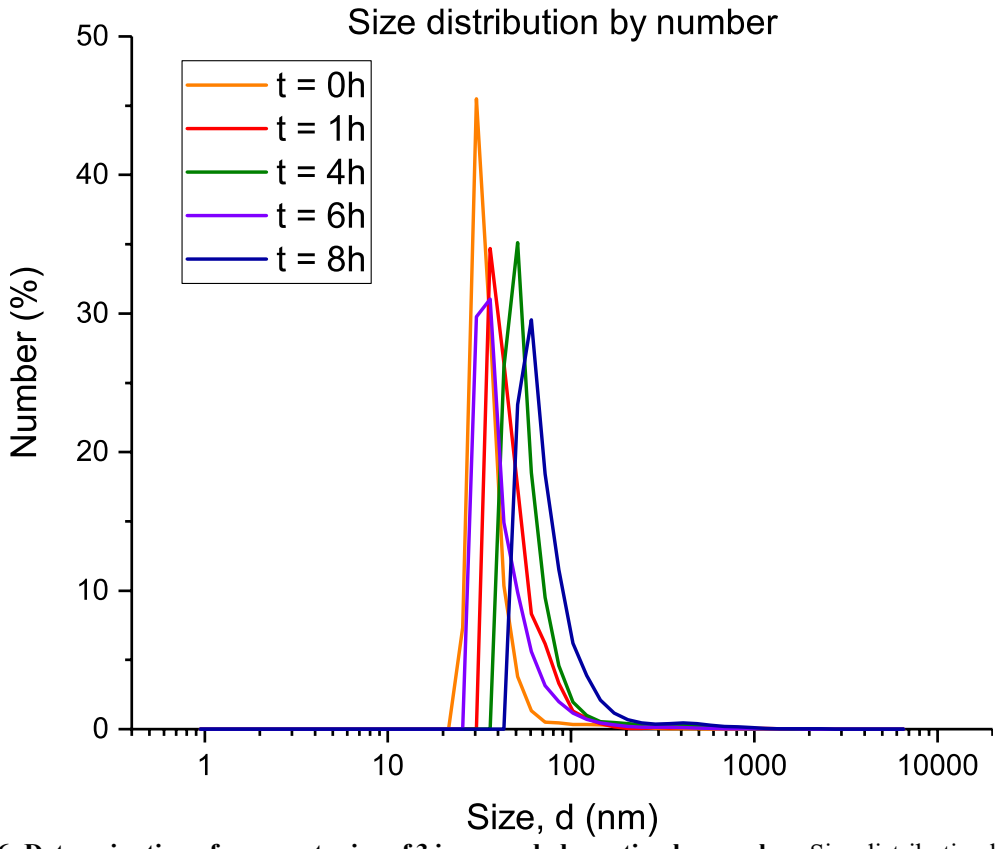

Figure S6: Determination of aggregate size of 3 in unseeded reaction by number. Size distribution by number of the aggregates in aliquots of the unseeded reaction (Fig. 2b, red squares) at different time points measured by DLS, related to Figure 2.

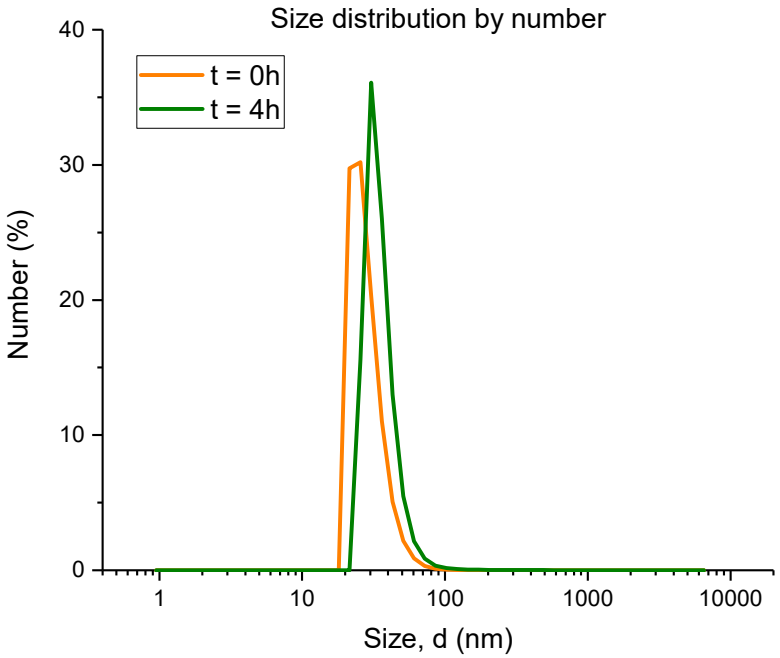

Figure S7: Determination of aggregate size of 3 in seeded reaction by number. Size distribution by number of the aggregates in aliquots of the seeded reaction (Fig. 2b, blue diamonds) at different time points measured by DLS, related to Figure 2.

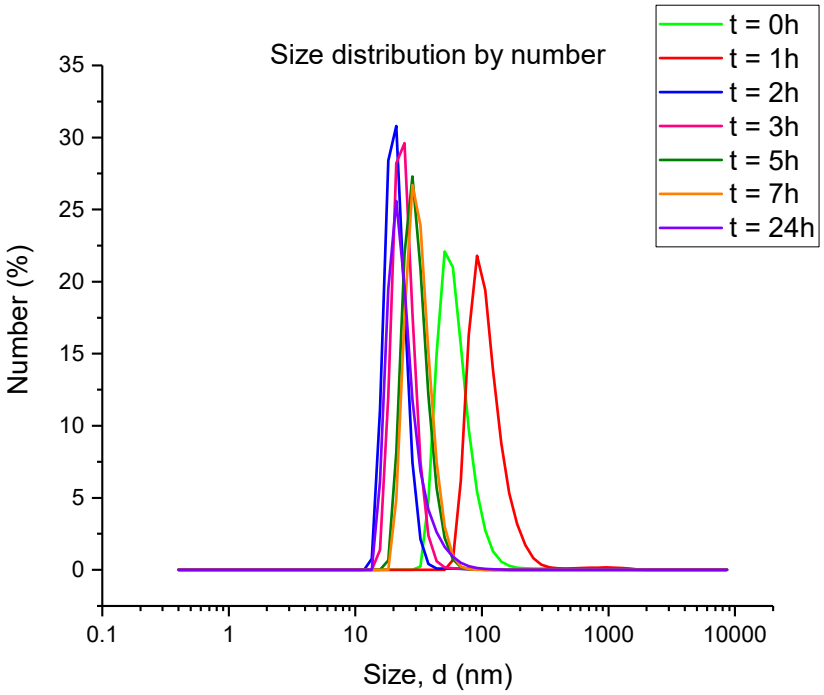

Figure S8: Determination of aggregate size of 3 in thin film seeded reaction by number. Size distribution by number of the aggregates in aliquots of the thin film seeded reaction (Fig. 2b, yellow triangles) at different time points measured by DLS.

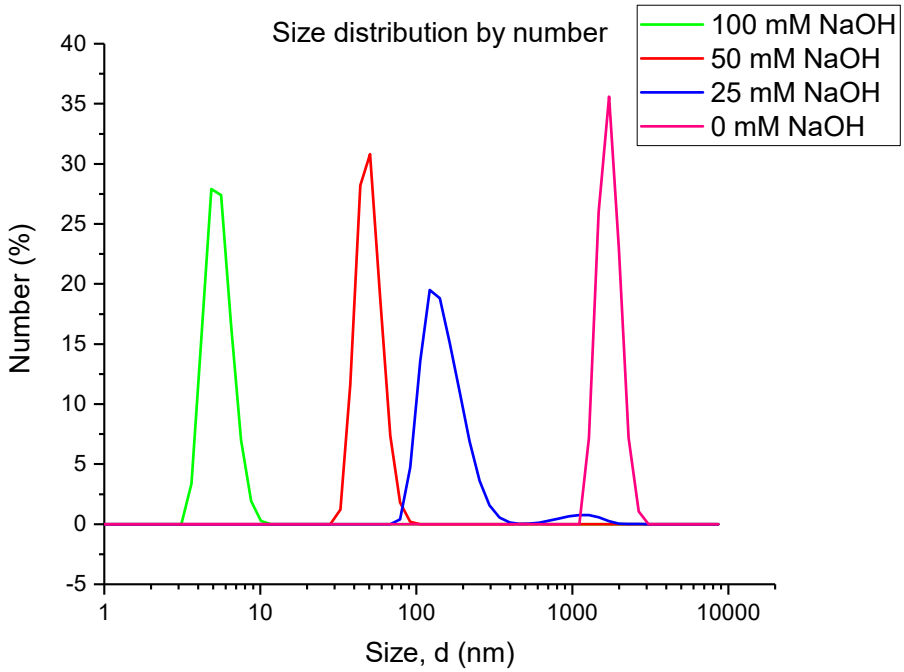

Figure S9: Determination of influence of NaOH concentration on aggregate size. Exposure of 4 mM of surfactant **3** to increasing concentrations of NaOH results in smaller aggregates due to higher degrees of hydrolysis: 25 mM NaOH yields 2.7 mM of **3** and 1.3 mM of **4**; 50 mM NaOH yields 1 mM of **3**, 2.3 mM of **4** and 0.7 mM of **5**; 100 mM NaOH yields 4 mM of **5**, related to Figure 3.

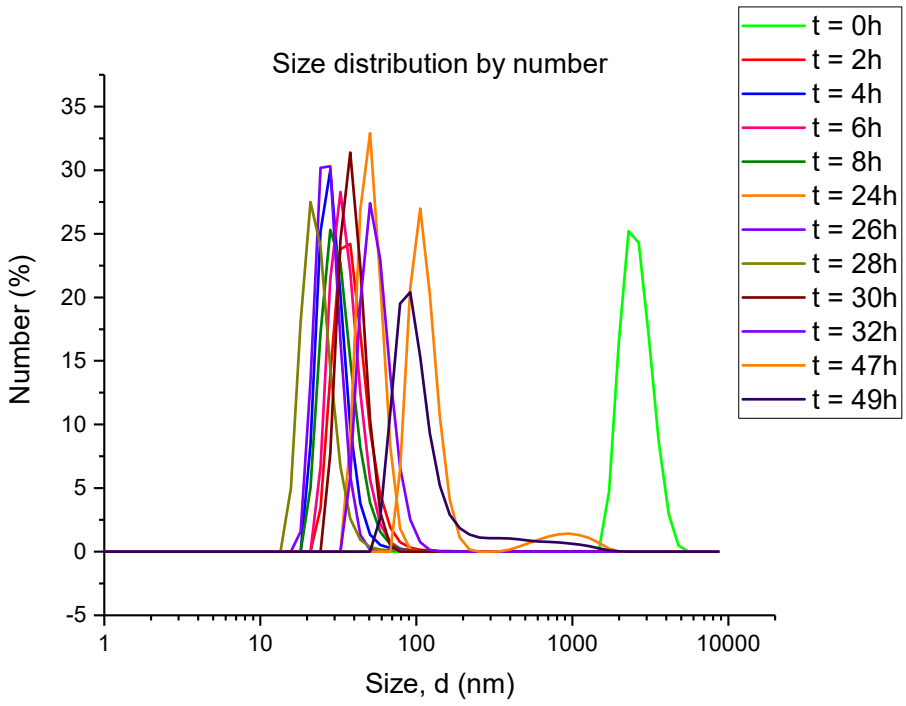

Figure S10: Determination of aggregate size under out-of-equilibrium conditions. Size distribution by number of the aggregates in aliquots of out-of-equilibrium reaction (Fig. 3c) at different time points measured by DLS.

Turbidity Measurements

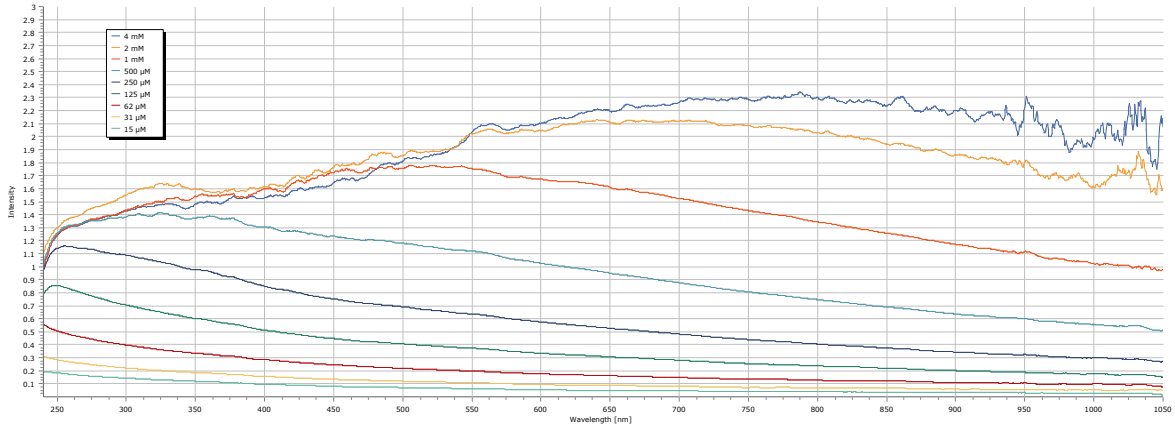

Figure S11: A wavelength independent increase in absorbance was observed with increasing concentration of **3** indicating an increase in turbidity of the solution, related to Figure 2.

TEM Data

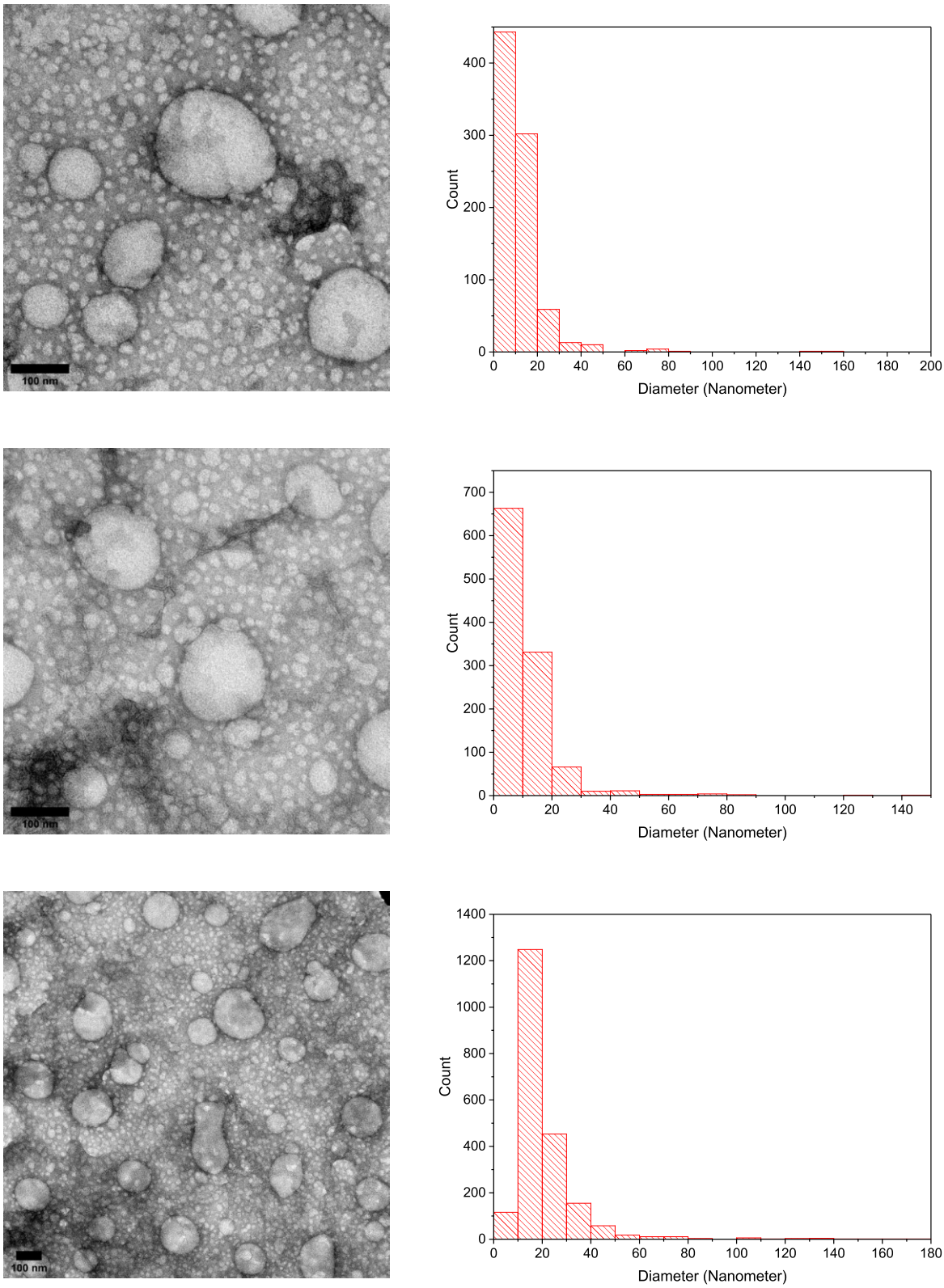

Figure S12: TEM micrographs of **3** (4 mM) deposited on a copper grid and stained with 2% uranyl acetate, related to Figure 2. Aggregates in the range 1-40 nm and some up to 40-180 nm are observed. Scale bar, 100 nm.

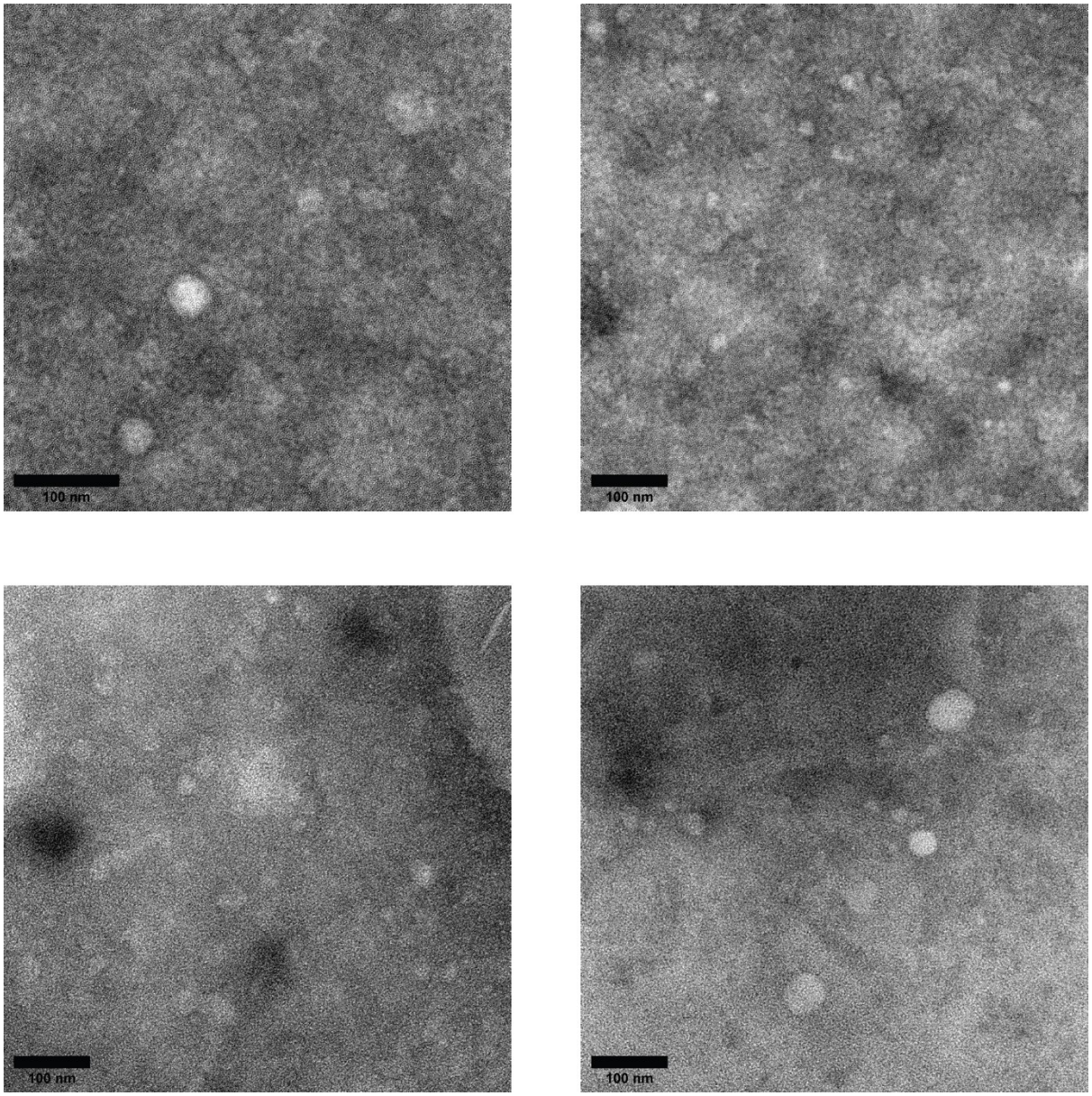

Figure S13: TEM micrographs of **7** (4 mM) deposited on a copper grid and stained with 2% uranyl acetate, related to Figure 4. Micelles largely in the 10-30 nm range are observed. Scale bar, 100 nm.

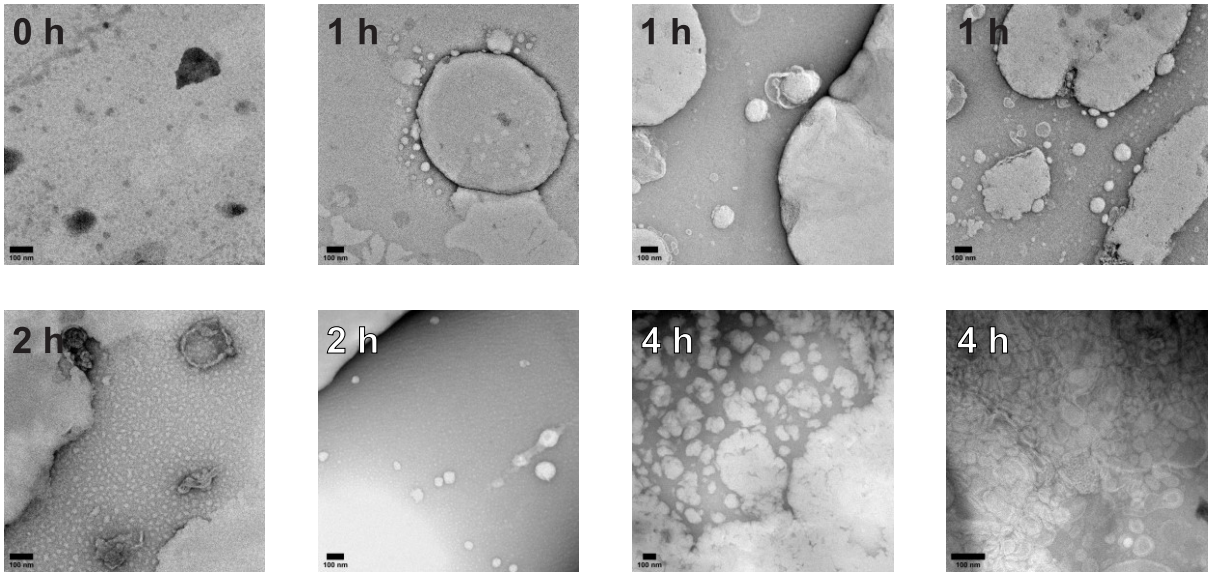

Figure S14: Additional TEM micrographs to Fig. 2c of aliquots of the unseeded reaction. Scale bar, 100 nm.

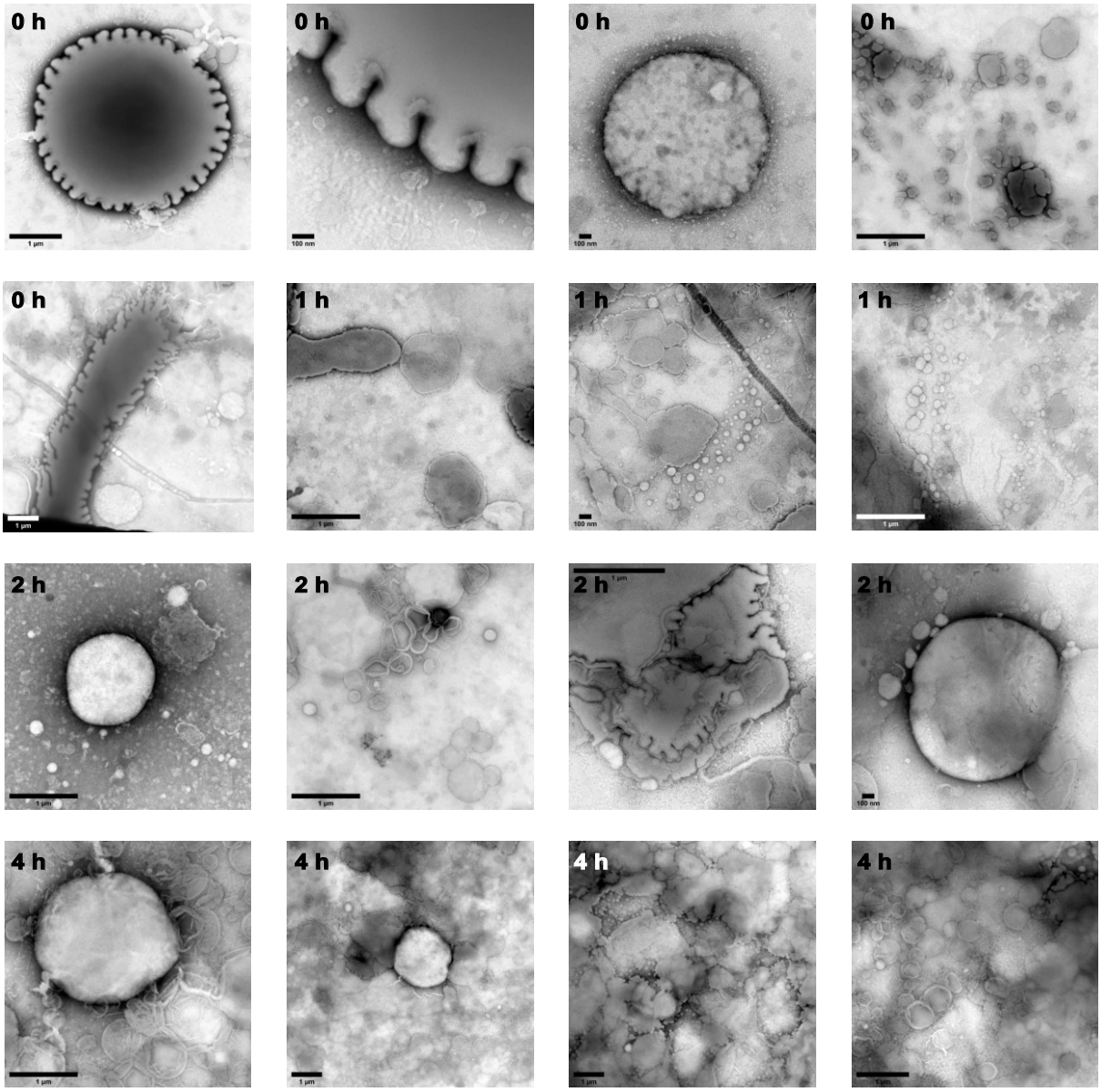

Figure S15: Additional TEM micrographs to Fig. 2d of aliquots of the seeded reaction. Scale bars, 1 µm and 100 nm.

Confocal Microscopy Data

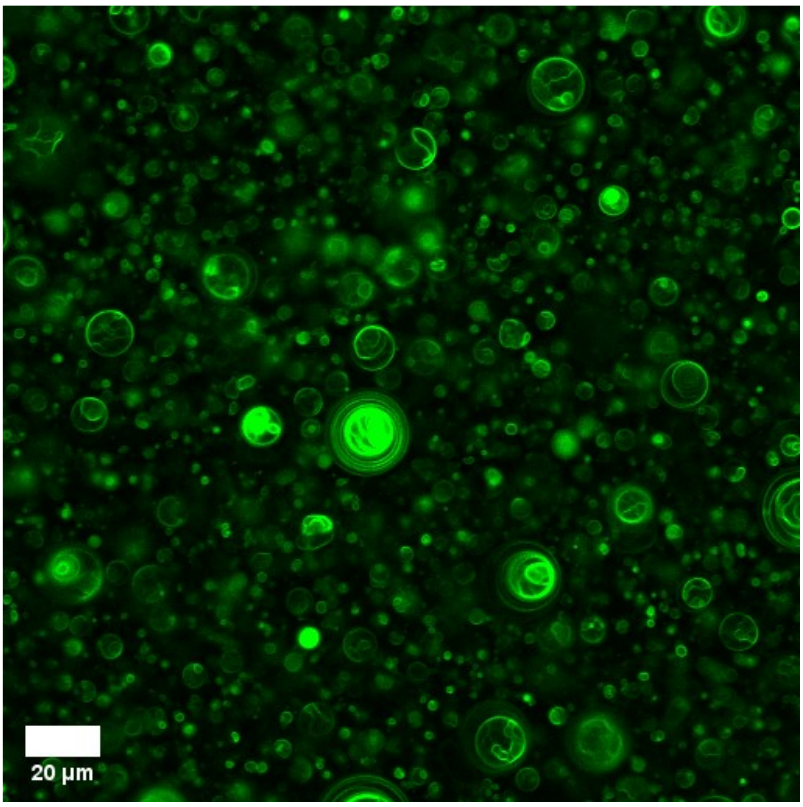

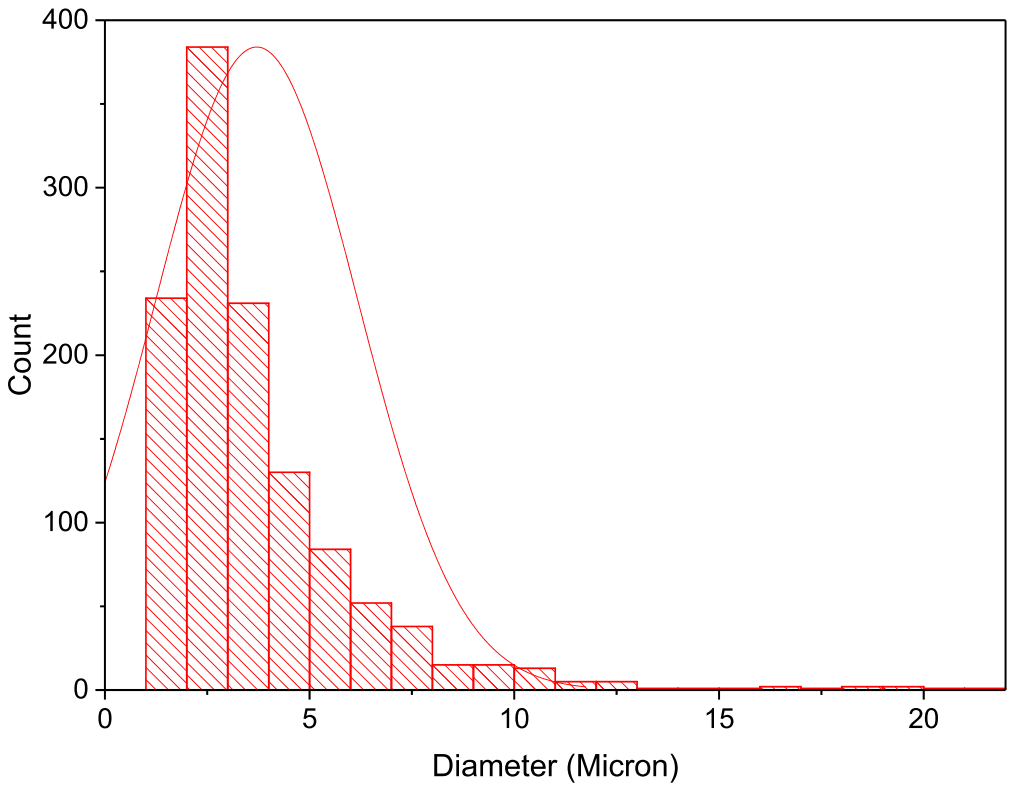

Figure S16: Confocal image of phospholipid vesicles of **3** (4 mM), related to Figure 2. A polydisperse range of multilaminar vesicles up to 20 µm is observed. Scale bar, 20 µm.

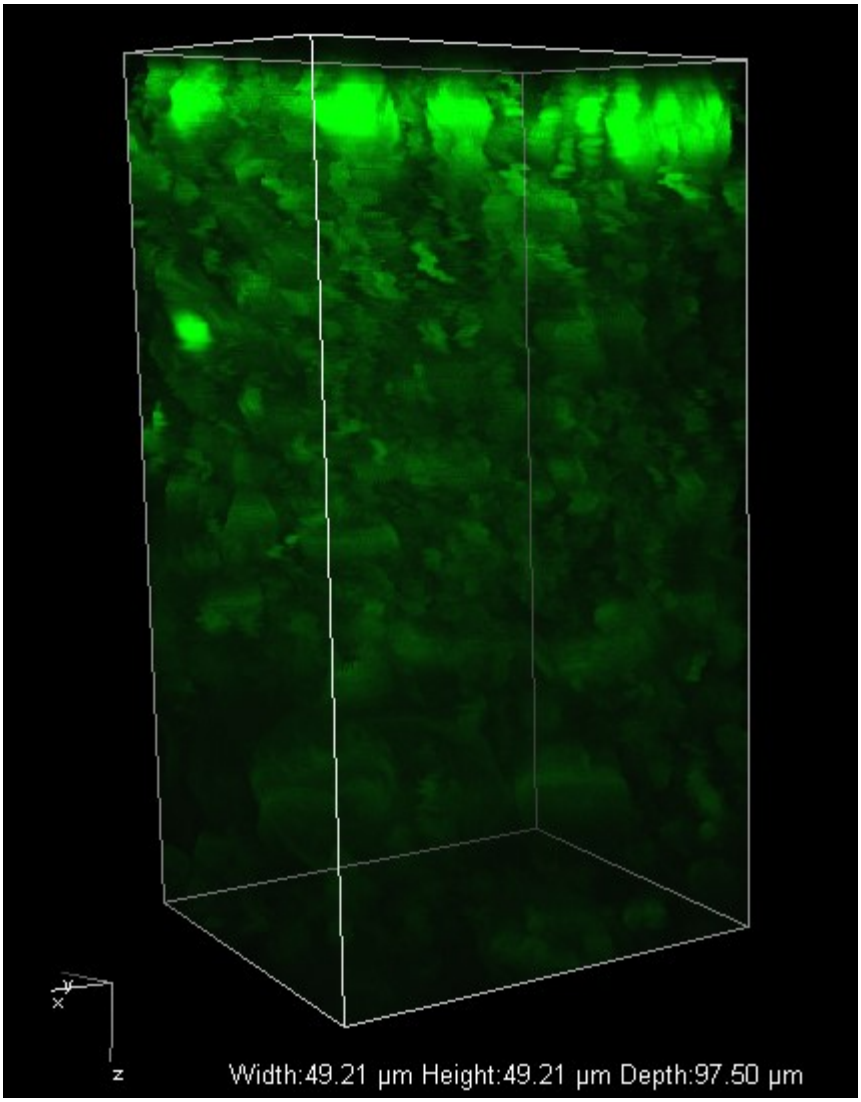

Figure S17: A Z-stack image of phospholipid vesicles of **3** (4 mM) after the sample has been left to sediment on to the coverslip overnight, related to Figure 2. A layer of about 100 µm that decreases in density as the distance to the coverslip increases is observed.

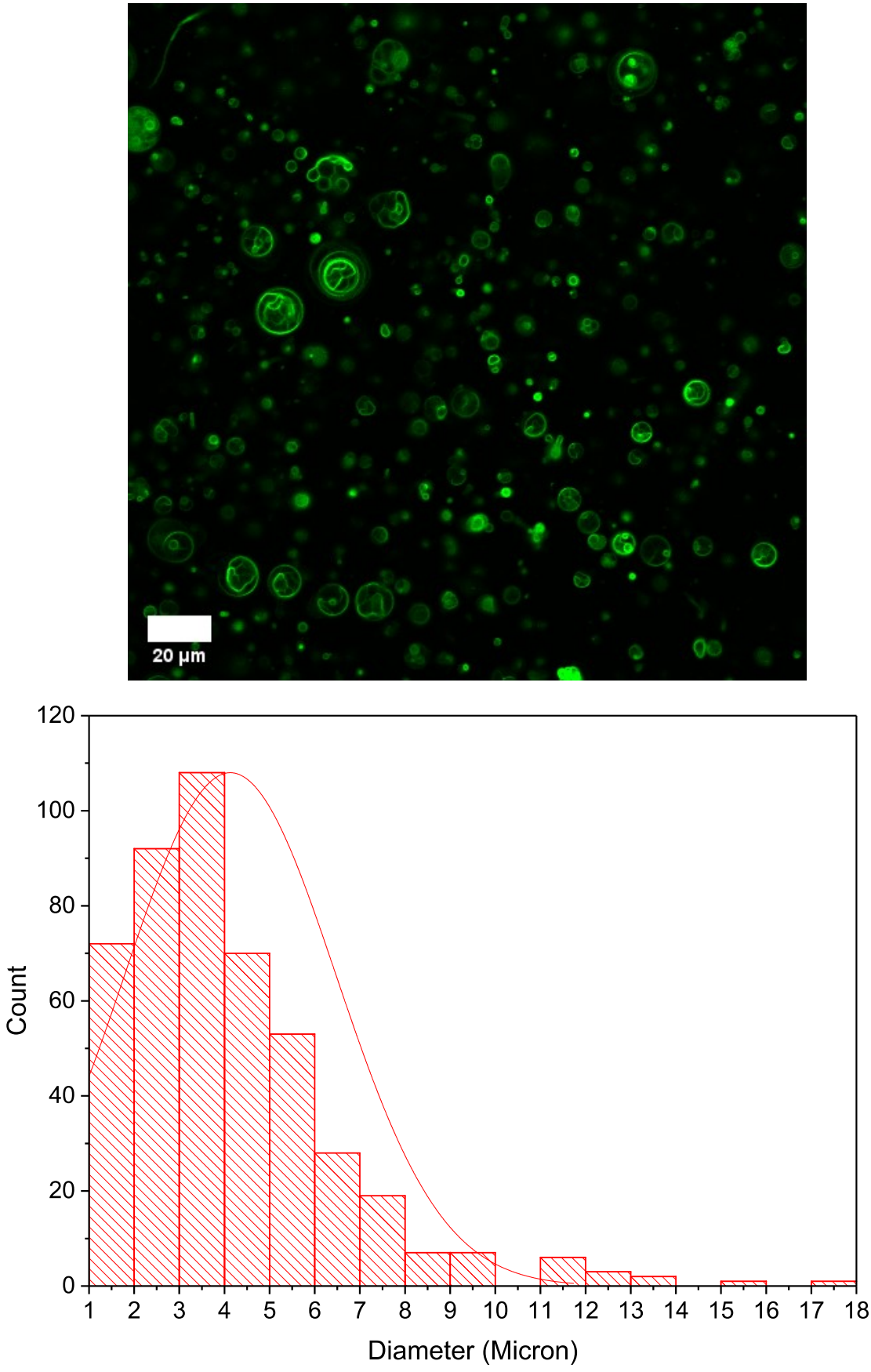

Figure S18: Confocal image of phospholipid vesicles of **3** (400 µM), related to Figure 2. A less dense and smaller range of multilaminar vesicles up to 18 µm is observed at this lower concentration. Scale bar, 50 µm.

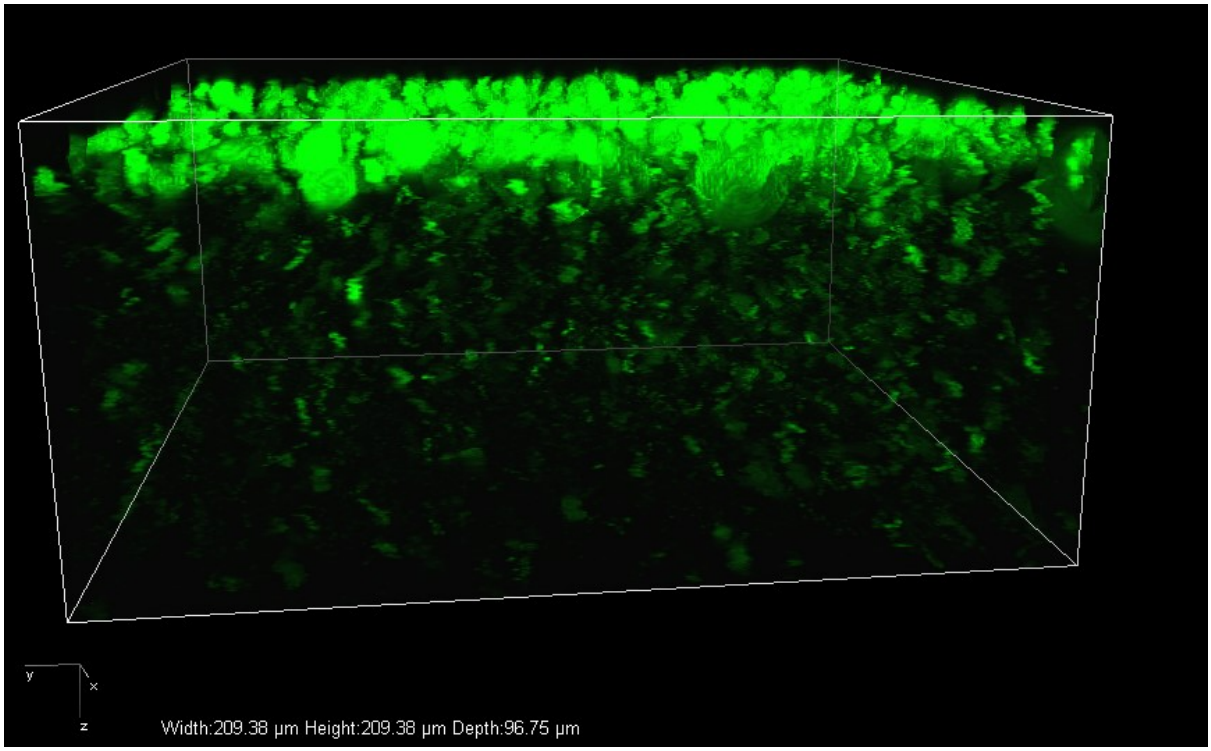

Figure S19: A Z-stack image of phospholipid vesicles of **3** (400 µM) after the sample has been left to sediment on to the coverslip overnight, related to Figure 2. A thinner layer of about 30 µm that decreases in density as the distance to the coverslip increases is observed at this concentration.

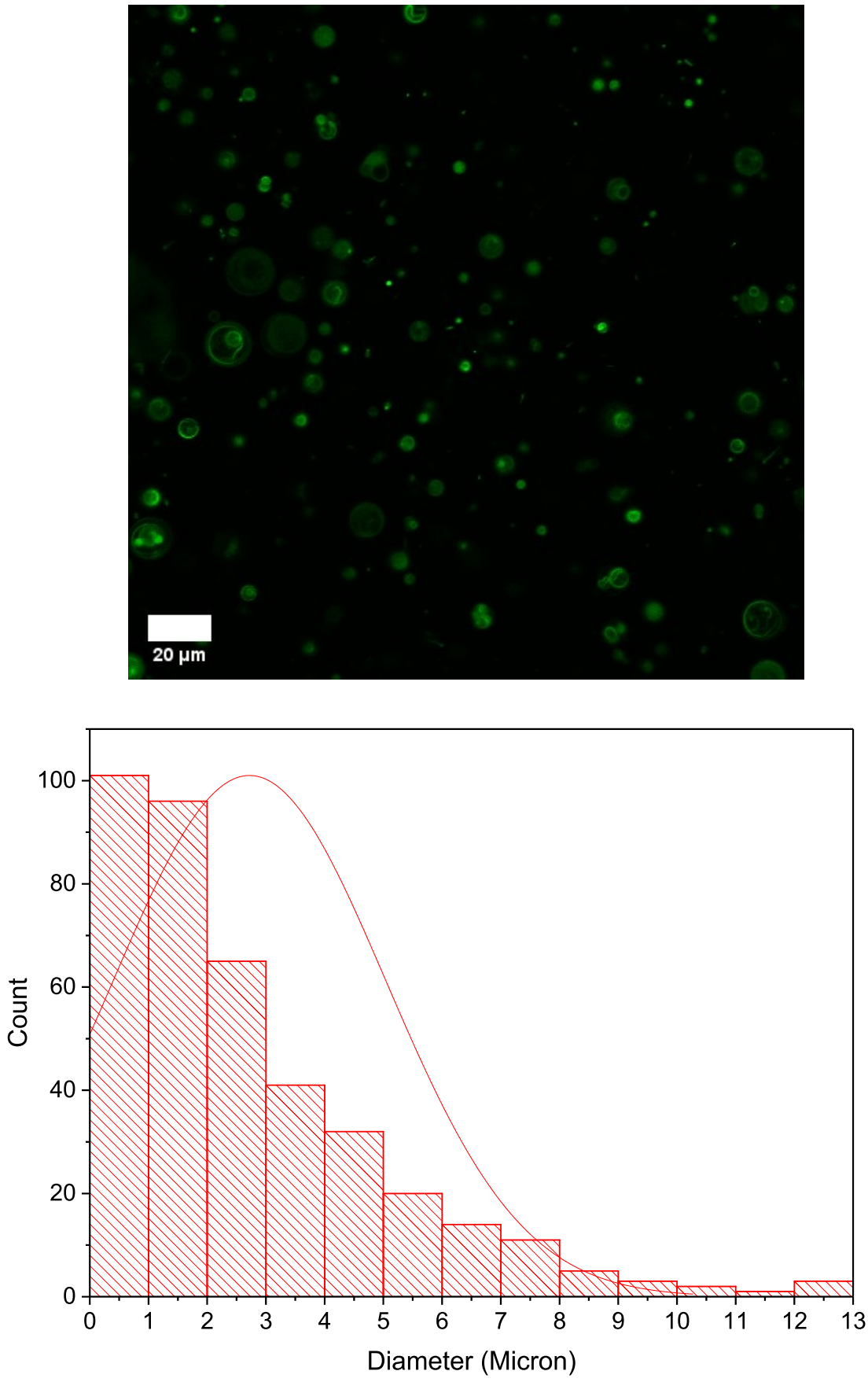

Figure S20: Confocal image of phospholipid vesicles of **3** (40 µM) in solution, related to Figure 2. A very dilute and smaller population of mainly <5 µm vesicles is observed at this concentration in solution. Scale bar, 20 µm.

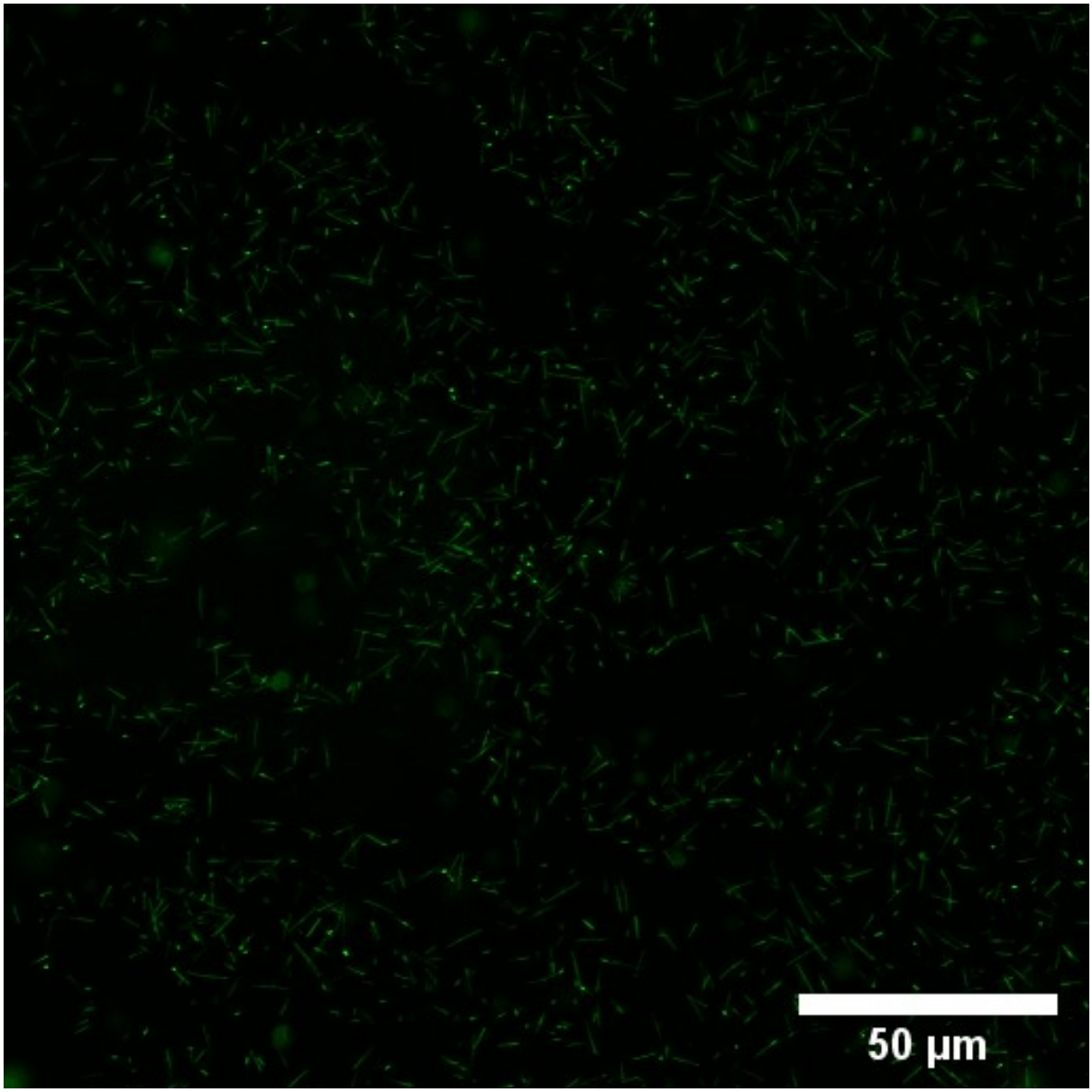

Figure S21: Confocal image of phospholipid vesicles of **3** (40 µM) on the coverslip, related to Figure 2. Rod-like structures of 1 µm width and 2-6 µm length are observed. Scale bar, 50 µm.

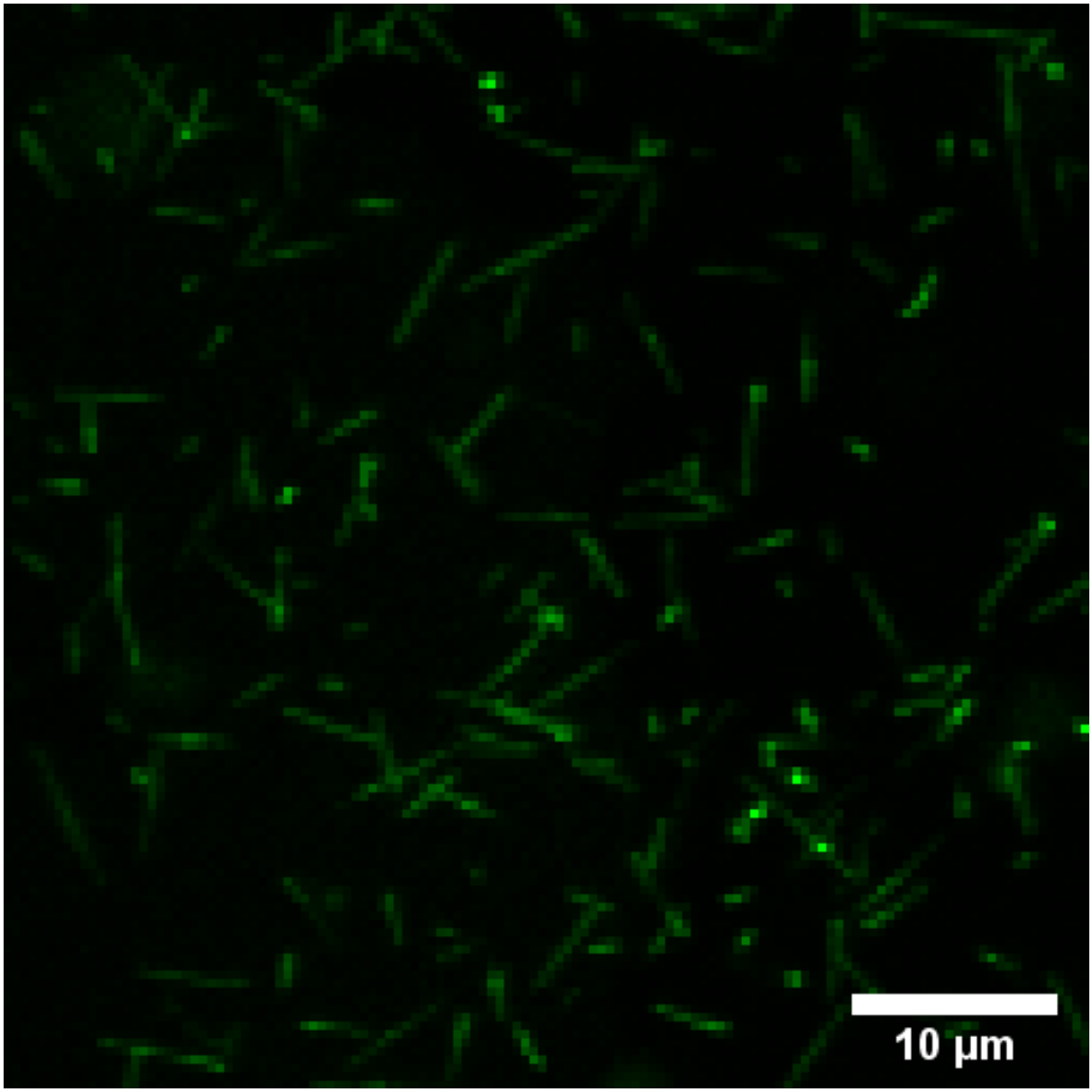

Figure S22: Zoomed in area of Figure S21, related to Figure 2.

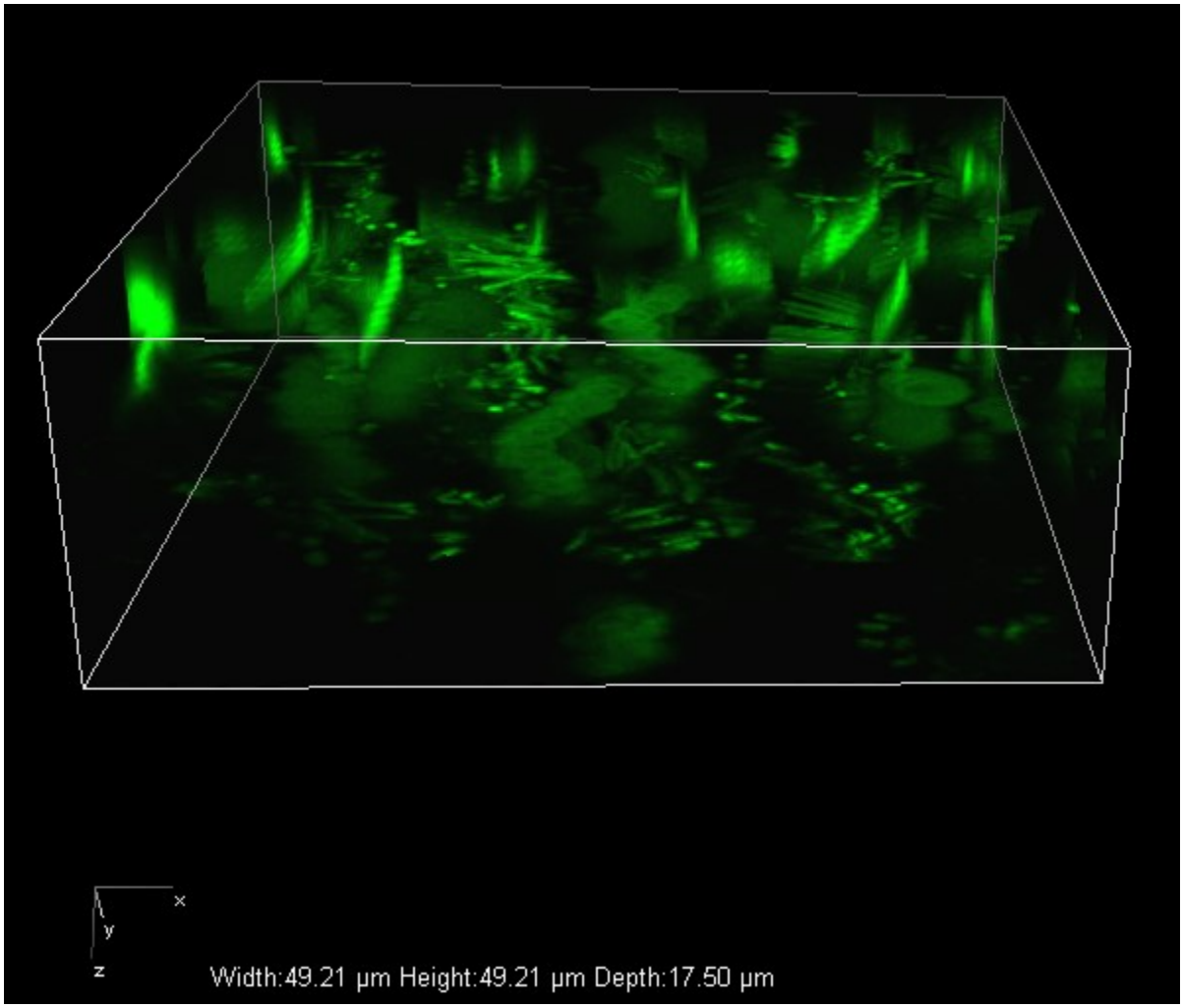

Figure S23: A Z-stack image of phospholipid vesicles of **3** (40 µM) after the sample has been left to sediment on to the coverslip overnight, related to Figure 2. A very thin layer of about 10 µm is observed. The Z-stack also captured the "wiggling" motion of the rod-like structures at the coverslip.

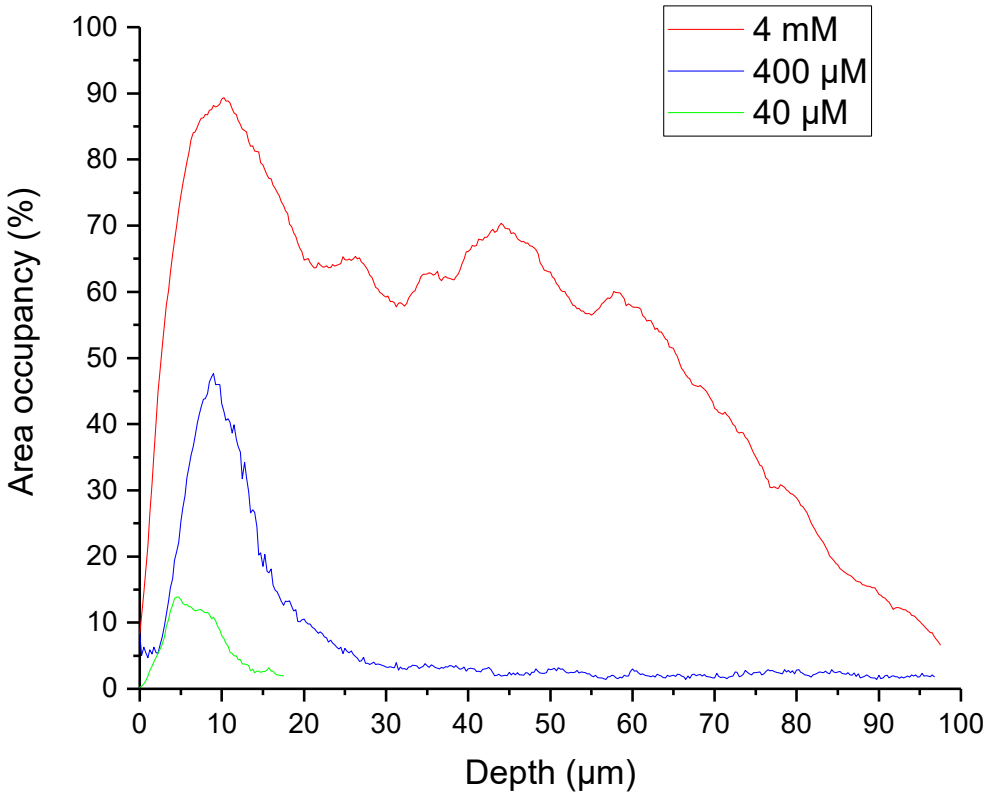

Figure S24: A threshold limit for the pixel intensity was set to calculate the number of green pixels relative to black pixels in the Z-stacks of S17, S19 and S23, related to Figure 2. This allowed us to quantify the occupancy of stained membrane of **3** at each slice of the Z-stack. The graph shows that at higher concentrations the layer of sedimented vesicles is not only thicker but the amount of membrane present at each depth is higher as well.

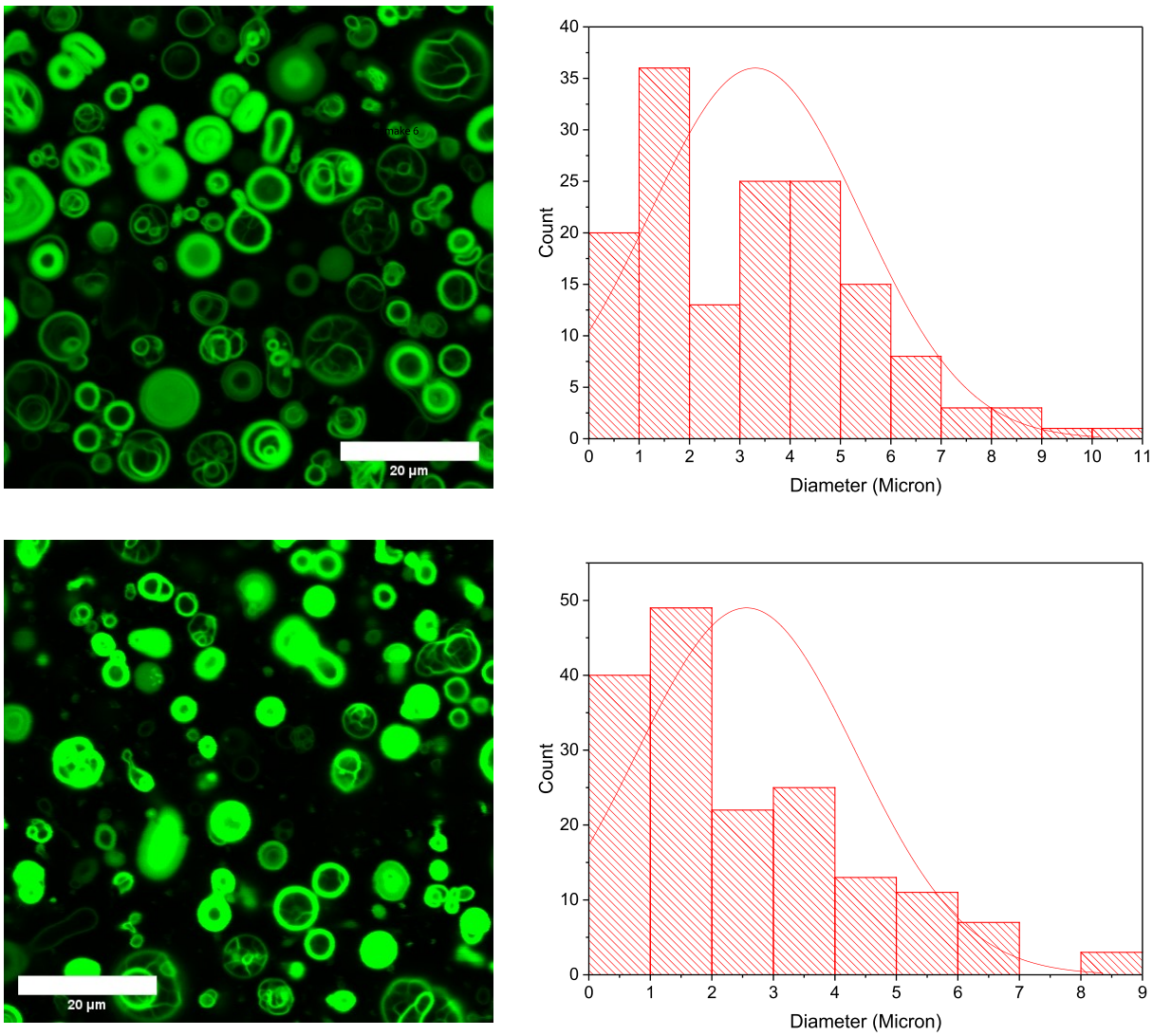

Figure S25: Confocal image thin film hydrated phospholipid vesicles of **3** (4 mM), related to Figure 2. Largely unilaminar vesicles up to 9 µm in size are observed. Scale bar, 20 µm.

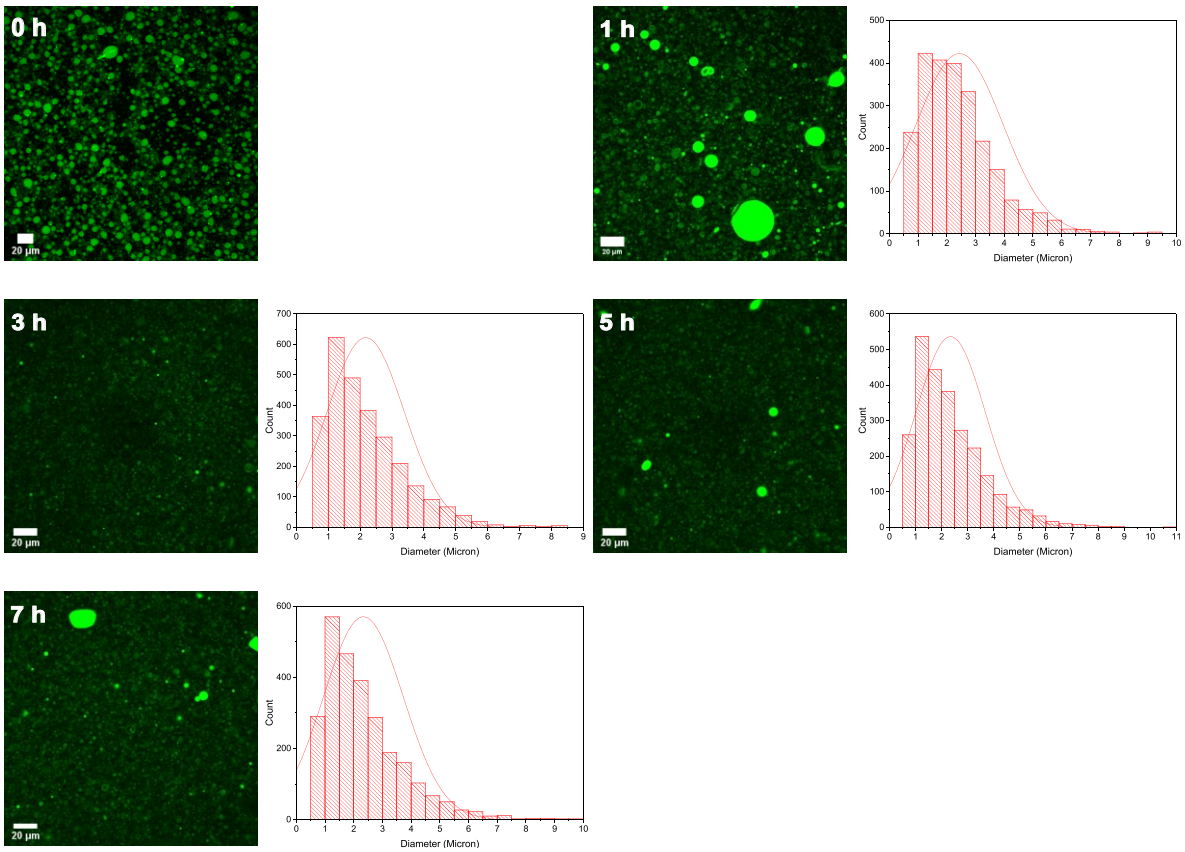

Figure S26: Additional confocal micrographs to Fig. 2e of aliquots of the unseeded reaction. Scale bar, 20 µm.

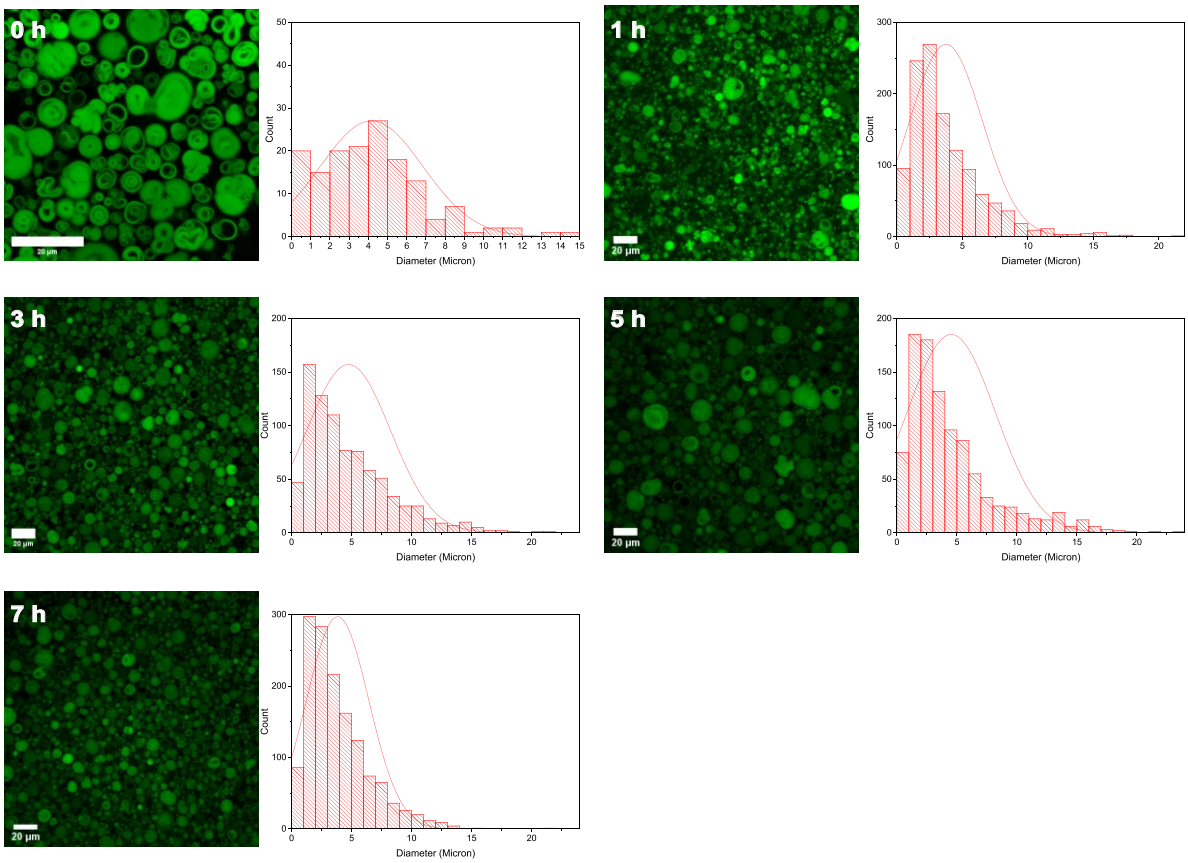

Figure S27: Additional confocal micrographs to Figure 2f of aliquots of the seeded reaction. Scale bar, 20 µm.

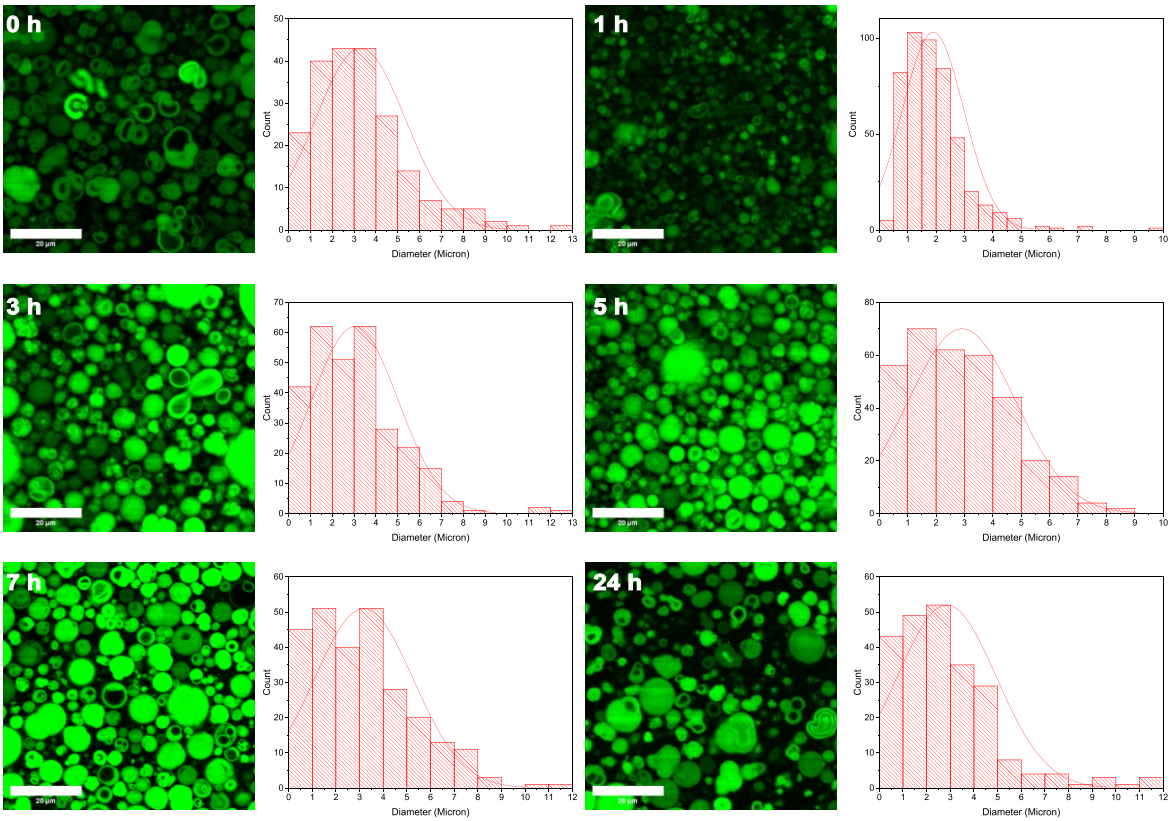

Figure S28: Confocal micrographs of aliquots of the thin film seeded reaction (yellow triangles in Figure 2b). Scale bar, 20 μm.

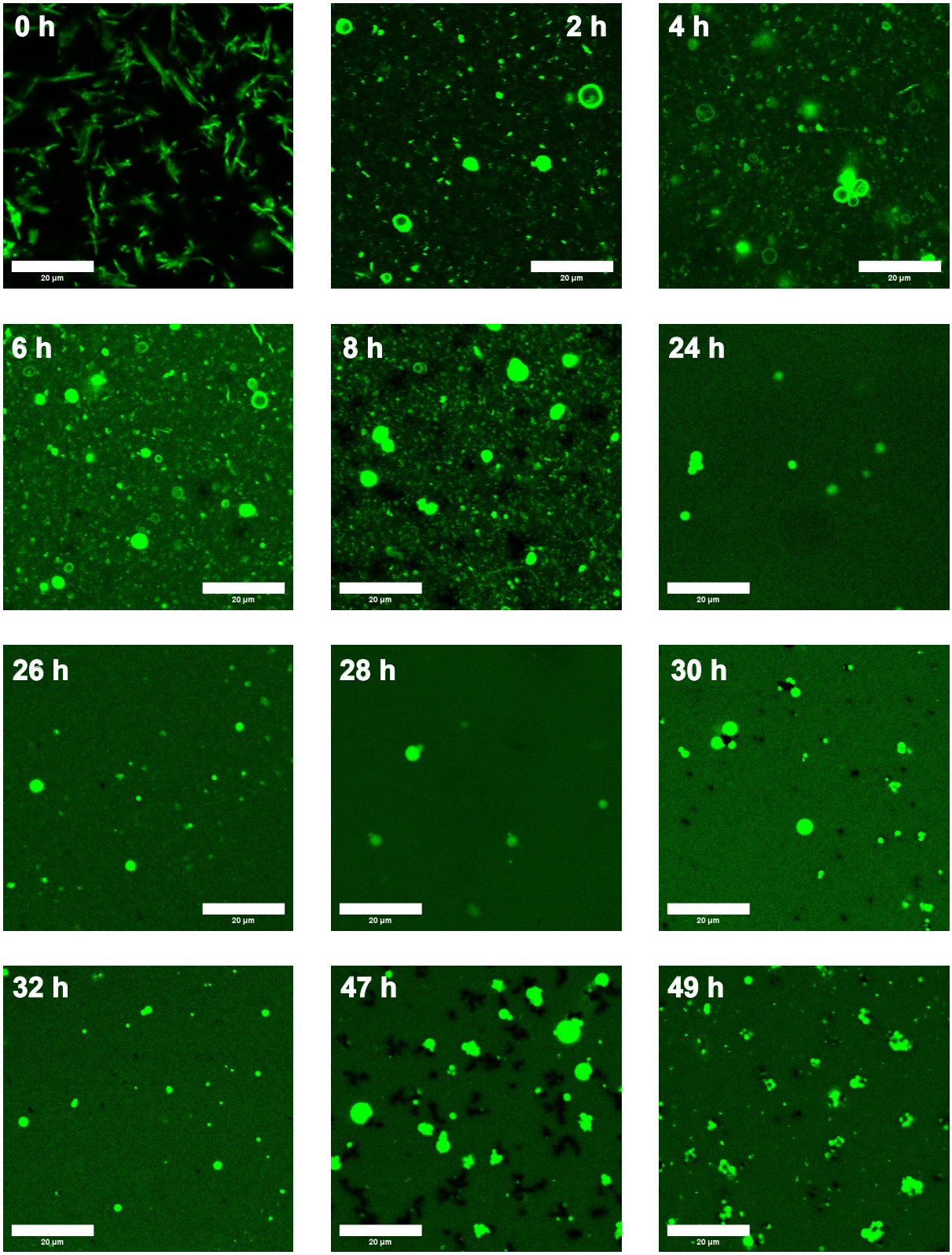

Figure S29: Confocal micrographs of aliquots of the out-of-equilibrium reaction (Figure 3c). Scale bar, 20 µm. At t = 0h amorphous oil of **1** is observed. From t = 2 to 8 h an mixture of vesicles and amorphous material is observed, at later time points (after t= 24 h) when the out-of-equilibrium steady state is reached only oil droplets are observed. Any aggregates present at these later time points are of sizes below the detection limit of confocal microscopy.

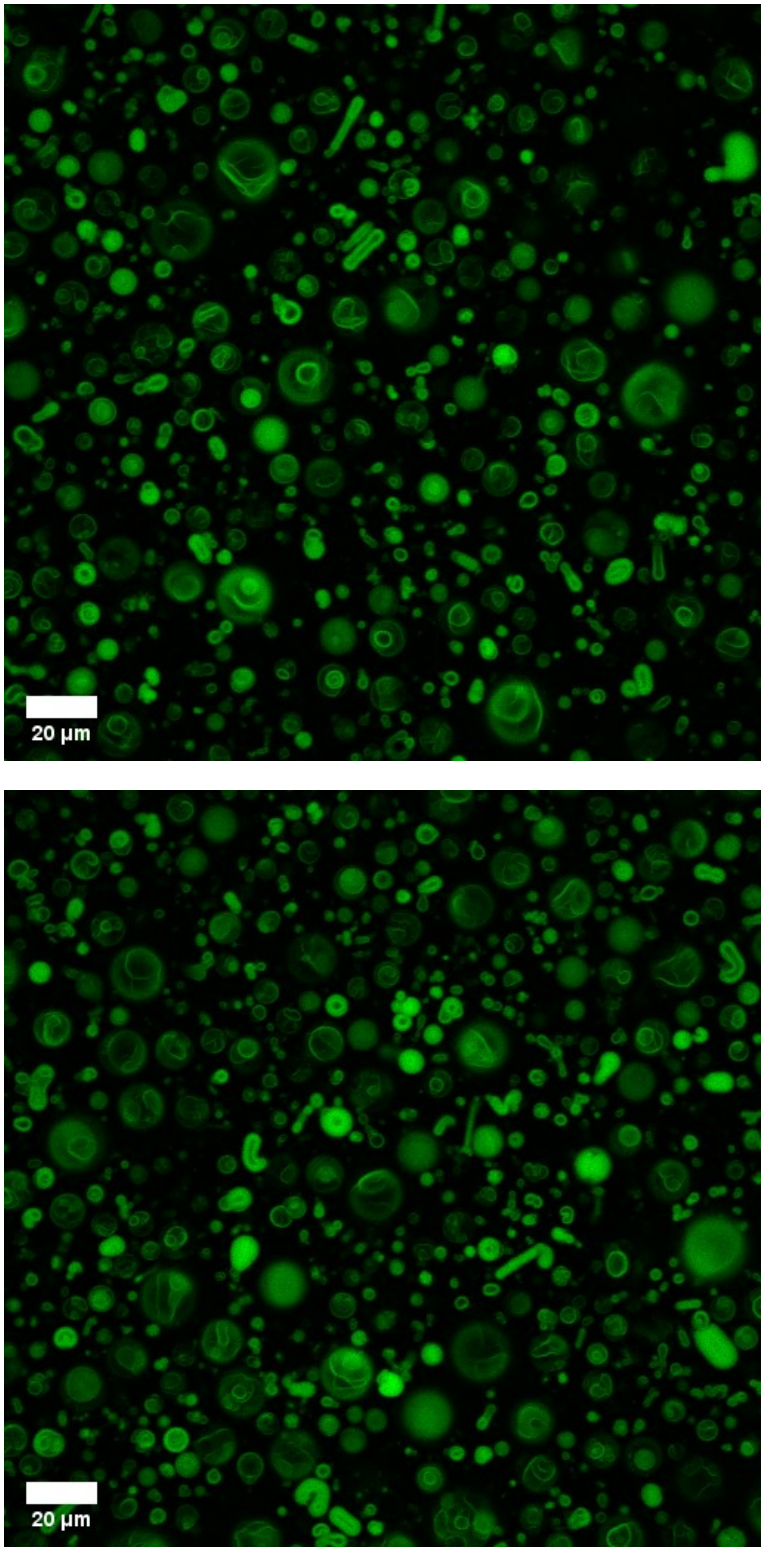

Figure S30: Confocal images of phospholipid vesicles of a mixture of **3** (4 mM) with **7** (10 mM), related to Figure 4. Not just spherical but also tubular vesicles are observed as are cases where multiple vesicles appear to be fused together. Scale bar, 20 µm.

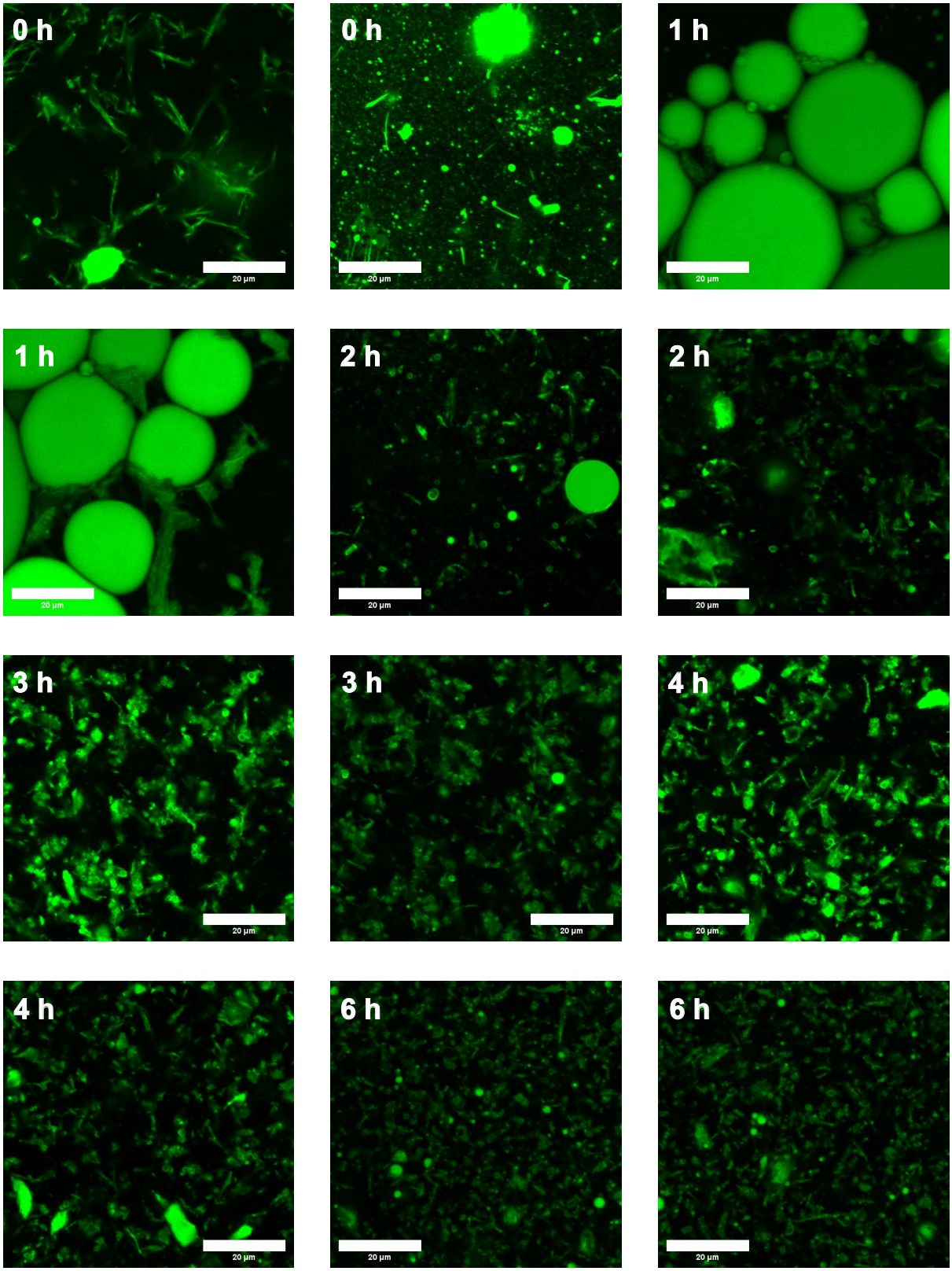

Figure S31: Confocal micrographs of aliquots of the competition reaction (Figure 4c) for the formation of compound **3** and **7** in the presence of 50 mM NaOH. Scale bar, 20 µm. Initially oil droplets stabilized by surfactants are observed, followed by the formation of amorphous aggregates and clusters of vesicles.

UPLC Calibration Curves

A calibration plot was prepared for the various compounds that were analysed by UPLC by plotting the peak area against the concentration of pure compound and fitting a trendline through the data points. These curves were used to calculate the concentration of compounds in the aliquots during kinetic monitoring of the reactions.

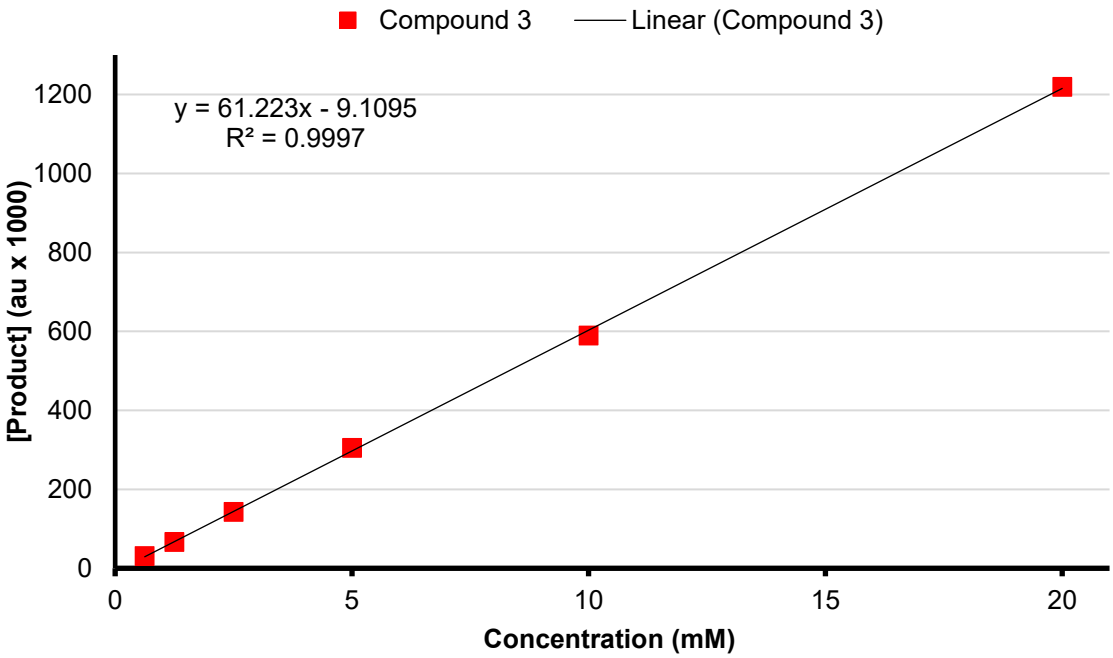

Figure S32: A linear calibration curve through data points of the area of pure **3** at different concentrations. Experimental conditions: 20 µL of aqueous sample diluted in 500 µL of standard solution of MeCN containing 0.7 mM of ethyl benzoate as internal standard. λ_{det} = 214.5 nm, injection volume = 5 µL, retention time: $t_{(3)}$ = 2.27 min.

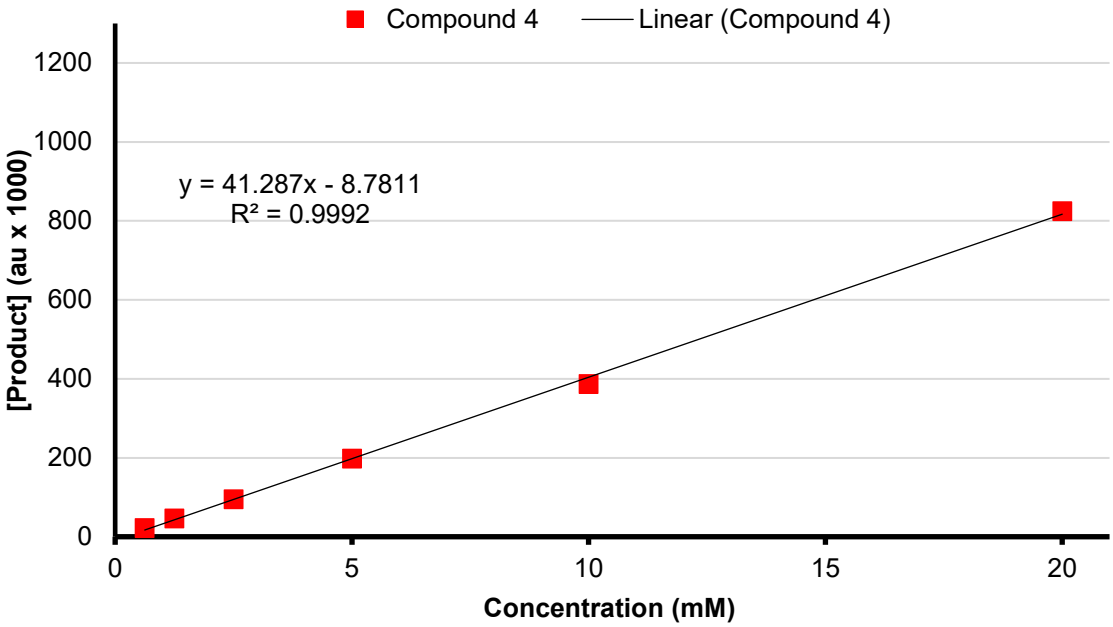

Figure S33: A linear calibration curve through data points of the area of pure **4** at different concentrations. Experimental conditions: 20 µL of aqueous sample diluted in 500 µL of standard solution of MeCN containing 0.7 mM of ethyl benzoate as internal standard. λ_{det} = 214.5 nm, injection volume = 5 µL, retention time: $t_{(4)}$ = 2.74 min.

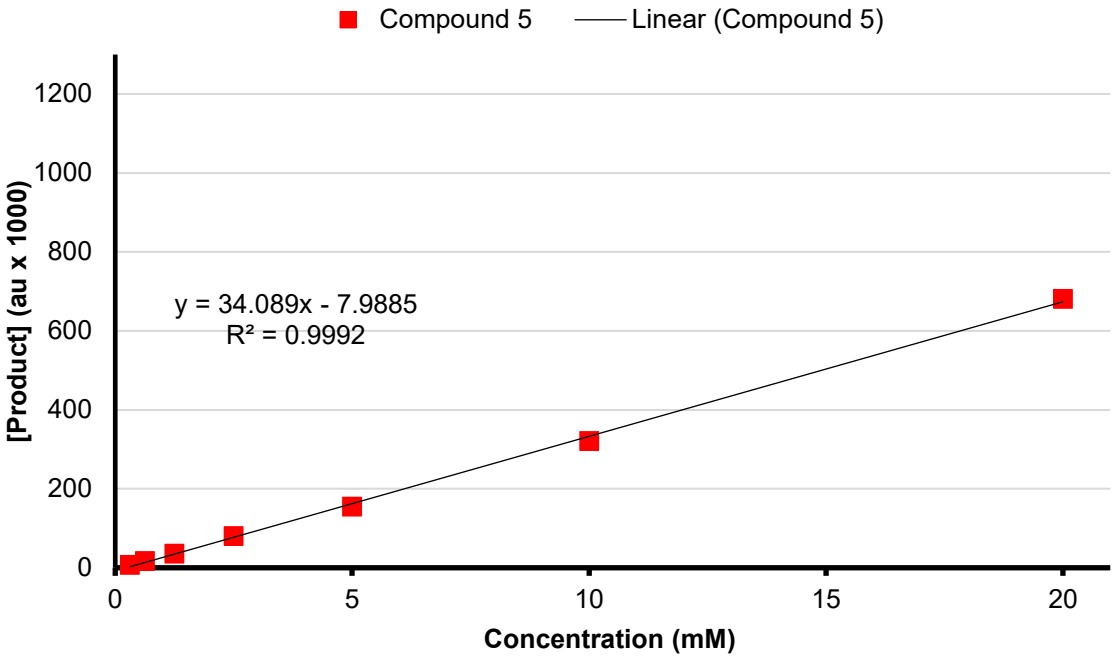

Figure S34: A linear calibration curve through data points of the area of pure **5** at different concentrations. Experimental conditions: 20 µL of aqueous sample diluted in 500 µL of standard solution of MeCN containing 0.7 mM of ethyl benzoate as internal standard. λ_{det} = 214.5 nm, injection volume = 5 µL, retention time: $t_{(5)}$ = 3.86 min.

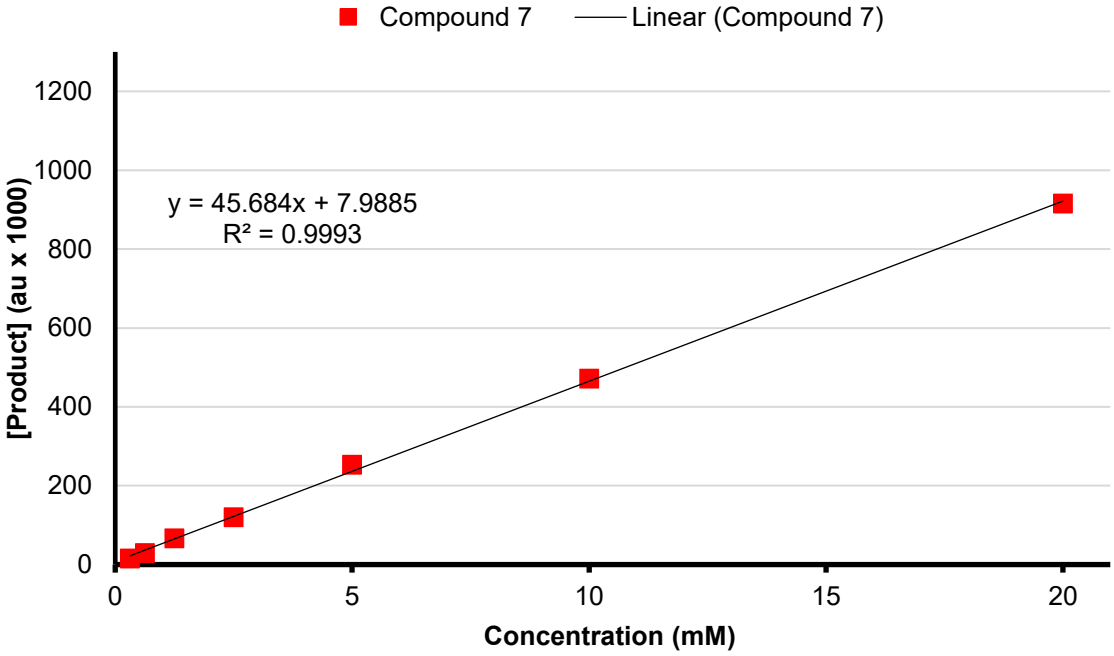

Figure S35: A linear calibration curve through data points of the area of pure **7** at different concentrations. Experimental conditions: 20 µL of aqueous sample diluted in 500 µL of standard solution of MeCN containing 0.7 mM of ethyl benzoate as internal standard. λ_{det} = 214.5 nm, injection volume = 5 µL, retention time: $t_{(7)}$ = 2.62 min.

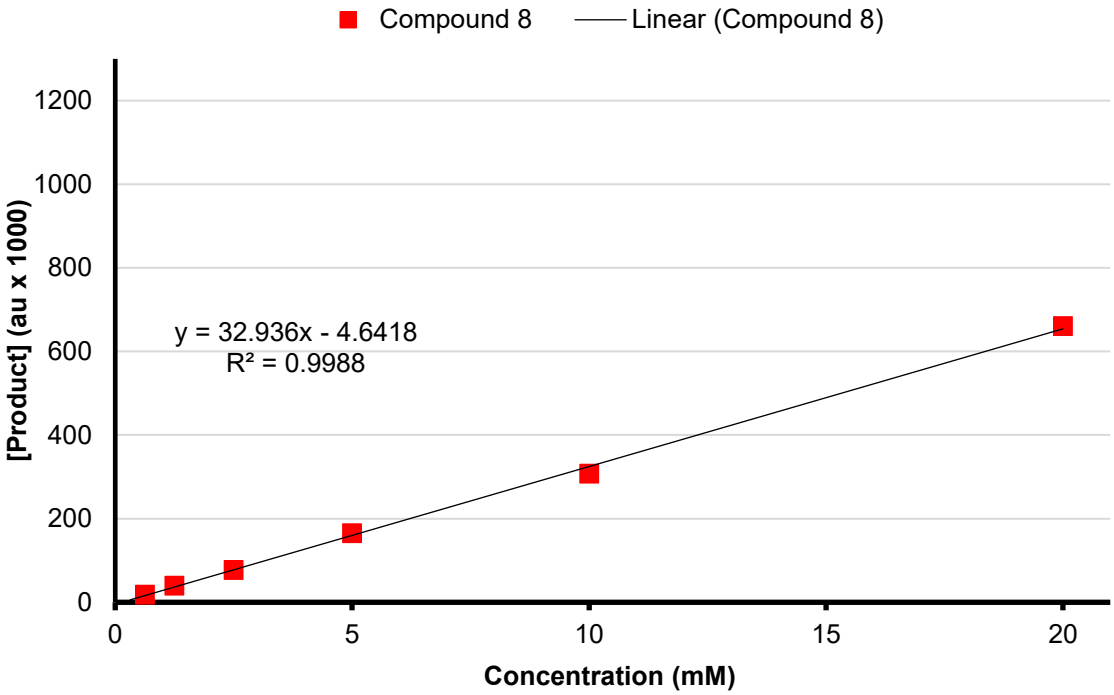

Figure S36: A linear calibration curve through data points of the area of pure **8** at different concentrations. Experimental conditions: 20 µL of aqueous sample diluted in 500 µL of standard solution of MeCN containing 0.7 mM of ethyl benzoate as internal standard. λ_{det} = 214.5 nm, injection volume = 5 µL, retention time: $t_{(\mathbf{8})}$ = 3.02 min.

Kinetic Data

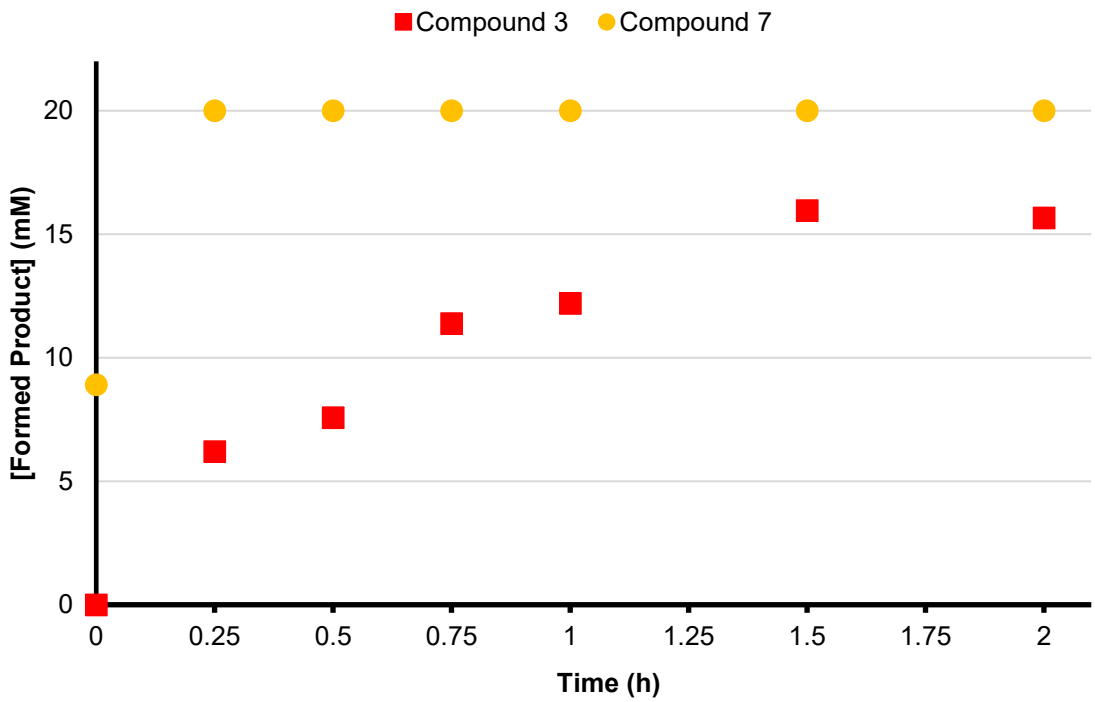

Figure S37: Reaction kinetics for the formation of surfactant under *t*BuOH/H_2O (1:1) conditions. Compound **3** (red squares) shows no lag period and complete conversion in 1.5 hours. Compound **7** (yellow circles) shows complete conversion in 15 minutes, related to Figure 2 and 4 respectively. Experimental conditions: Performed in batch in the presence with a 2 mM copper(I) catalyst loading while stirring at 1000 rpm for formation of **3** and stirring at 400 rpm for **7**.

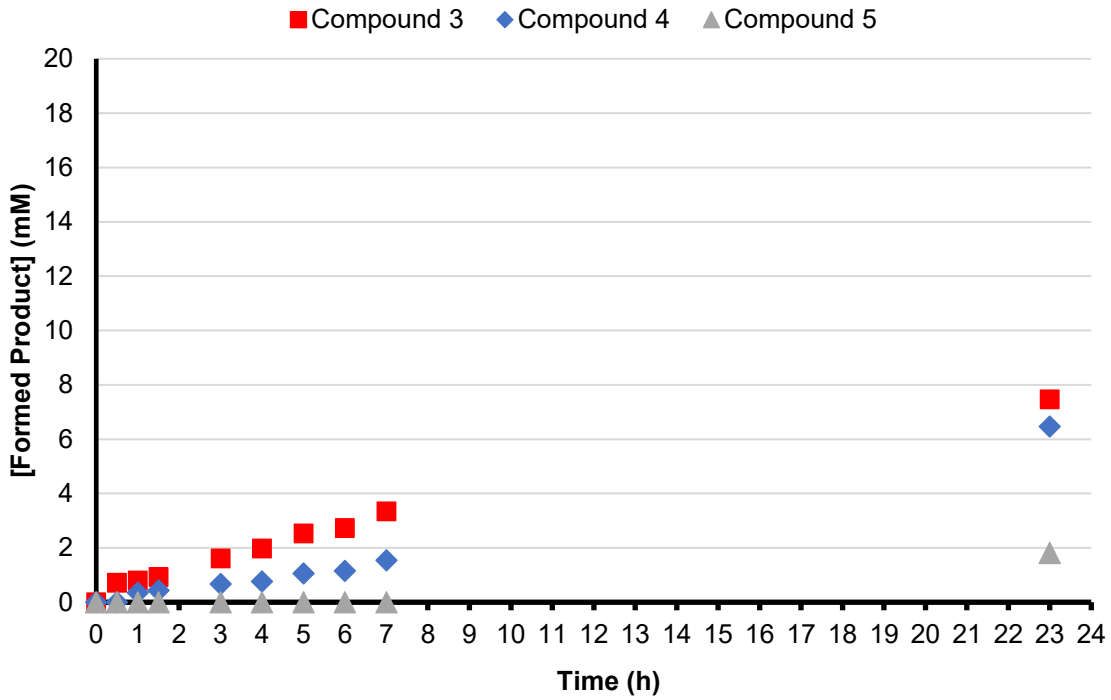

Figure S38: Reaction kinetics for the formation of compound 3 (red squares), 4 (blue diamonds) and 5 (grey triangles). Results indicate that **3** is relatively stable to hydrolysis but that a higher catalyst loading is required to obtain significant product formation at convenient time scales. Experimental conditions: Performed in batch in the presence of 50 mM NaOH with 8 mM copper(I) catalyst loading while stirring at 1000 rpm, related to Figure 3.

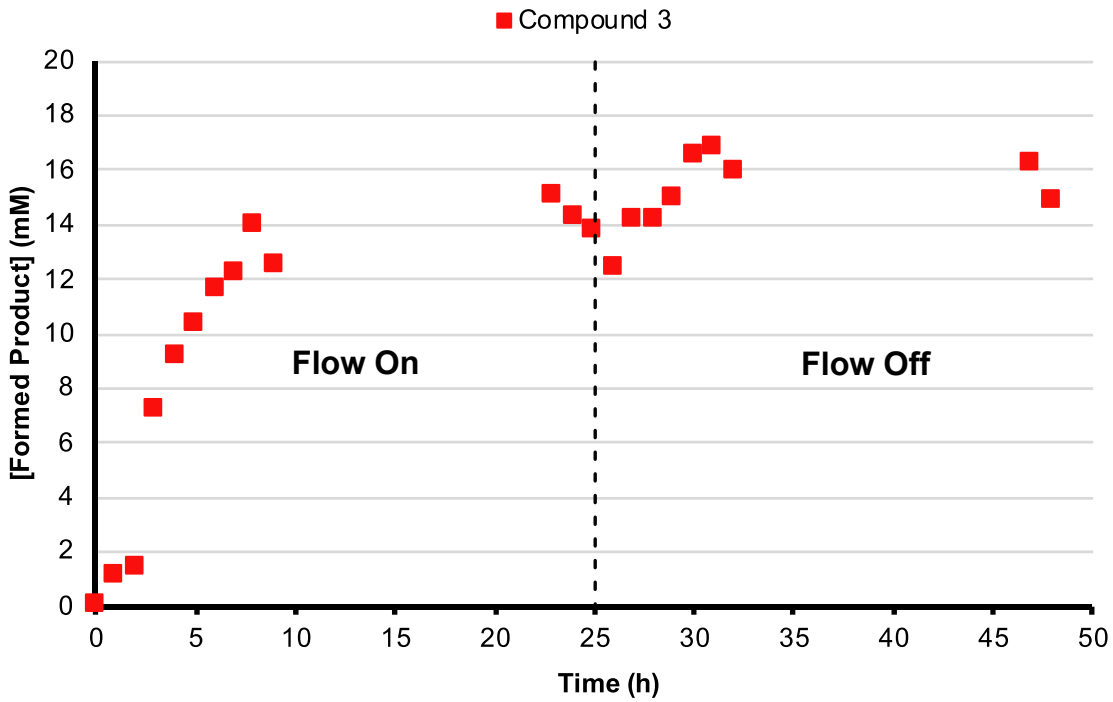

Figure S39: Reaction kinetics for the formation of compound 3 (red squares) in CSTR setup. Results indicate that no out-of-equilibrium steady-state can be obtained at 0 mM NaOH. Experimental conditions: Performed in CSTR setup in the presence of 0 mM NaOH with 8 mM copper(I) catalyst loading while stirring at 1000 rpm, related to Figure 3. The flow was turned off at t = 25 h.

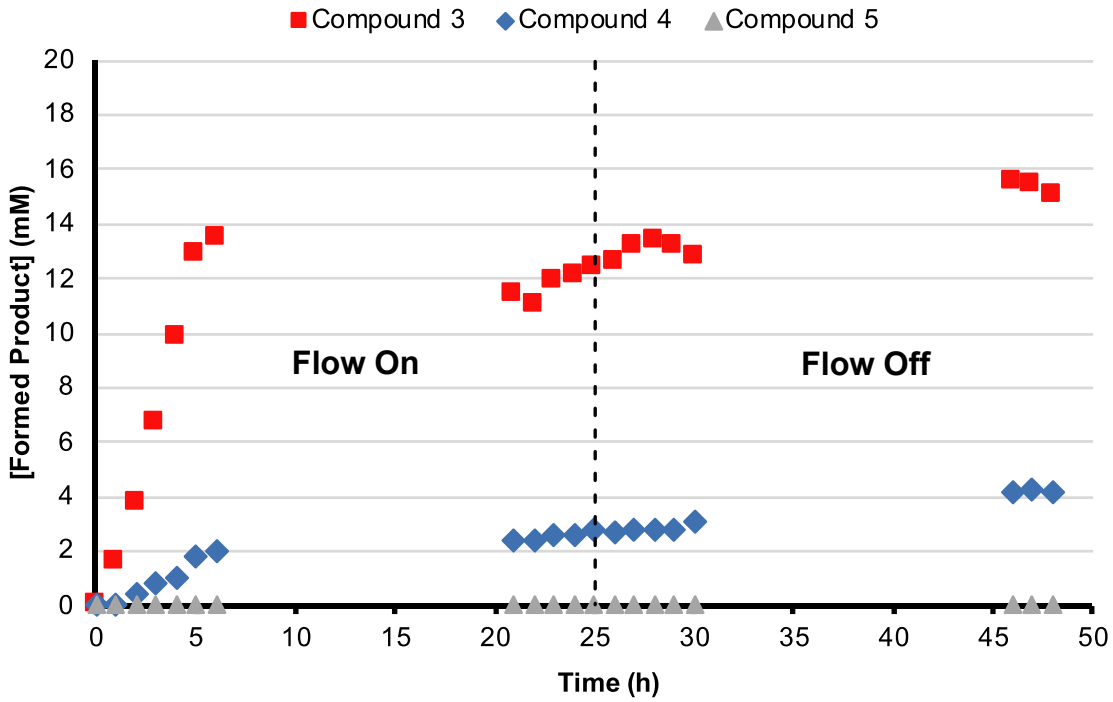

Figure S40: Reaction kinetics for the formation of compound 3 (red squares), 4 (blue diamonds) and 5 (grey triangles) in CSTR setup. Results indicate that no out-of-equilibrium steady-state can be obtained at 25 mM NaOH. Experimental conditions: Performed in CSTR setup in the presence of 25 mM NaOH with a 8 mM copper(I) catalyst loading while stirring at 1000 rpm, related to Figure 3. The flow was turned off at t = 25 h.

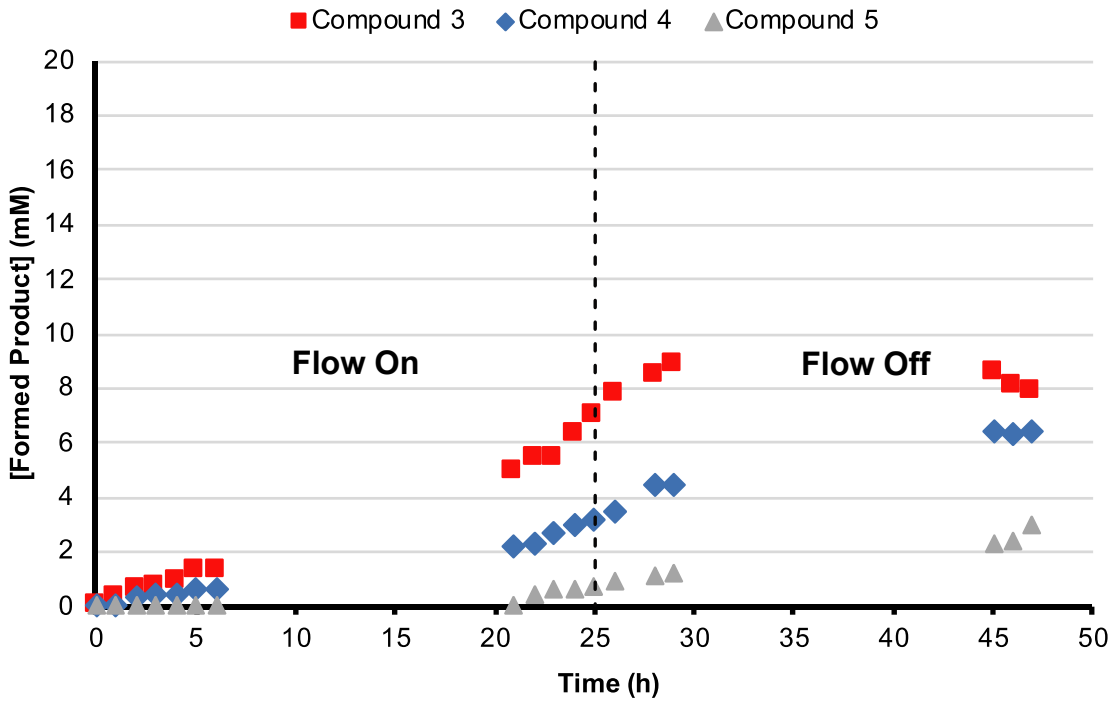

Figure S41: Reaction kinetics for the formation of compound 3 (red squares), 4 (blue diamonds) and 5 (grey triangles) in CSTR setup. Results indicate that no out-of-equilibrium steady-state can be obtained at 50 mM NaOH. Experimental conditions: Performed in CSTR setup in the presence of 50 mM NaOH with a 8 mM copper(I) catalyst loading while stirring at 1000 rpm, related to Figure 3. The flow was turned off at t = 25 h.

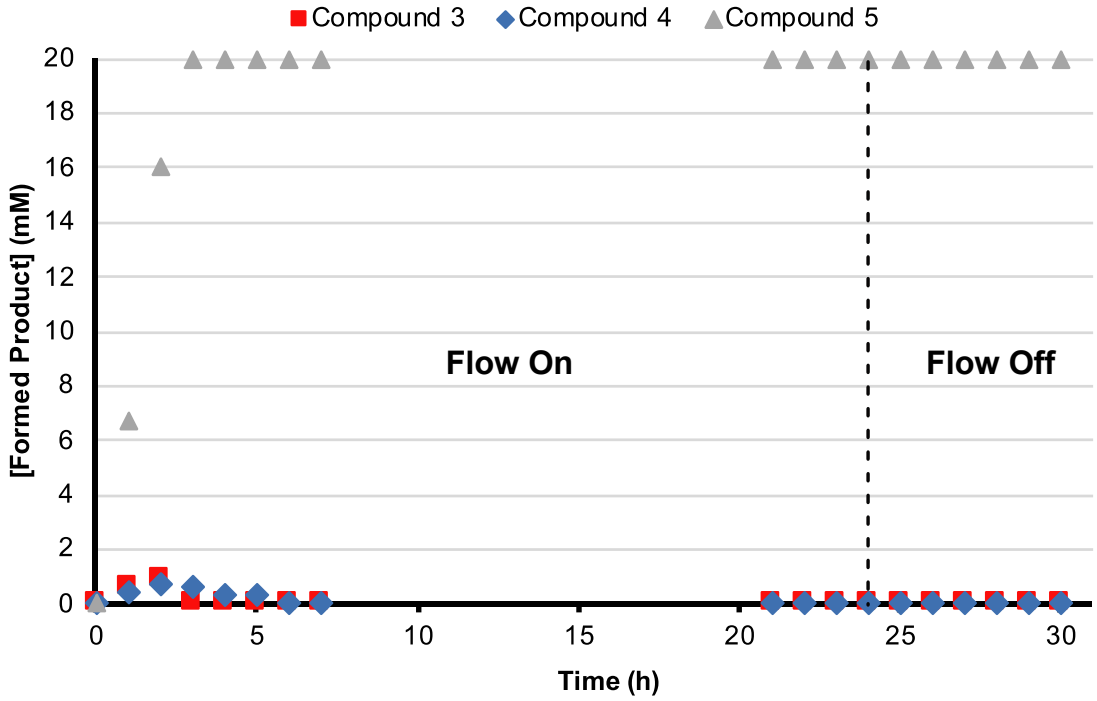

Figure S42: Reaction kinetics for the formation of compound 3 (red squares), 4 (blue diamonds) and 5 (grey triangles) in CSTR setup. Complete conversion to **5** is observed within 5 hours and turning of the flow at t = 24 h does not lead to a change in composition. This shows that an out-of-equilibrium steady-state requires phase-separation, and hence product aggregation, allowing the autocatalytic mechanism to operate. Experimental conditions: Performed in flow in the presence of 100 mM NaOH with a 8 mM copper(I) catalyst loading while stirring at 1000 rpm in *t*BuOH/H_2O (1:1), related to Figure 3. The flow was turned off at t = 24 h.

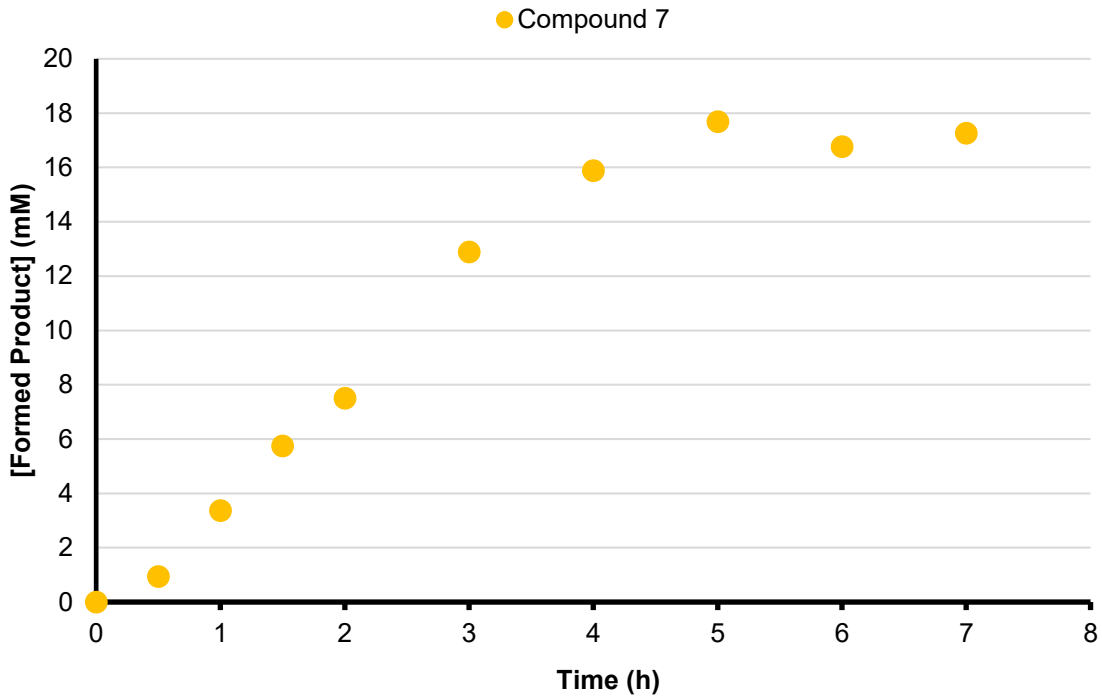

Figure S43: Reaction kinetics for the unseeded formation of compound 7 (yellow circles). Results indicate that formation of **7** is too fast when stirred at 1000 rpm resulting in no visible lag period. Experimental conditions: Performed in batch with 2 mM copper(I) catalyst loading while stirring at 1000 rpm, related to Figure 4.

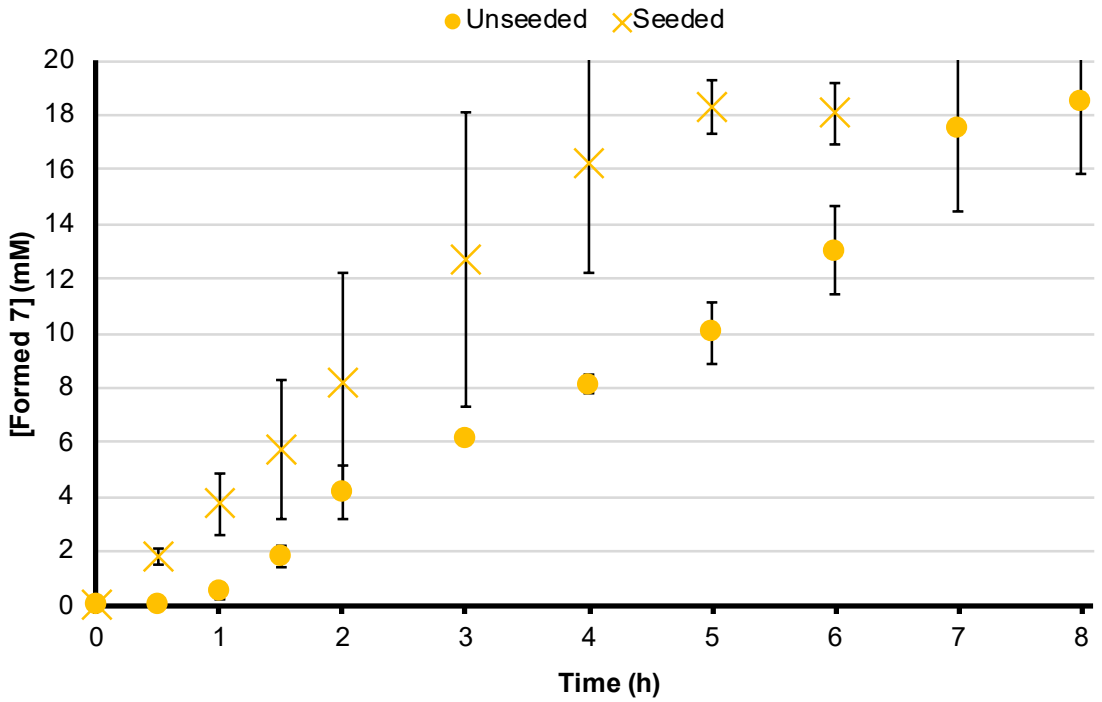

Figure S44: Reaction kinetics for the formation of surfactant 7 when unseeded (yellow circles) and seeded (yellow crosses) with product 7 (4 mM). The unseeded reaction (yellow circles) shows a lag period of 1 hour and complete conversion in 8 hours whereas the seeded reaction (yellow crosses) has no lag period and is complete in 5 hours, related to Figure 4. Experimental conditions: Performed in batch with a 2 mM copper(I) catalyst loading while stirring at 400 rpm. Points are the mean of three independent experiments and the error bars are the standard deviation.

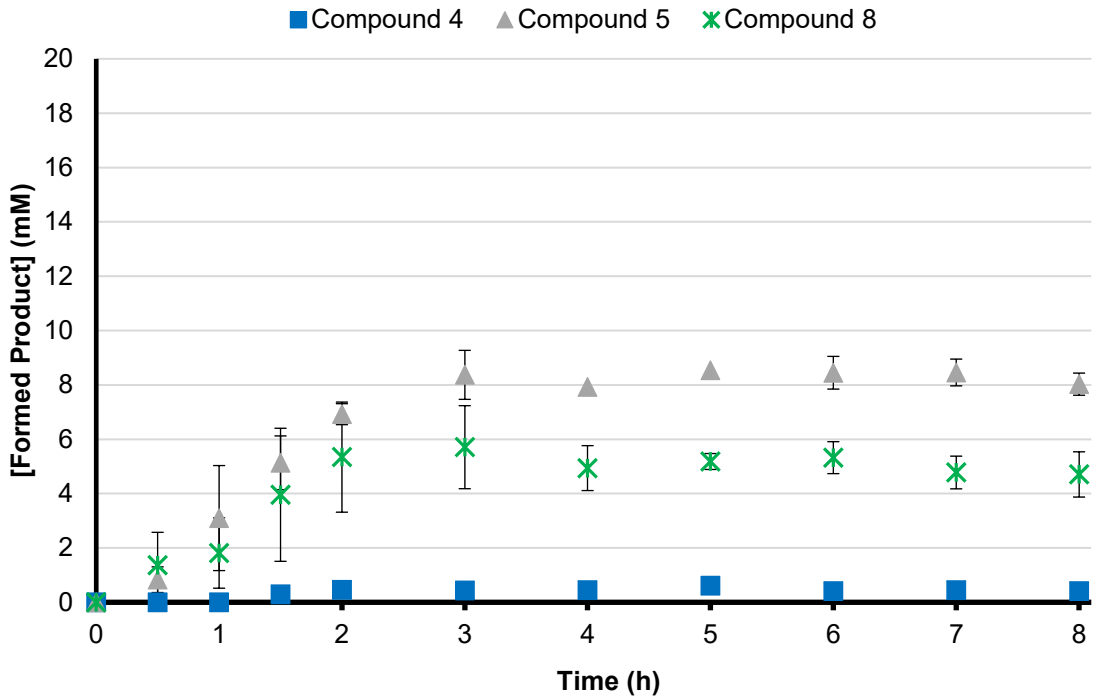

Figure S45: Complimentary figure to Fig. 4c showing the formation of hydrolysis products 4 (blue squares), 5 (grey triangles) and 8 (green stars). Results indicate significant formation of hydrolysis products **5** and **8** but not of **4** indicating hydrolysis of **7** but not of **3**. Experimental conditions: Performed in batch in the presence of 50 mM NaOH with a 8 mM copper(I) catalyst loading while stirring at 1000 rpm. Points are the mean of three independent experiments and the error bars are the standard deviation.

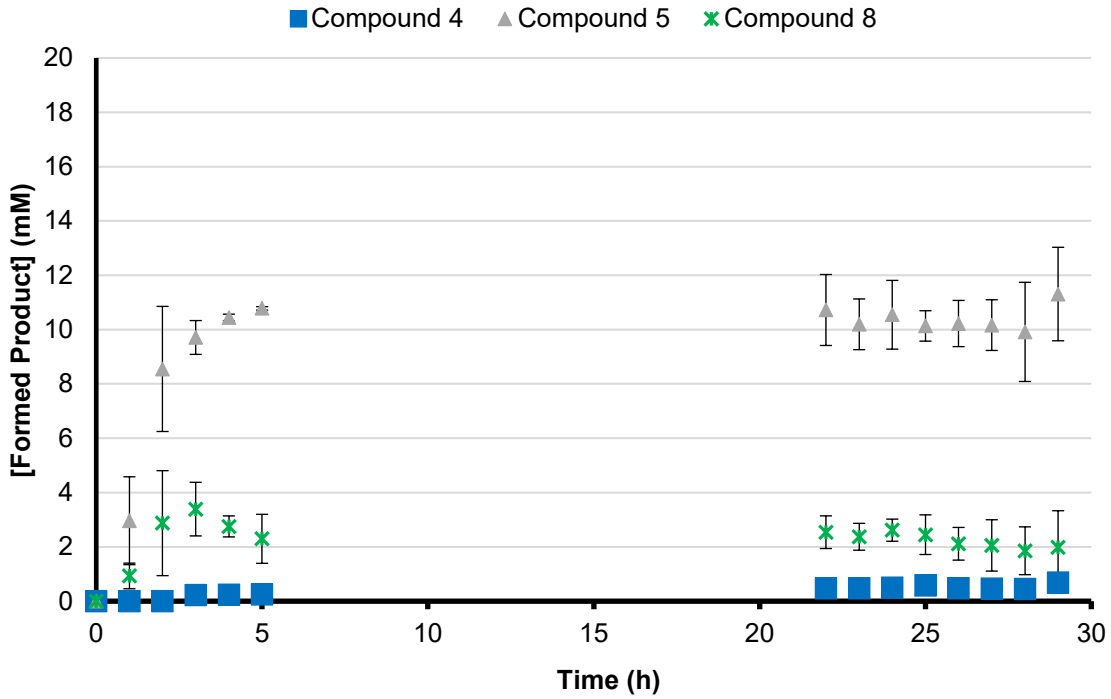

Figure S46: Complimentary figure to Fig. 4d showing the formation of hydrolysis products 4 (blue squares), 5 (grey triangles) and 8 (green stars) in CSTR setup. Results indicate significant formation of hydrolysis products **5** and **8** but not of **4** indicating hydrolysis of **7** but not of **3**. Experimental conditions: Performed in CSTR setup in the presence of 50 mM NaOH with a 8 mM copper(I) catalyst loading while stirring at 1000 rpm. The flow was turned off at t = 25 h. Points are the mean of three independent experiments and the error bars are the standard deviation.

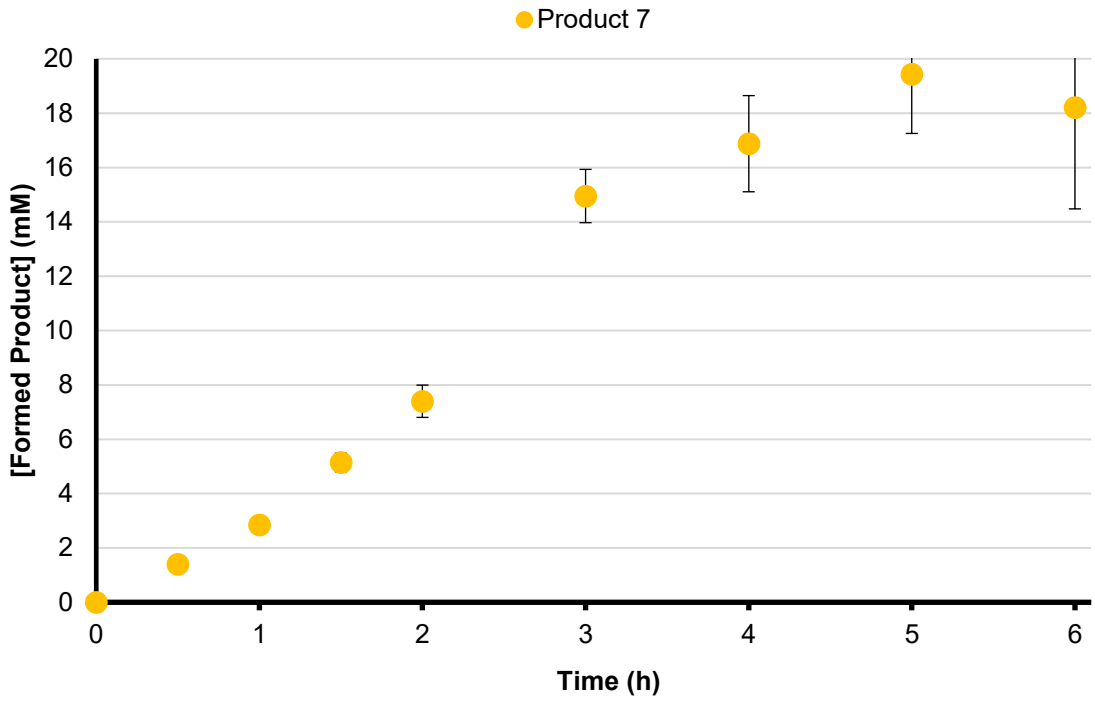

Figure S47: Reaction kinetics for the formation of compound 7 (yellow circles) when cross-seeded with 4 mM of 3. Results indicate that vesicles of **3** have a similar efficiency at accelerating formation of **7** as micelles of **7**. Experimental conditions: Performed in batch with 8 mM copper(I) catalyst loading while stirring at 400 rpm, related to Figure 4e. Points are the mean of three independent experiments and the error bars are the standard deviation.

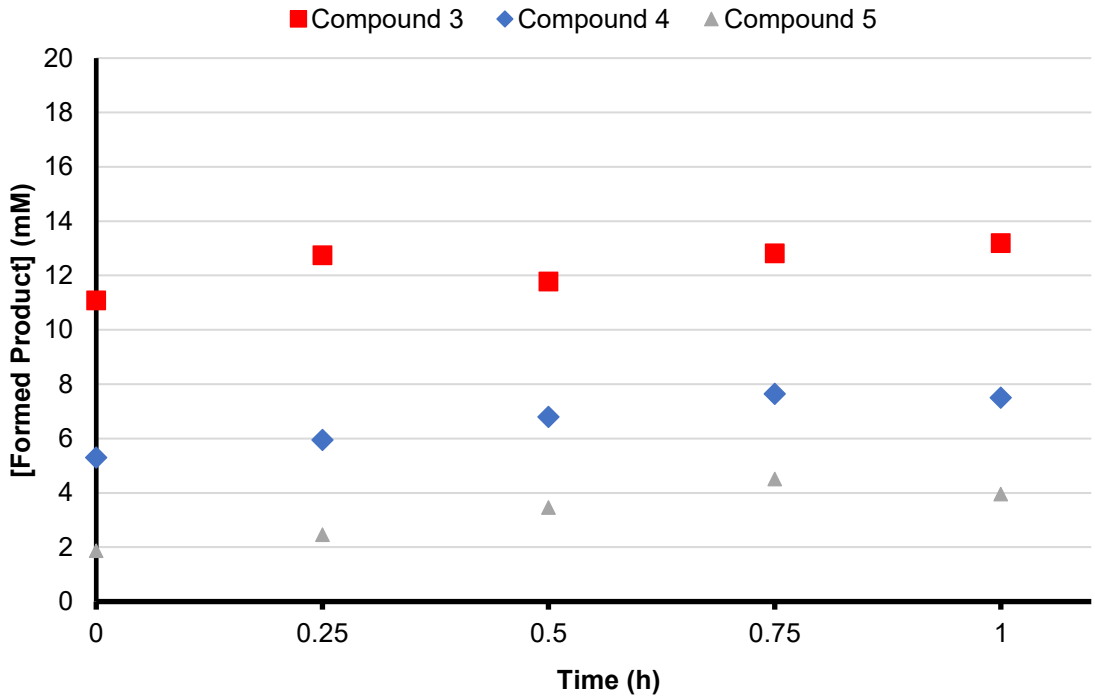

Figure S48: Reaction kinetics for the hydrolysis of compound 3 (red squares) to 4 (blue diamonds) and 5 (grey triangles). Results indicate the relative stability of **3** to hydrolysis. Experimental conditions: Performed in batch by stirring 20 mM of **3** in the presence of 50 mM NaOH at 1000 rpm, related to Figure 4.

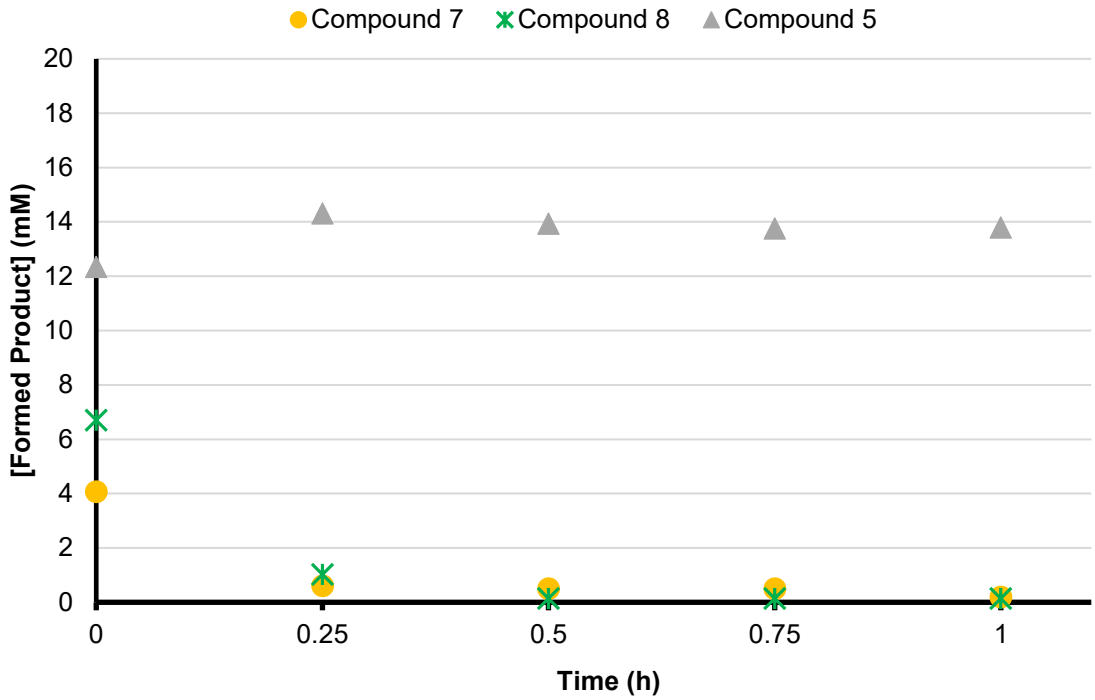

Figure S49: Reaction kinetics for the hydrolysis of compound 7 (yellow circles) to 8 (green stars) and 5 (grey triangles). Results show the instability of compound **7** to hydrolysis. Experimental conditions: Performed in batch by stirring 20 mM of **7** in the presence of 50 mM NaOH at 1000 rpm, related to Figure 4.

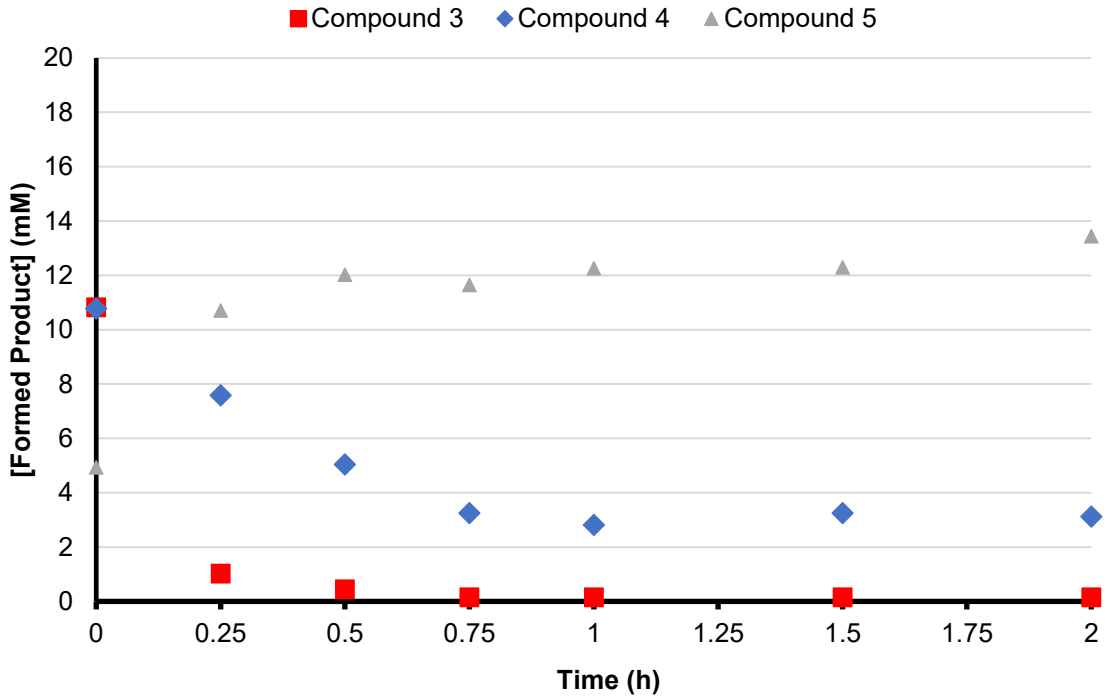

Figure S50: Reaction kinetics for the hydrolysis of compound 3 (red squares) to 4 (blue diamonds) and 5 (grey triangles) under *t*BuOH/H_2O (1:1) conditions. Results show that **3** becomes unstable to hydrolysis when in its unaggregated form. Experimental conditions: Performed in batch by stirring 20 mM of **3** in the presence of 50 mM NaOH at 1000 rpm in a 1:1 water/*tert*-butanol mixture, related to Figure 4.

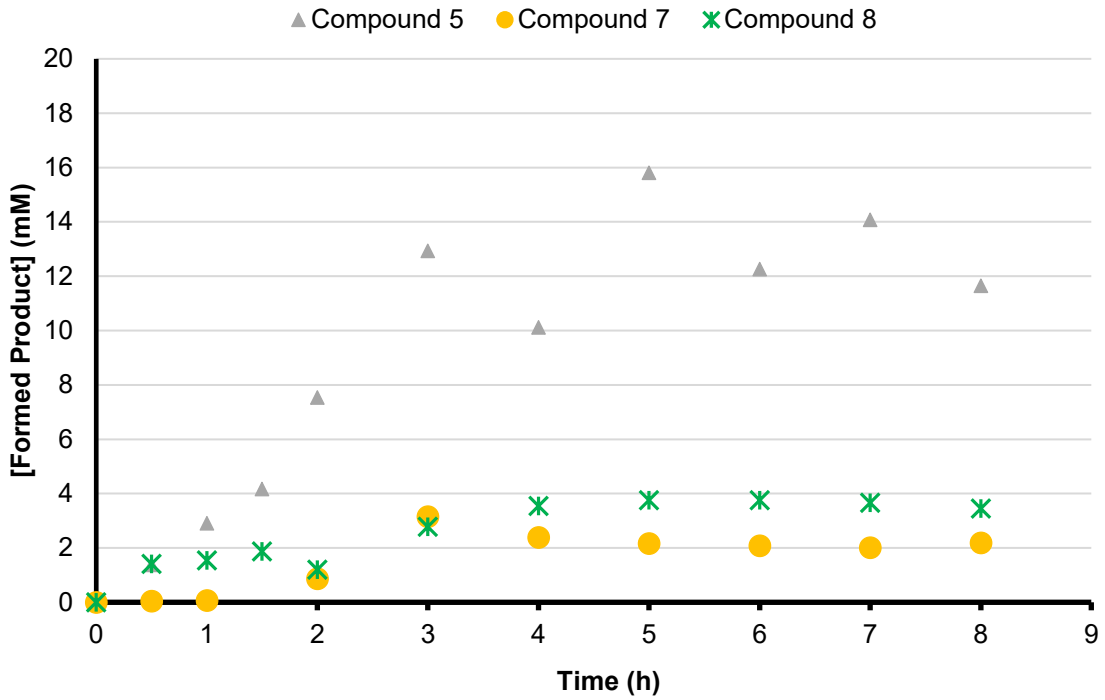

Figure S51: Reaction kinetics for the formation of compound 7 (yellow circles), 8 (green stars) and 5 (grey triangles) under hydrolysing conditions. Results show that in situ generated **7** is unstable to hydrolysis. Experimental conditions: Reaction between compound **2** and **6** performed in batch in the presence of 50 mM NaOH with a 8 mM copper(I) catalyst loading while stirring at 1000 rpm, related to Figure 4.

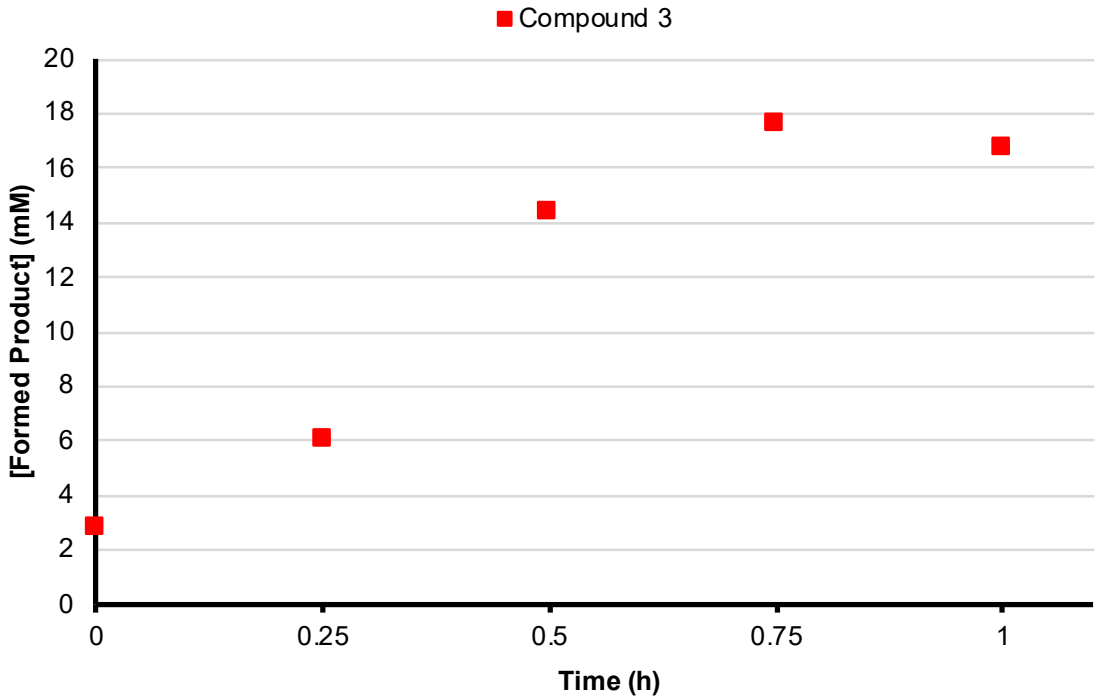

Figure S52: Reaction kinetics for the formation of compound 3 (red squares) when seeded with 4 mM of 7 under *t*BuOH/H_2O (1:1) conditions. Results show that **7** does not inhibit formation of **3** when there is no phase separation and supramolecular aggregation. Experimental conditions: Performed in batch with 8 mM copper(I) catalyst loading while stirring at 1000 rpm in *t*BuOH/H_2O (1:1), related to Figure 4.

DOSY Data

The diffusion coefficients were recorded for all reaction components at the concentrations present in the system during the synthesis of **7** in water. Due to the low CMC of **7** (27.6 μM) we were unable to get measurements below this value, however the diffusion coefficient (D) for the aggregated surfactant **7** at 4 mM is in agreement with that of micelles we have measured previously[14,15] and decreases with increasing concentration (20 mM) indicating a greater proportion of aggregated to free surfactant (Table S1, entry A-B). A compound associating with the micelle is expected to diffuse at a similar or slower rate as the surfactant. Control experiments show that azide **6** is insoluble in the absence of surfactant and associates strongly with **7** (entries C−E). However, azide **1** is only solubilized at high concentrations of **7** (20 mM) and is not observed in the absence or at lower concentrations of **7** (F−H). The hydrophobic copper ligand TBTA is not soluble in water even in the presence of high concentrations of **7** (entries I-K) contrary to previous systems investigated by us where other types of micelles were able to solubilize this compound. However, when the ligand is coordinated to copper a strong association with **7** is observed (entries L-N). Hydrophilic alkyne **2** is soluble without **7** present and does not associate with the micelles (entries O−Q).
Aggregates of **3** in water could not be studied by NMR due to the undefined broad peaks in the spectra that were obtained, likely due to long relaxation times. The rigid stacking of individual molecules of **3** in the vesicle bilayer plus the slow movement of the large aggregates possibly prevents them from relaxing after excitation.[16]

Entry	Species present	*D* (7)	*D* (6)	*D* (1)	*D* (ligand)	*D* (2)
A	**7** (4 mM)	3.4	-	-	-	-
B	**7** (20 mM)	2.8	-	-	-	-
C	**6** (saturated)	-	ND	-	-	-
D	**7** (4 mM) + **6** (saturated)	3.4	3.3	-	-	-
E	**7** (20 mM) + **6** (saturated)	2.7	0.44	-	-	-
F	**1** (saturated)	-	-	ND	-	-
G	**7** (4 mM) + **1** (saturated)	3.3	-	ND	-	-
H	**7** (20 mM) + **1** (saturated)	2.7	-	0.12	-	-
I	**TBTA** (saturated)	-	-	-	ND	-
J	**7** (4 mM) + **TBTA** (saturated)		-	-	ND	-
K	**7** (20 mM) + **TBTA** (saturated)	2.5	-	-	ND	-
L	**[Cu-TBTA]** (saturated)	-	-	-	ND	-
M	**7** (4 mM) + **[Cu-TBTA]** (saturated)	2.8			3.0	-
N	**7** (20 mM) + **[Cu-TBTA]** (saturated)	1.4	-	-	0.82	-
O	**2** (20 mM)	-	-	-	-	5.5
P	**7** (4 mM) + **2** (20 mM)	3.4	-	-	-	5.4
Q	**7** (20 mM) + **2** (20 mM)	2.8	-	-	-	5.2

Table S1: Diffusion coefficients extracted from DOSY experiments. The diffusion coefficients were recorded for all reaction components at the concentrations present in the system during the synthesis of **7** in water. *D* values reported in 10^{-10} m^2s^{-1}. A decrease in the diffusion coefficient in the presence of surfactant **7** above the CMC indicates a strong association with the micelle. ND indicates that the diffusion coefficient could not be extracted because of the limited solubility of the compound in water. For entries L-N sodium ascorbate (24 mM) was added to reduce $CuSO_4$.

NMR Spectra

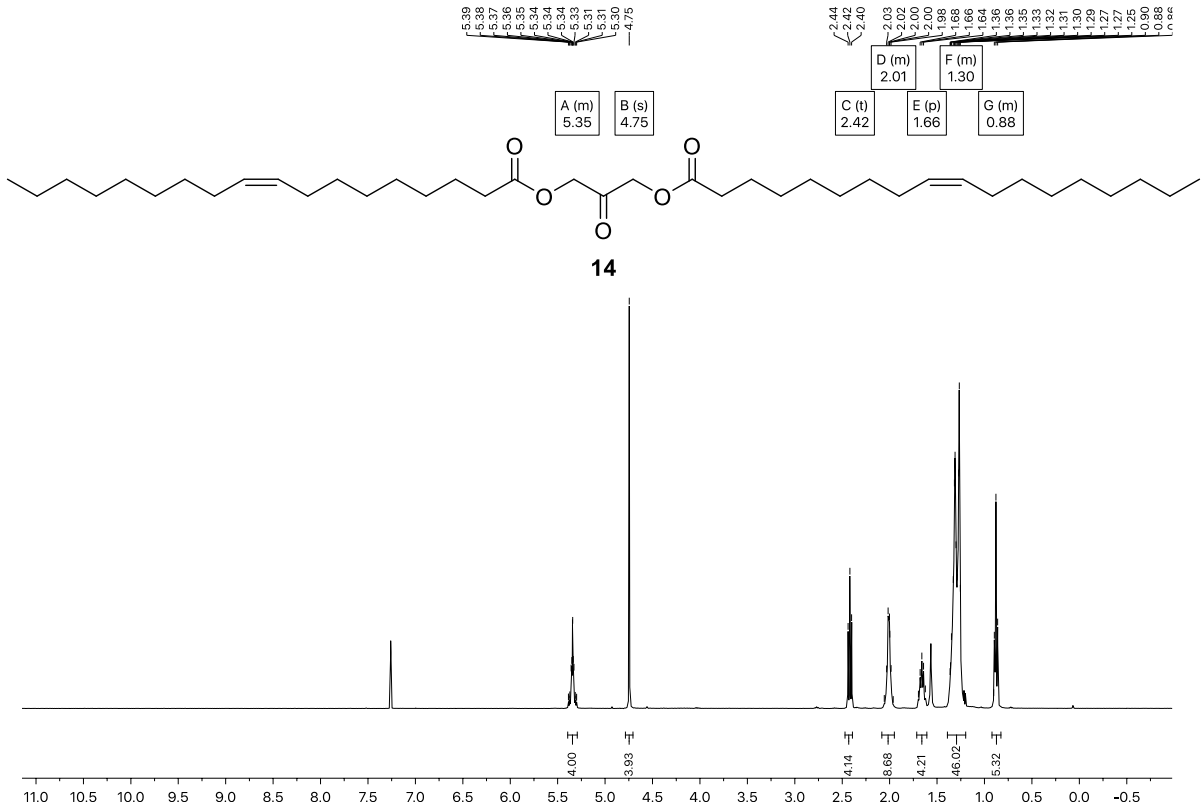

Figure S53: ^{1}H NMR spectrum of compound **14** in $CDCl_3$.

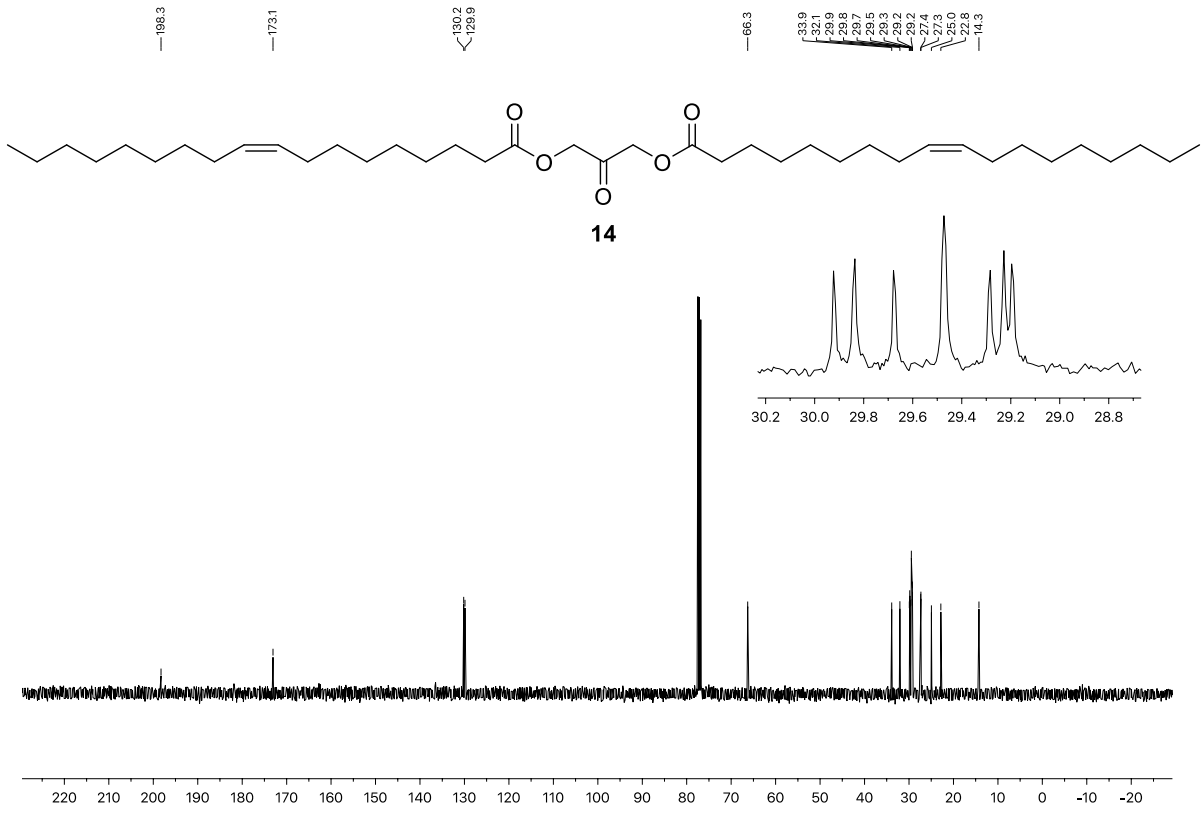

Figure S54: ^{13}C NMR spectrum of compound **14** in $CDCl_3$.

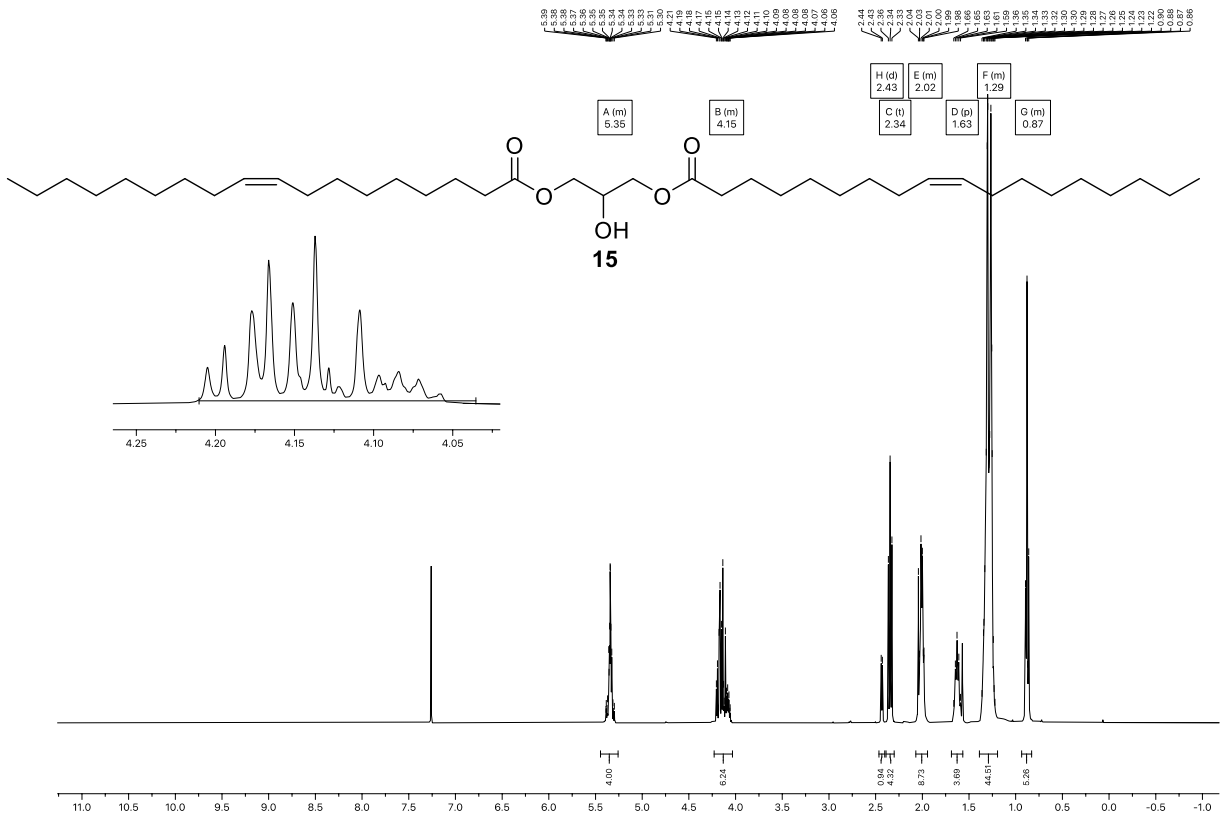

Figure S55: ^{1}H NMR spectrum of compound **15** in $CDCl_3$.

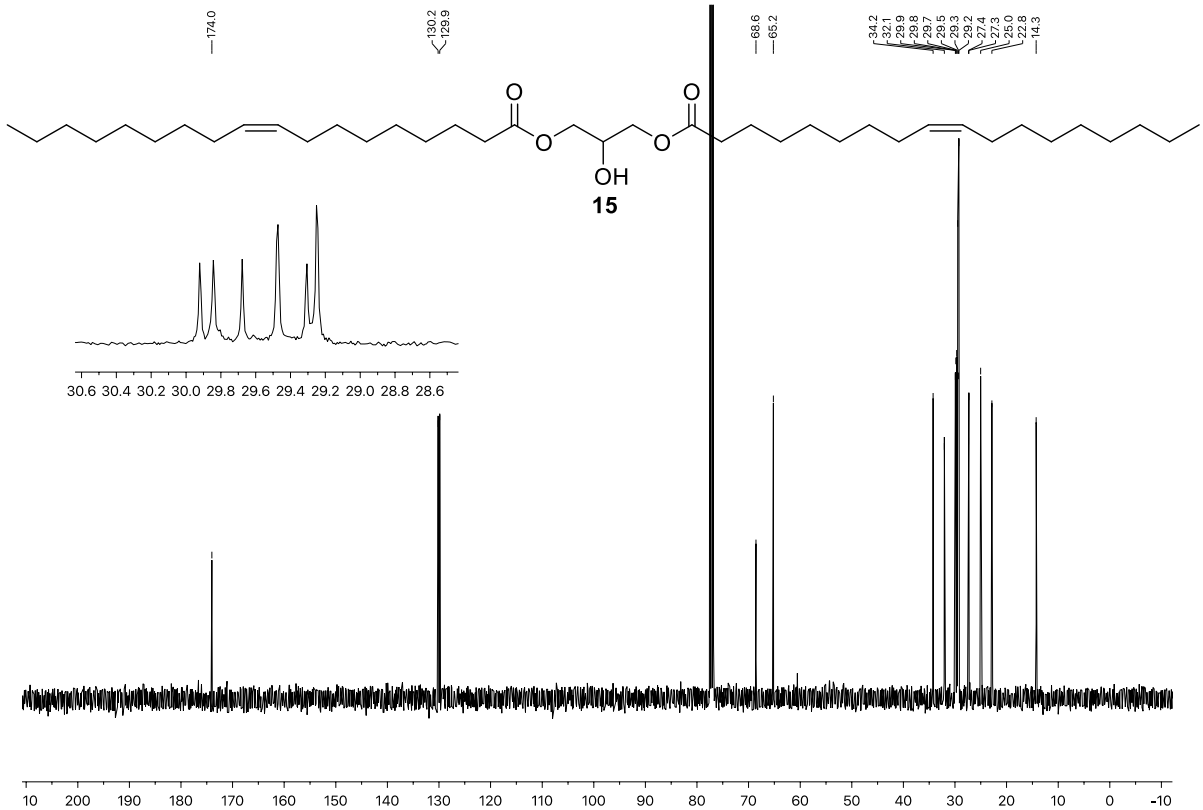

Figure S56: ^{13}C NMR spectrum of compound **15** in $CDCl_3$.

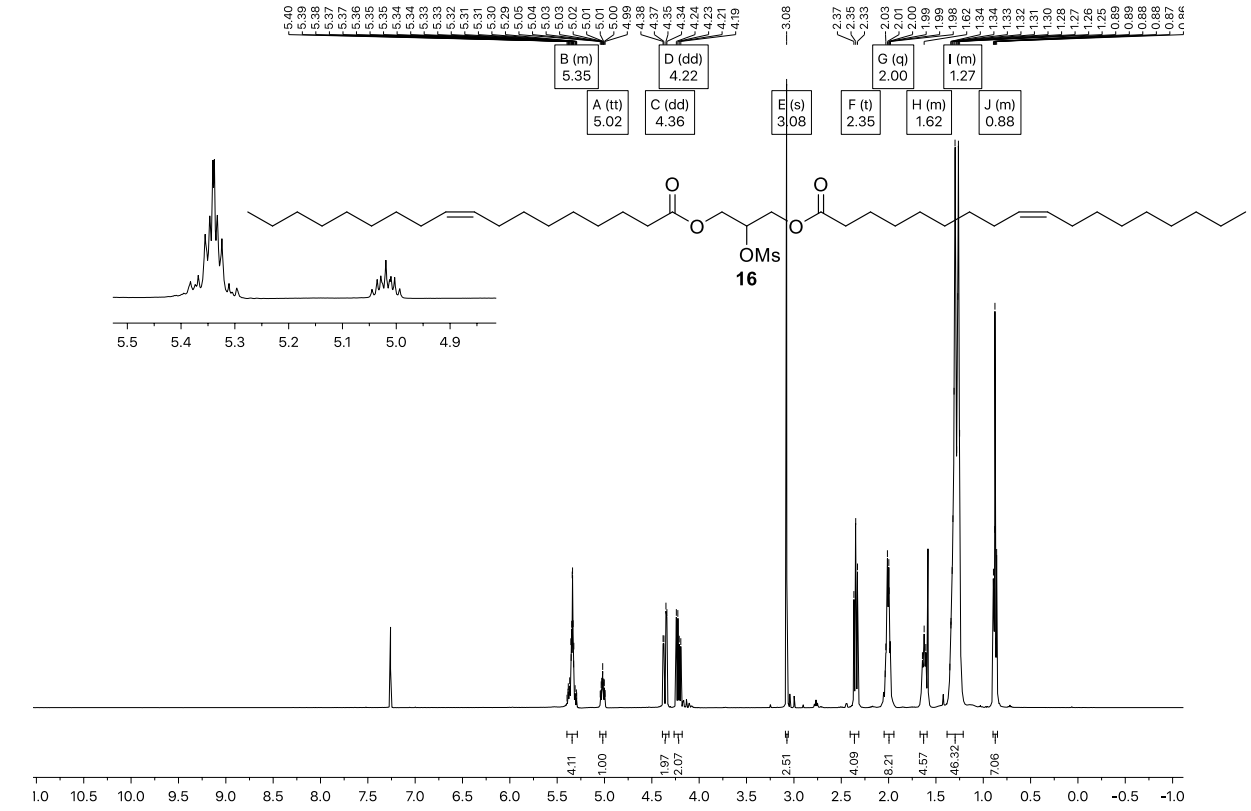

Figure S57: ^{1}H NMR spectrum of compound **16** in $CDCl_3$.

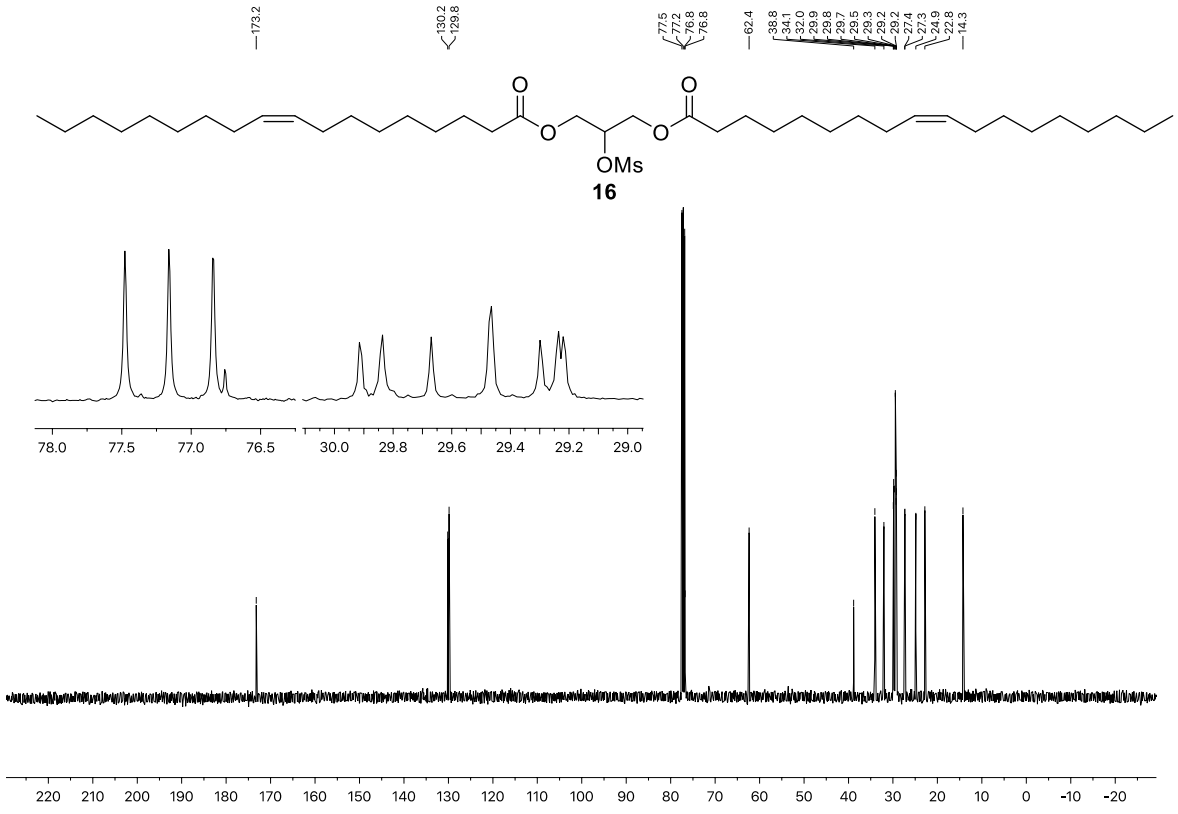

Figure S58: ^{13}C NMR spectrum of compound **16** in $CDCl_3$.

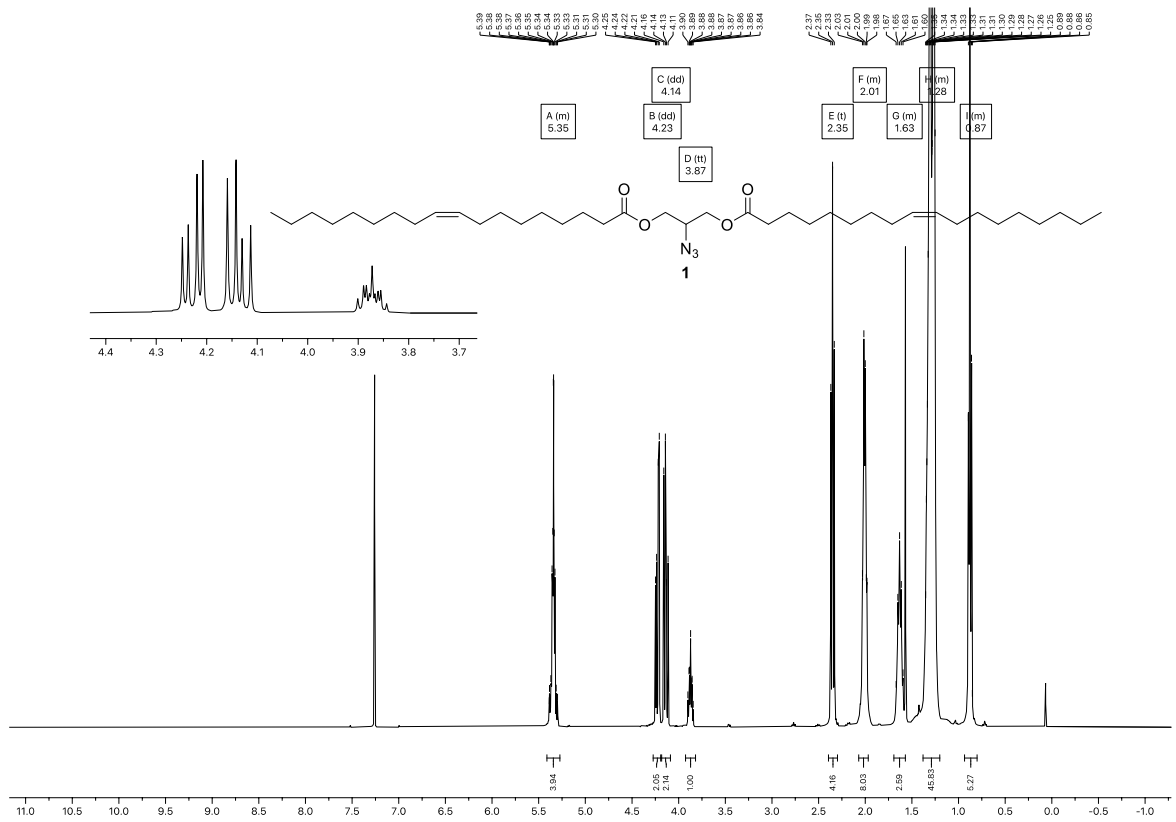

Figure S59: ^{1}H NMR spectrum of compound **1** in $CDCl_3$.

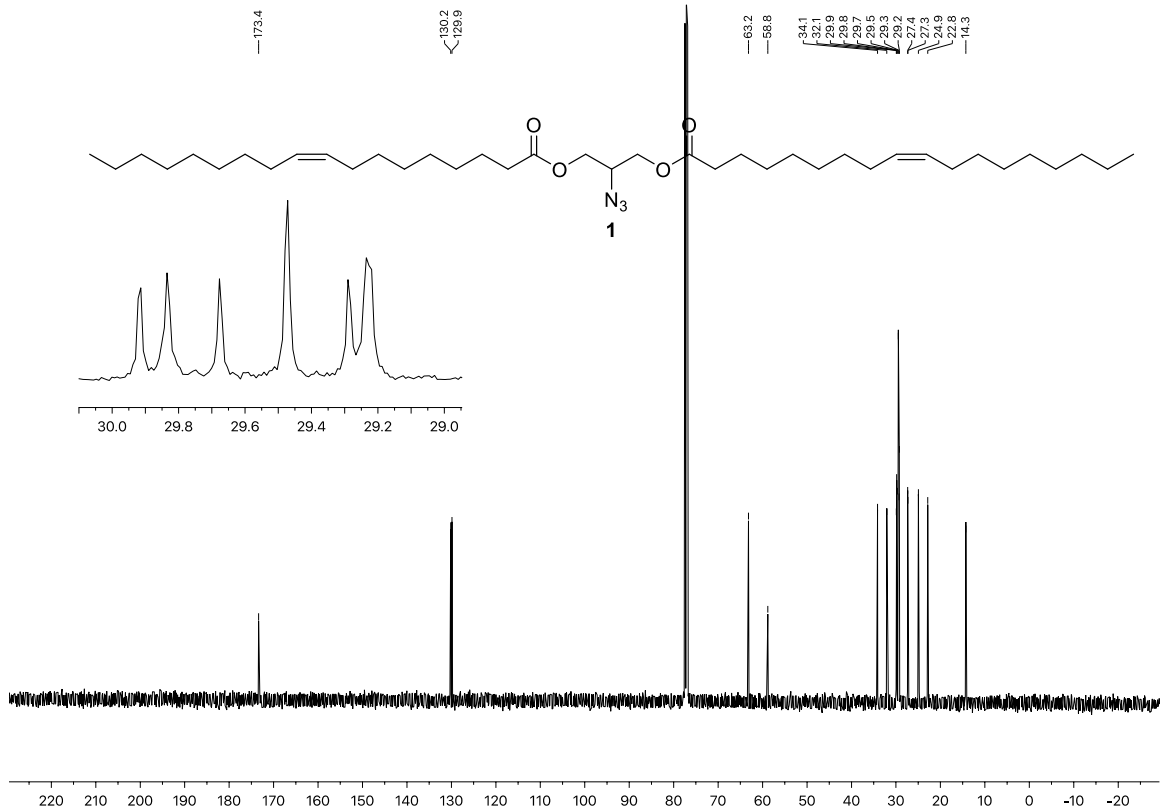

Figure S60: ^{13}C NMR spectrum of compound **1** in $CDCl_3$.

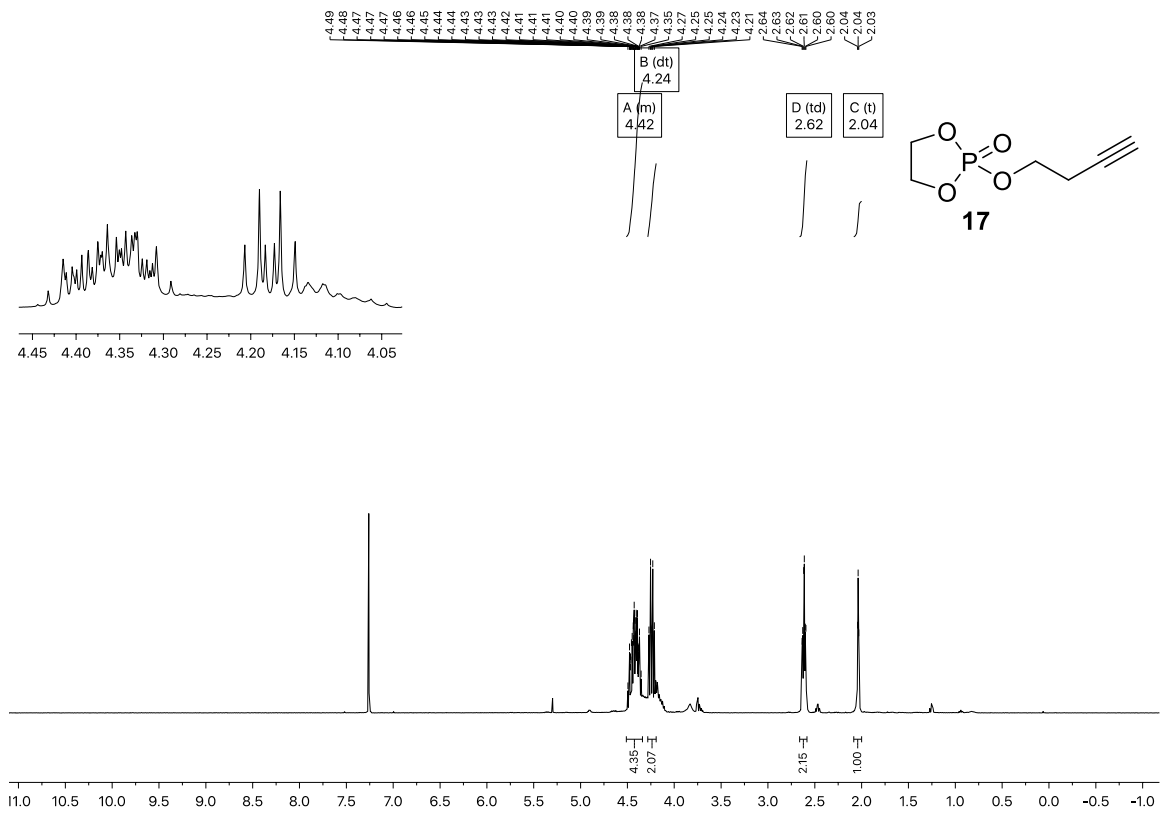

Figure S61: ^{1}H NMR spectrum of compound **17** in $CDCl_3$.

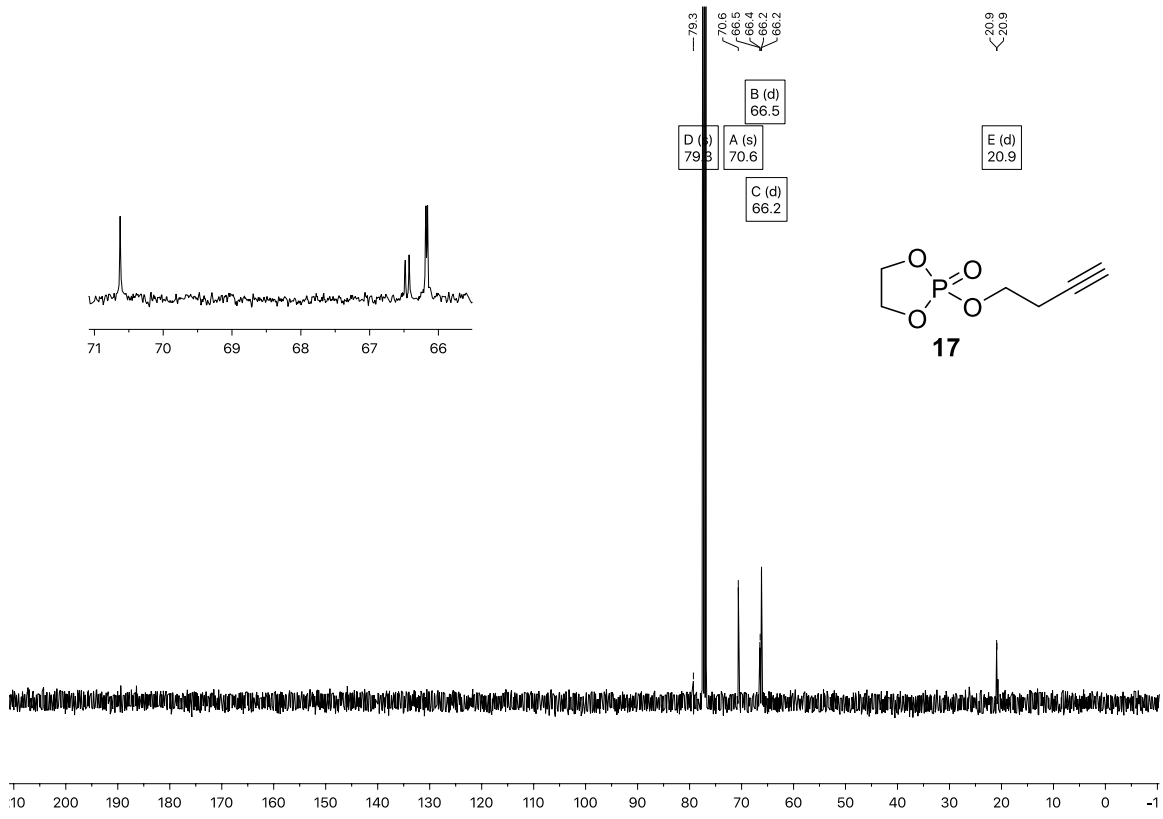

Figure S62: ^{13}C NMR spectrum of compound **17** in $CDCl_3$.

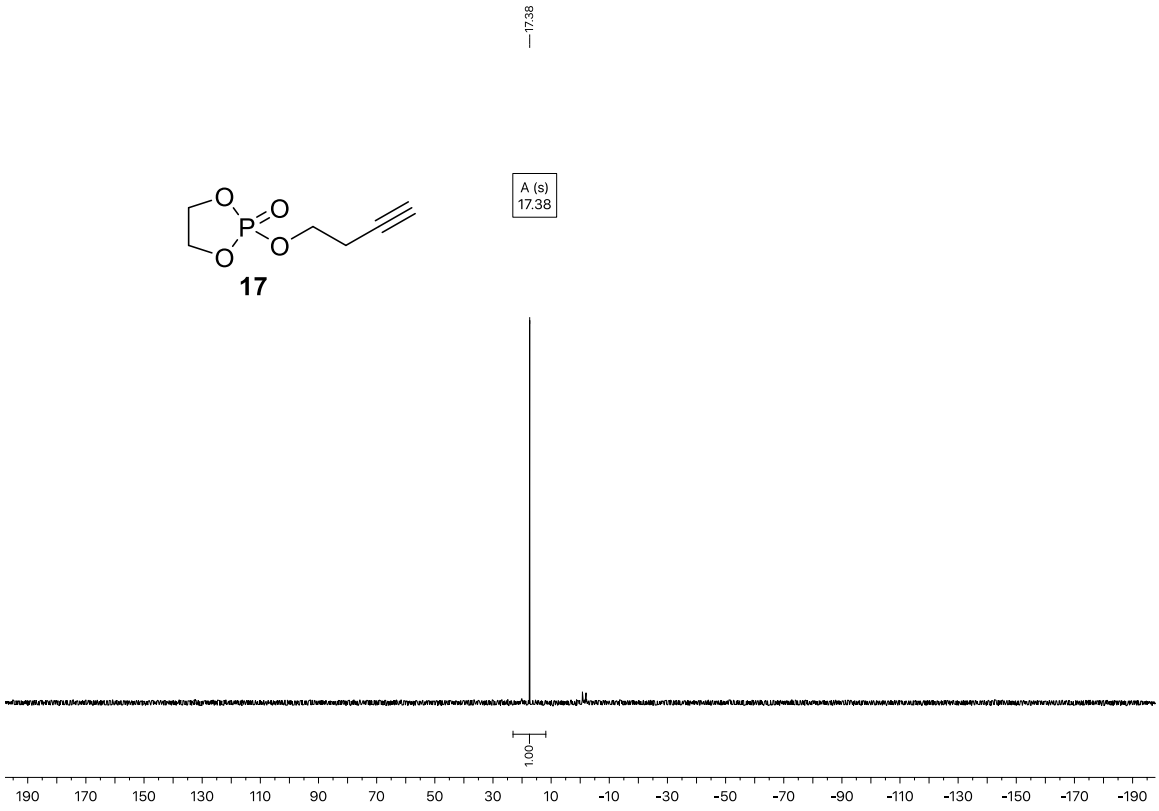

Figure S63: ^{31}P NMR spectrum of compound **17** in $CDCl_3$.

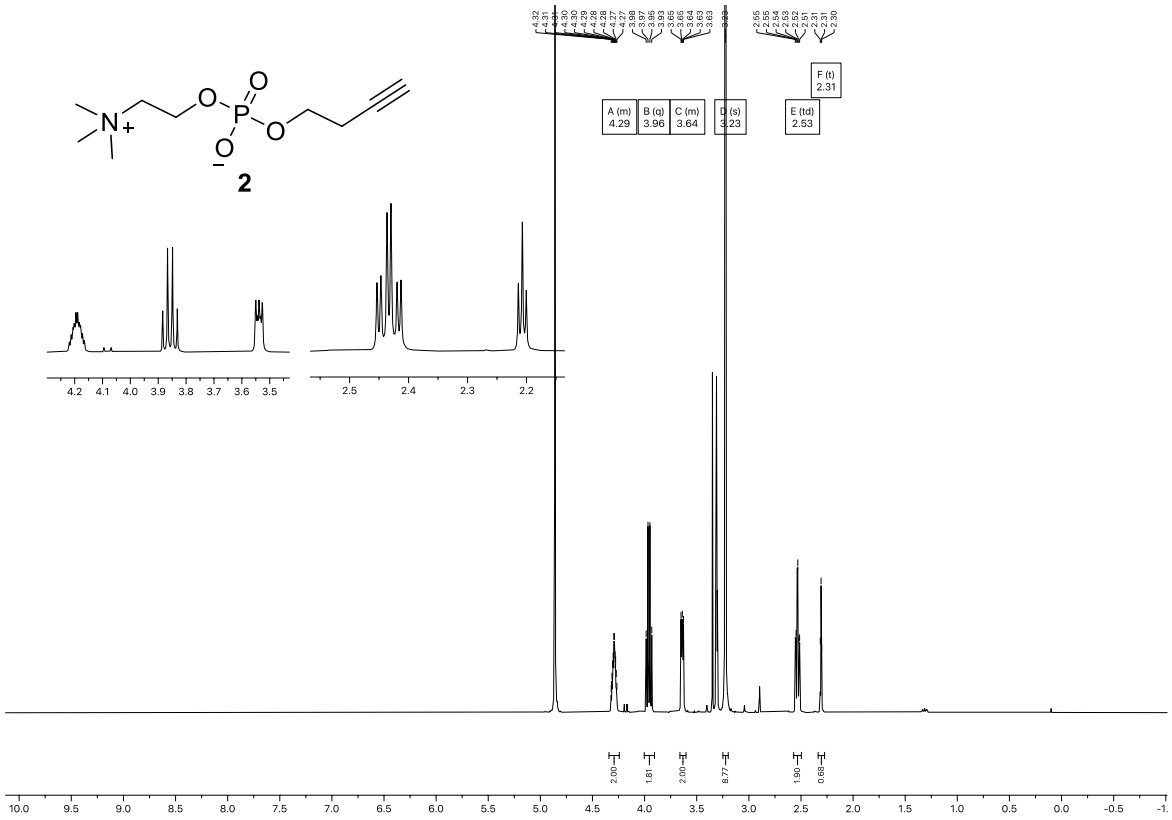

Figure S64: ^{1}H NMR spectrum of compound **2** in CD_3OD.

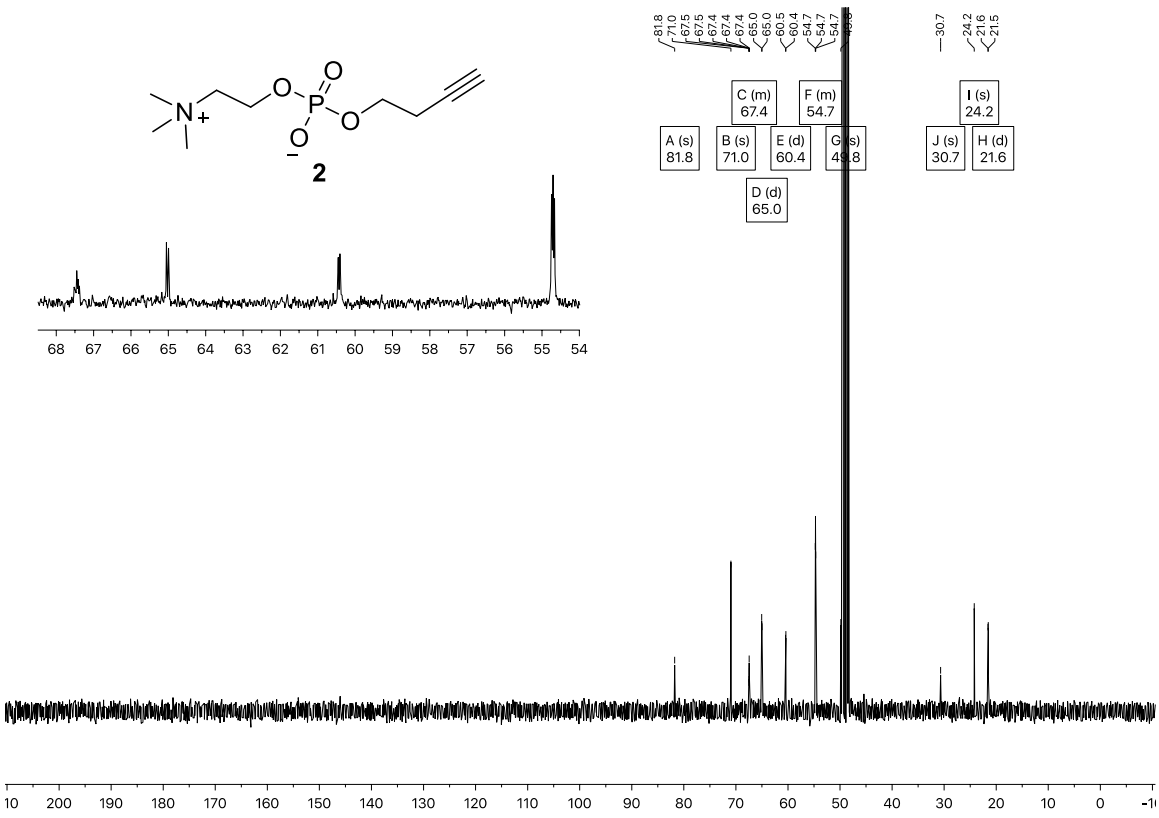

Figure S65: ^{13}C NMR spectrum of compound **2** in CD_3OD.

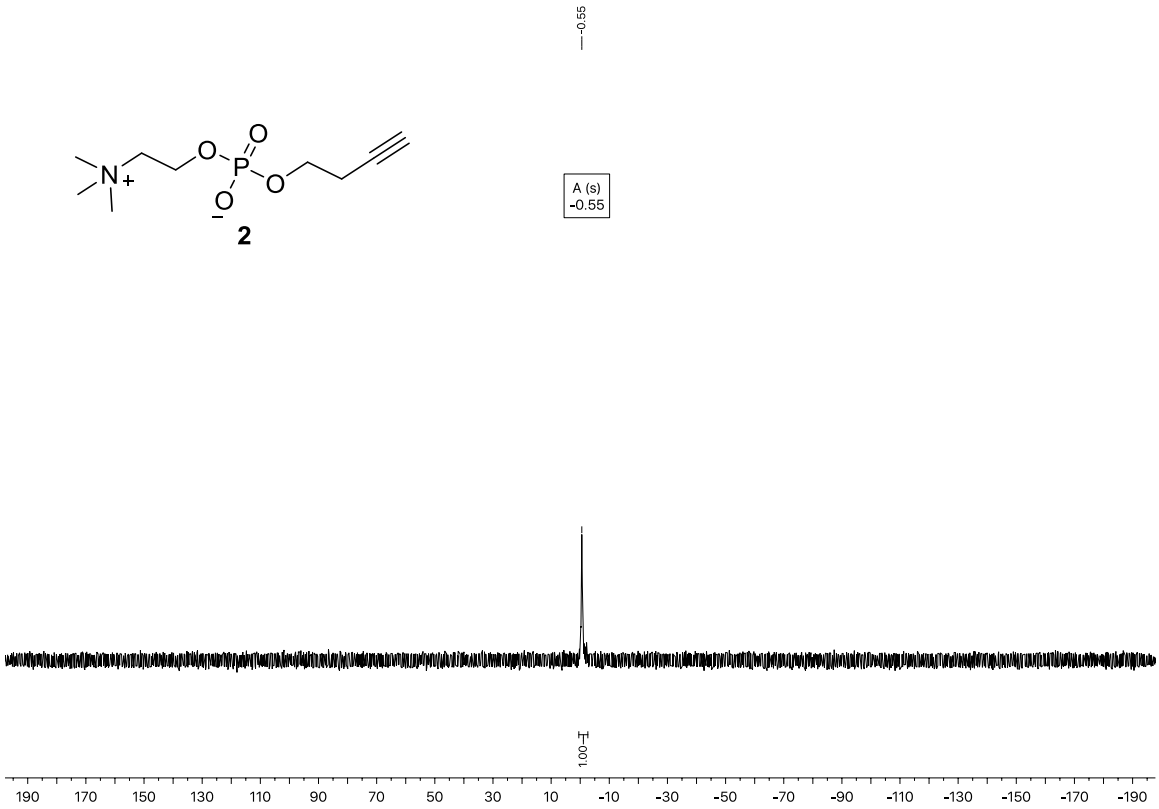

Figure S66: ^{31}P NMR spectrum of compound **2** in CD_3OD.

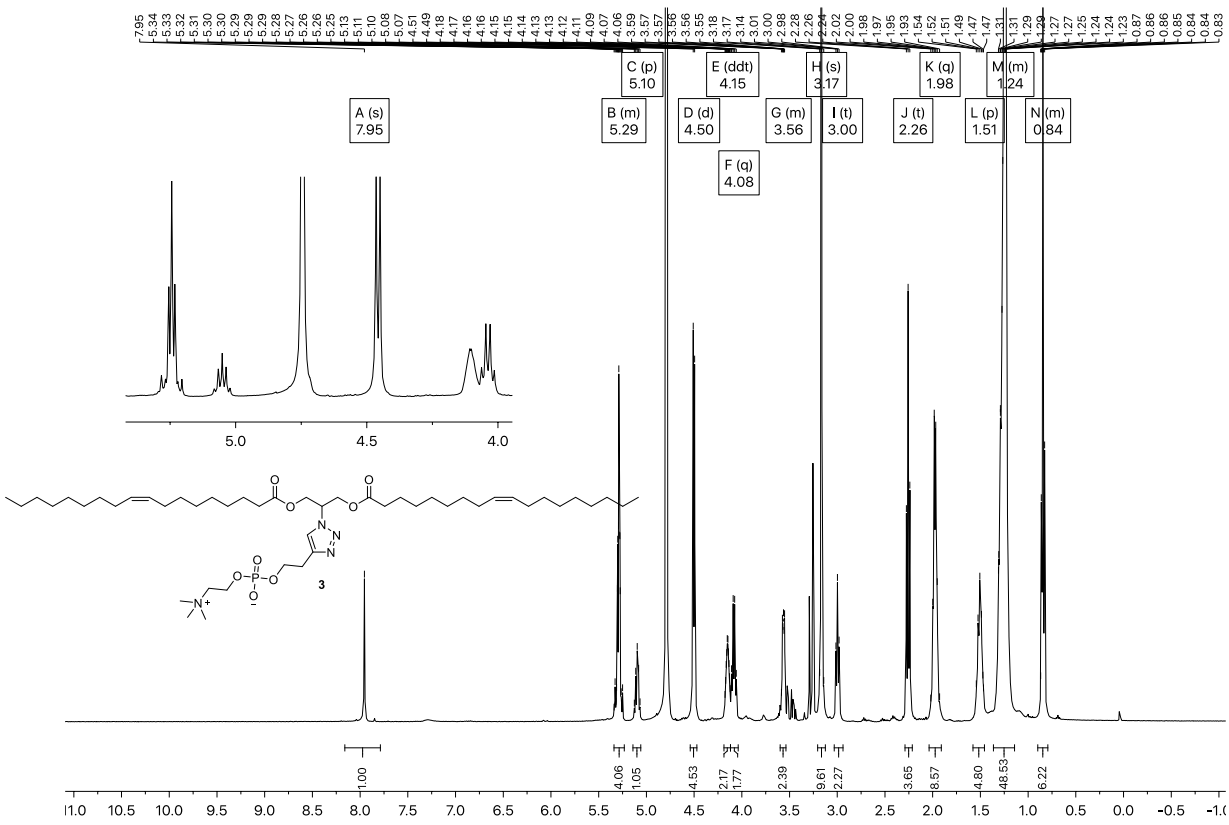

Figure S67: ^{1}H NMR spectrum of compound **3** in CD_3OD.

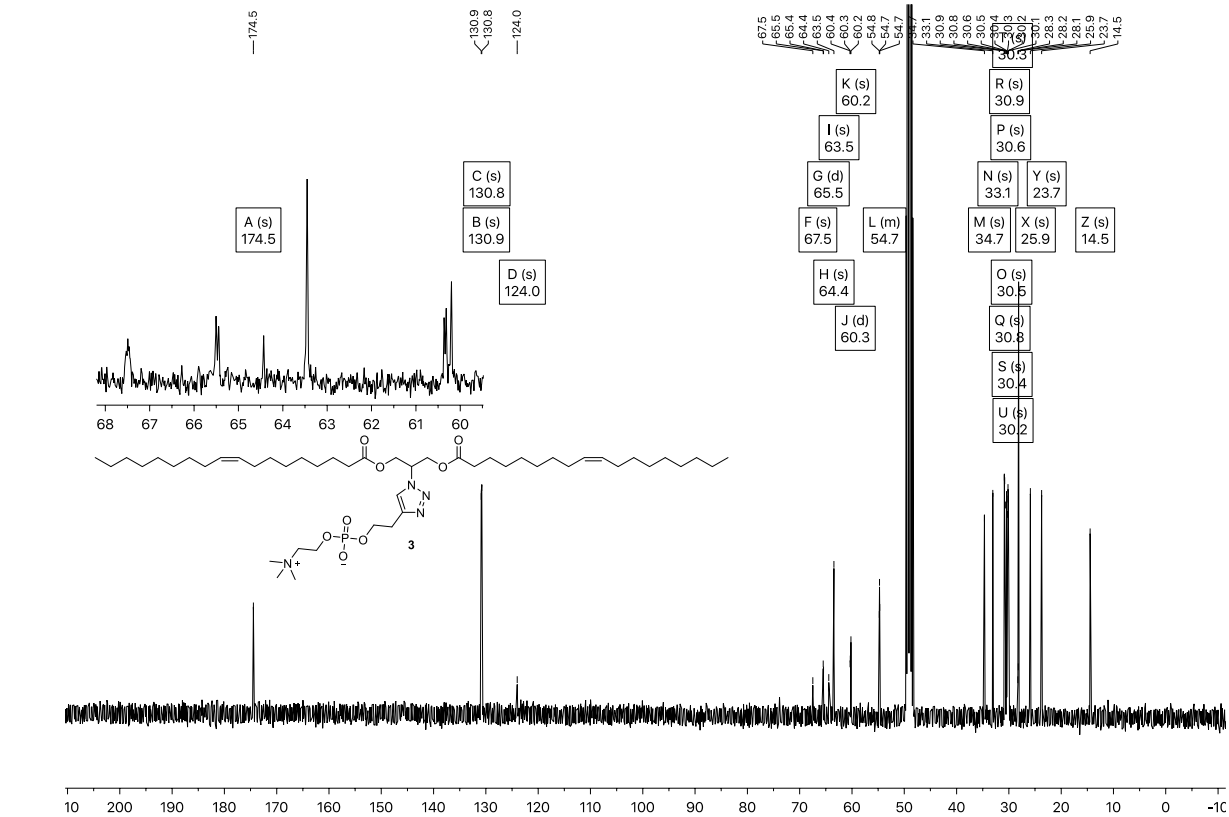

Figure S68: ^{13}C NMR spectrum of compound **3** in CD_3OD.

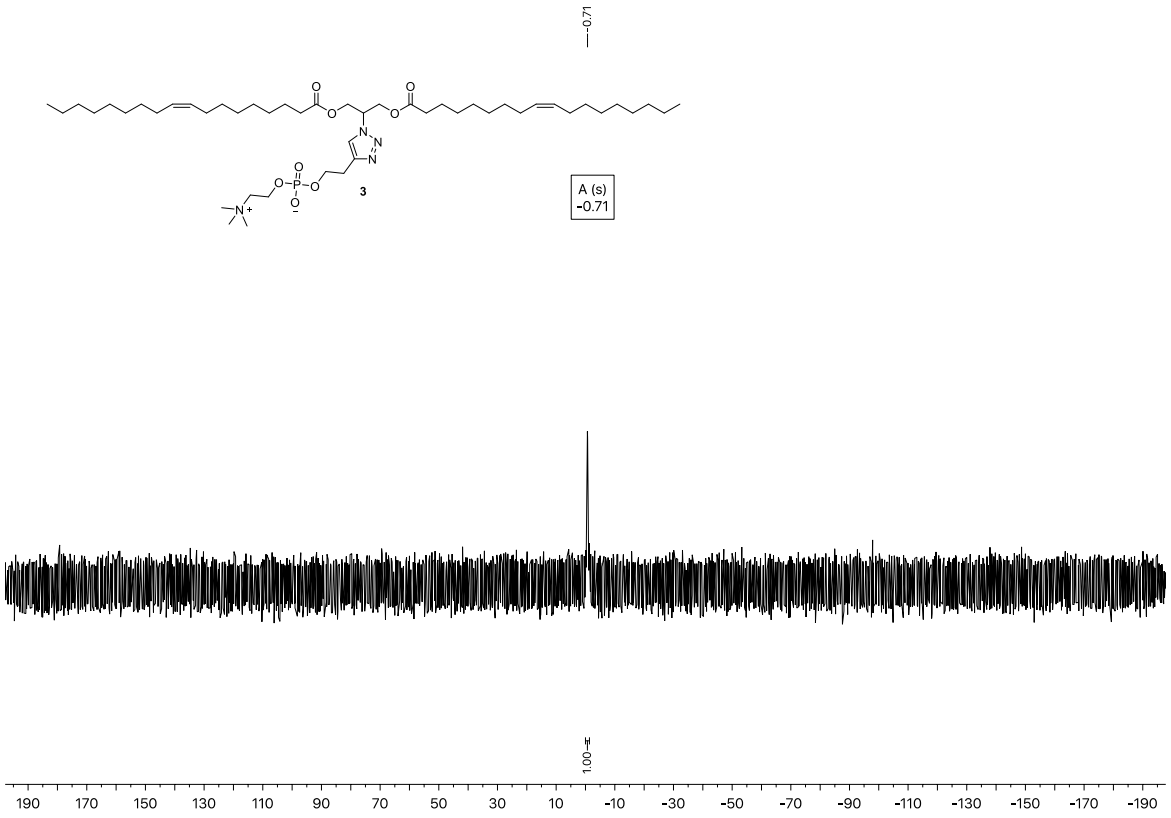

Figure S69: ^{31}P NMR spectrum of compound **3** in CD_3OD.

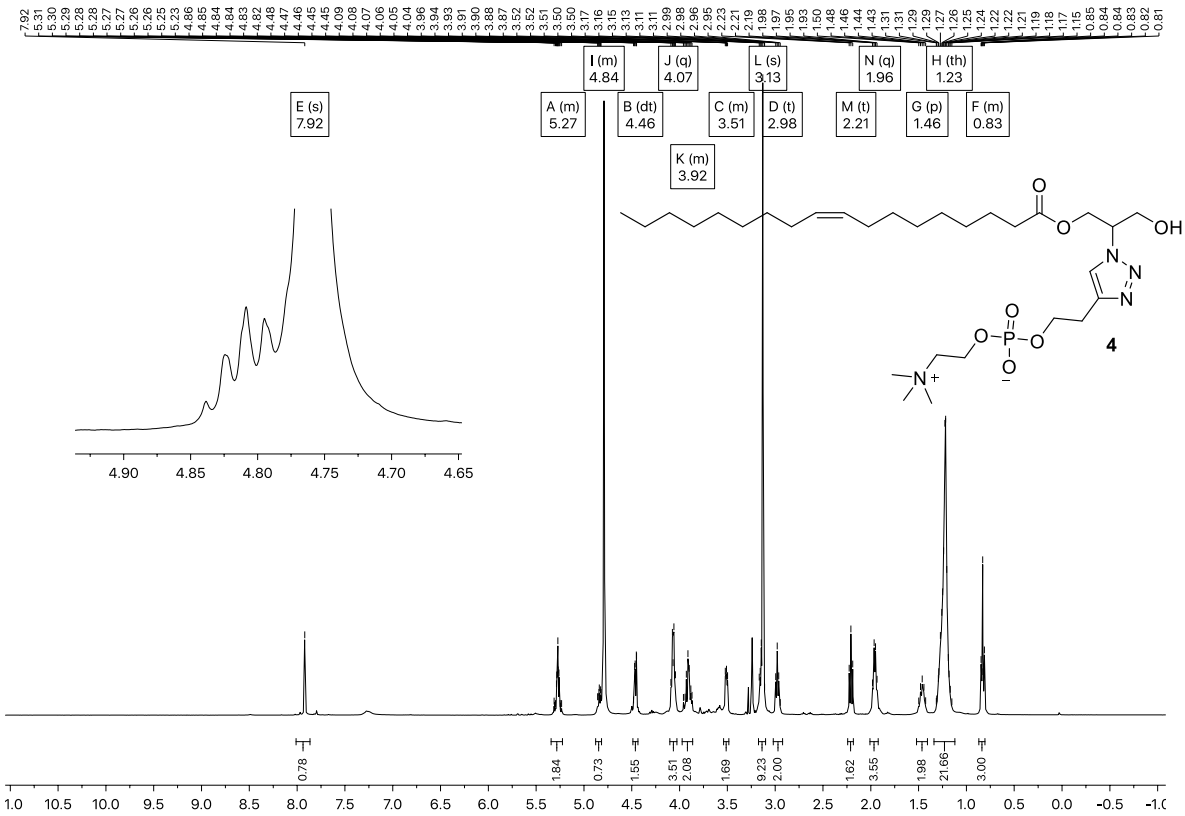

Figure S70: ^{1}H NMR spectrum of compound **4** in CD_3OD.

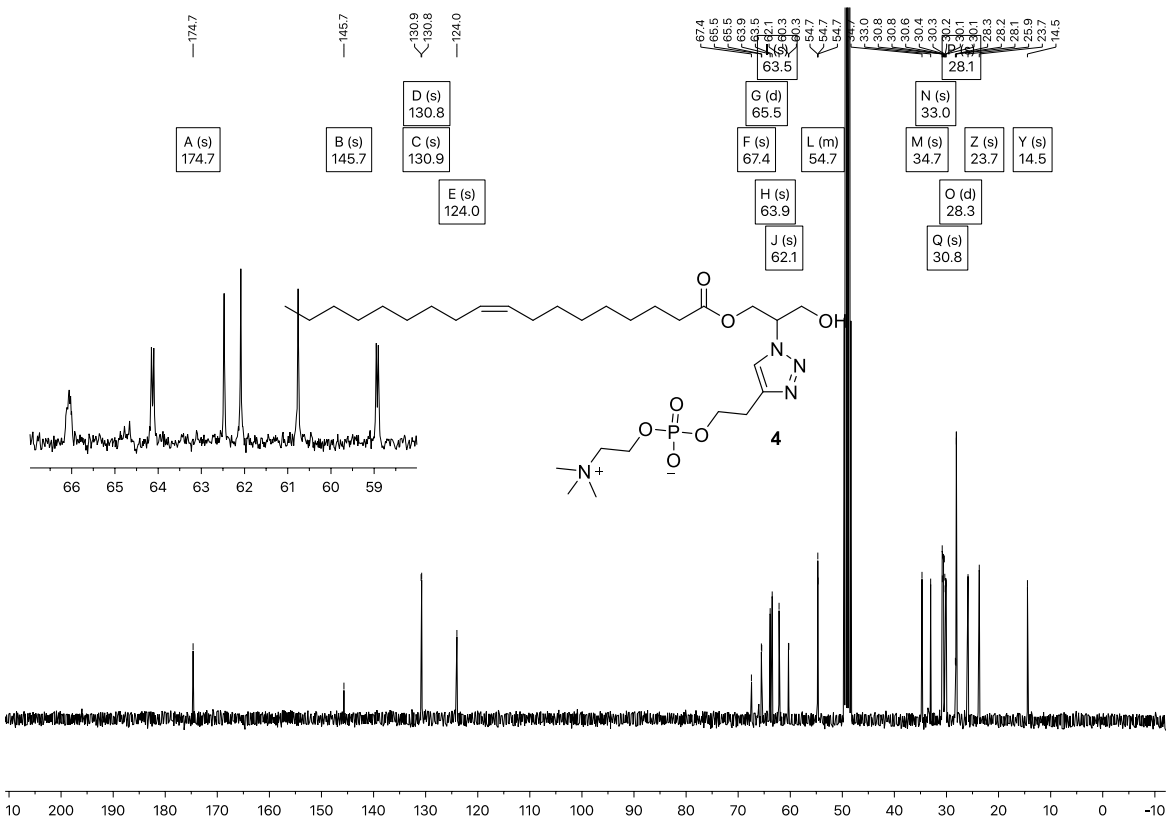

Figure S71: ^{13}C NMR spectrum of compound **4** in CD_3OD.

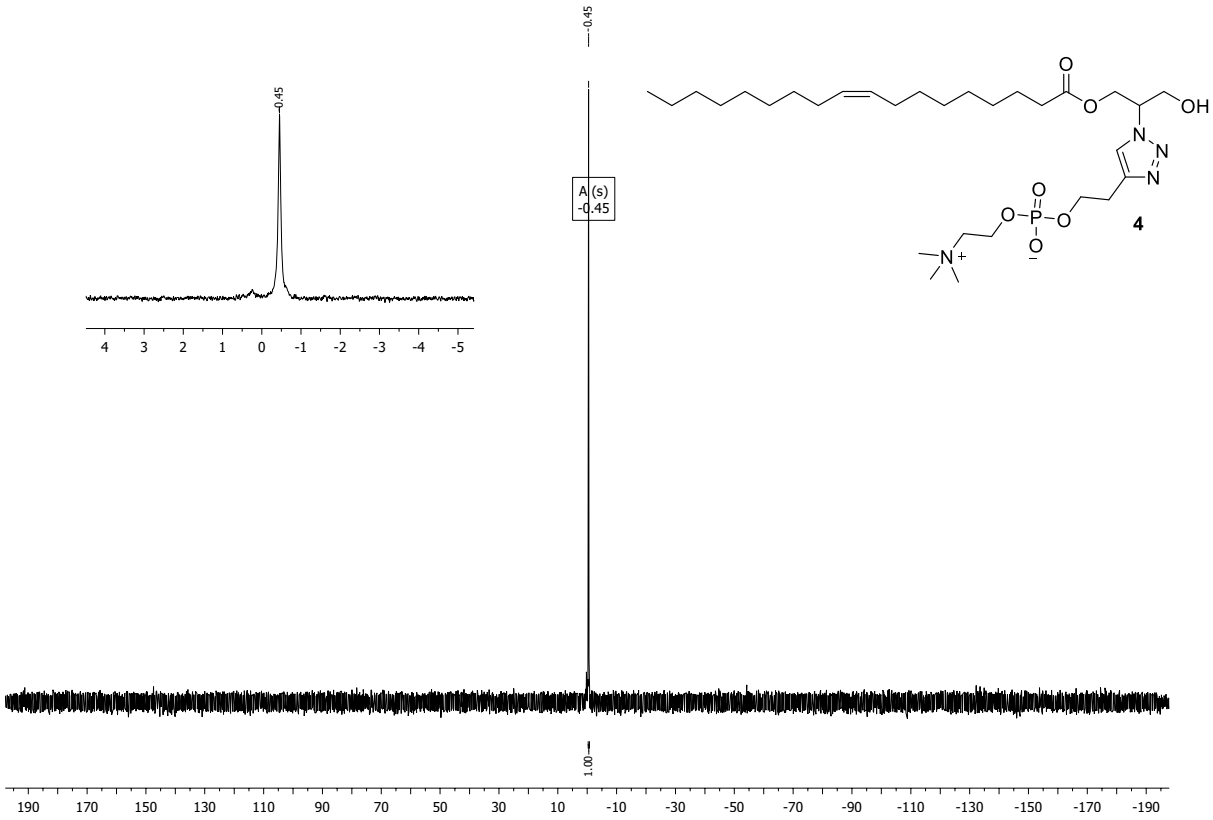

Figure S72: ^{31}P NMR spectrum of compound **4** in CD_3OD.

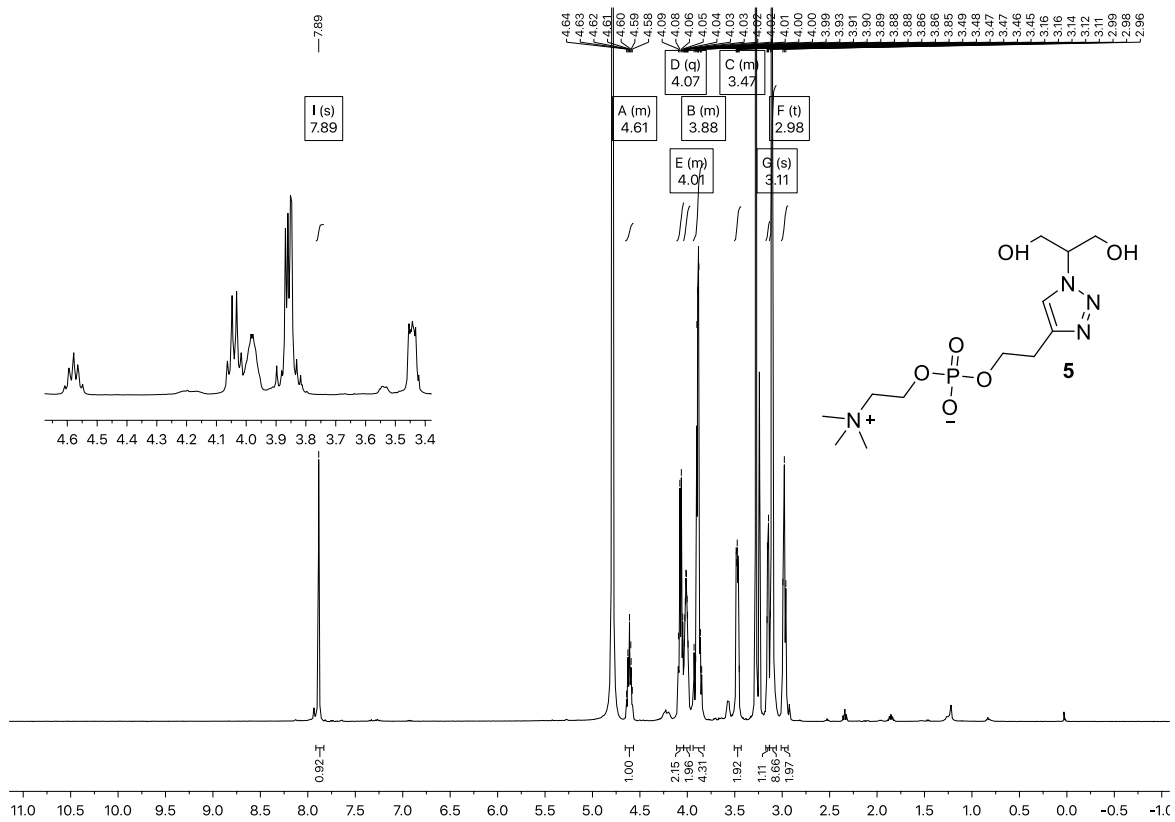

Figure S73: ^{1}H NMR spectrum of compound **5** in CD_3OD.

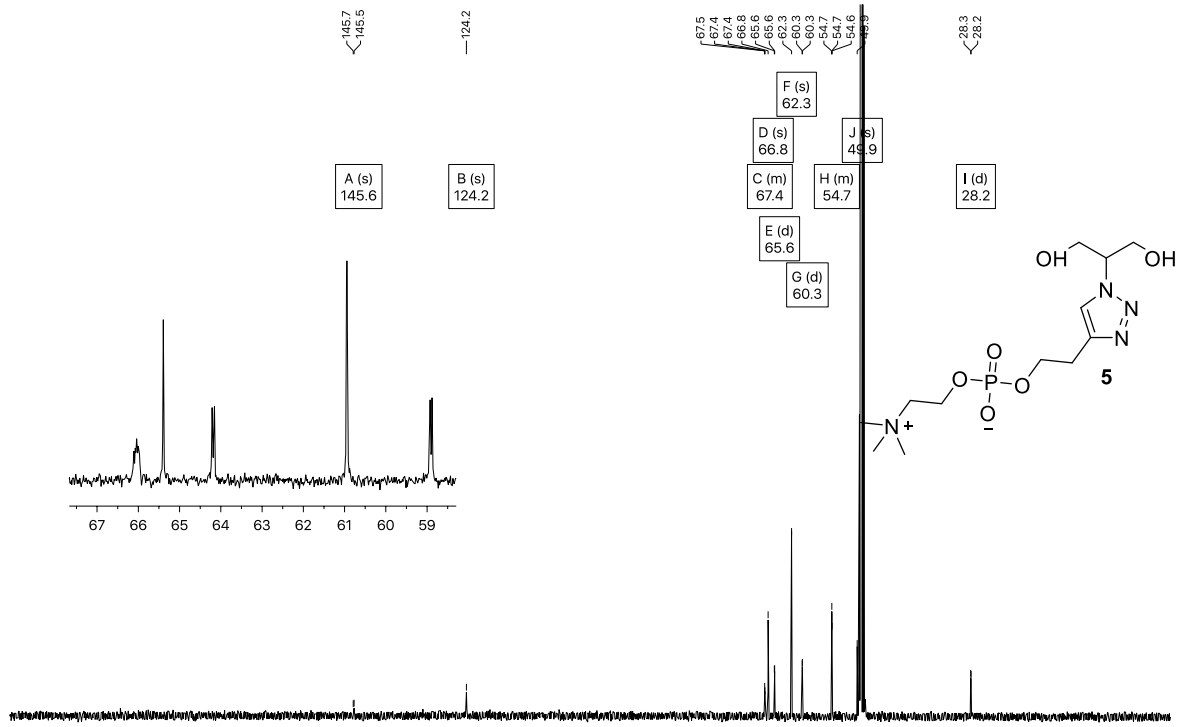

Figure S74: ^{13}C NMR spectrum of compound **5** in CD_3OD.

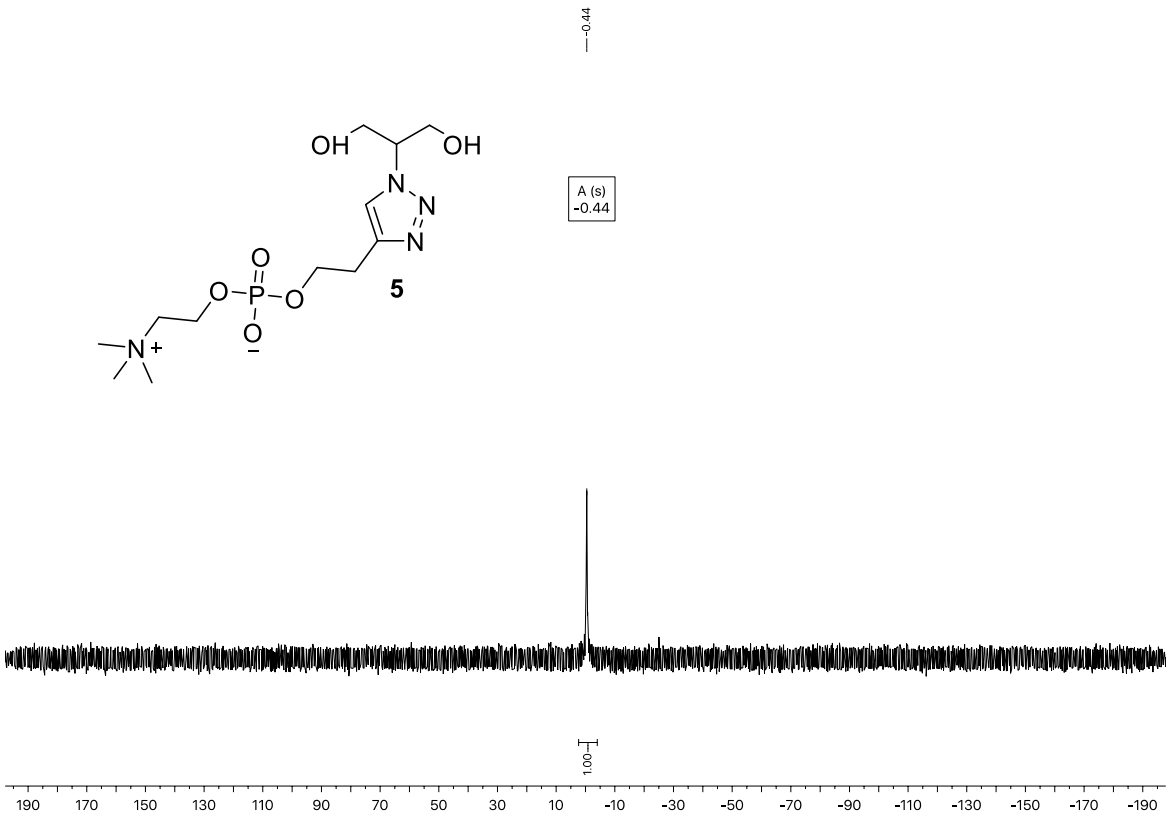

Figure S75: ^{31}P NMR spectrum of compound **5** in CD_3OD.

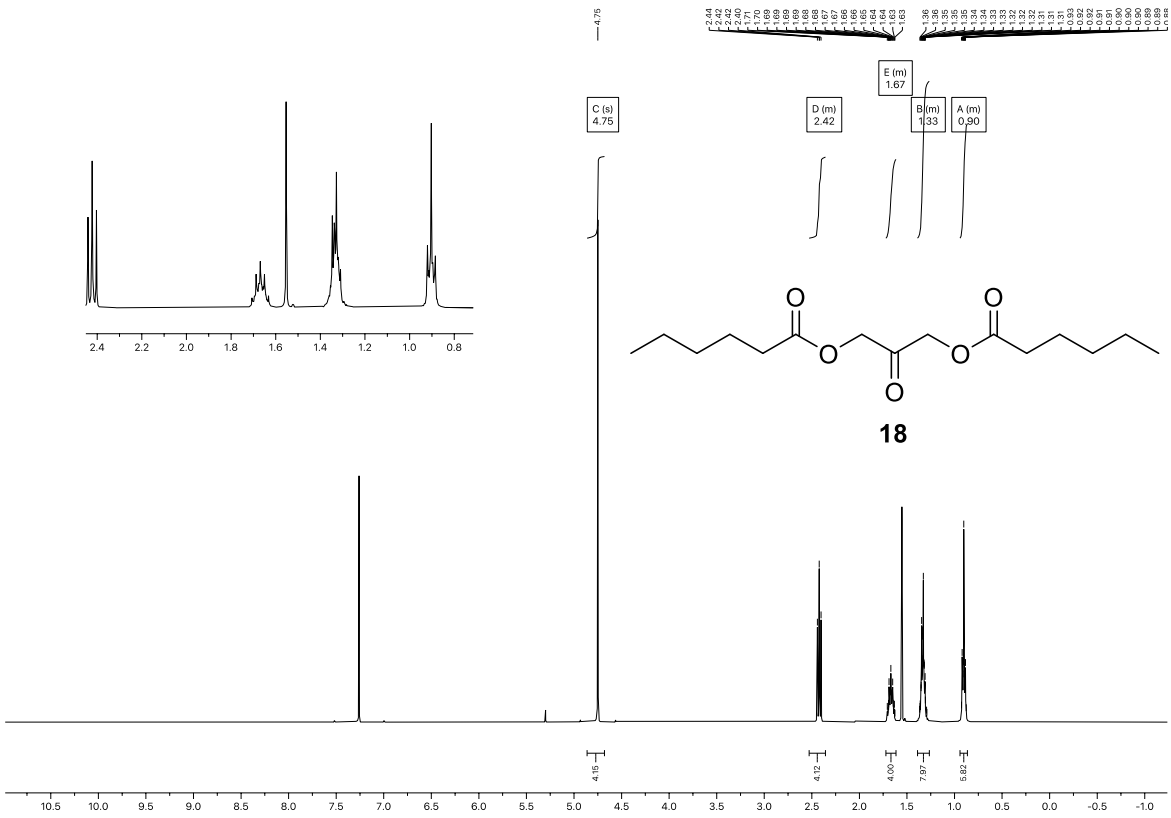

Figure S76: ^{1}H NMR spectrum of compound **18** in $CDCl_3$.

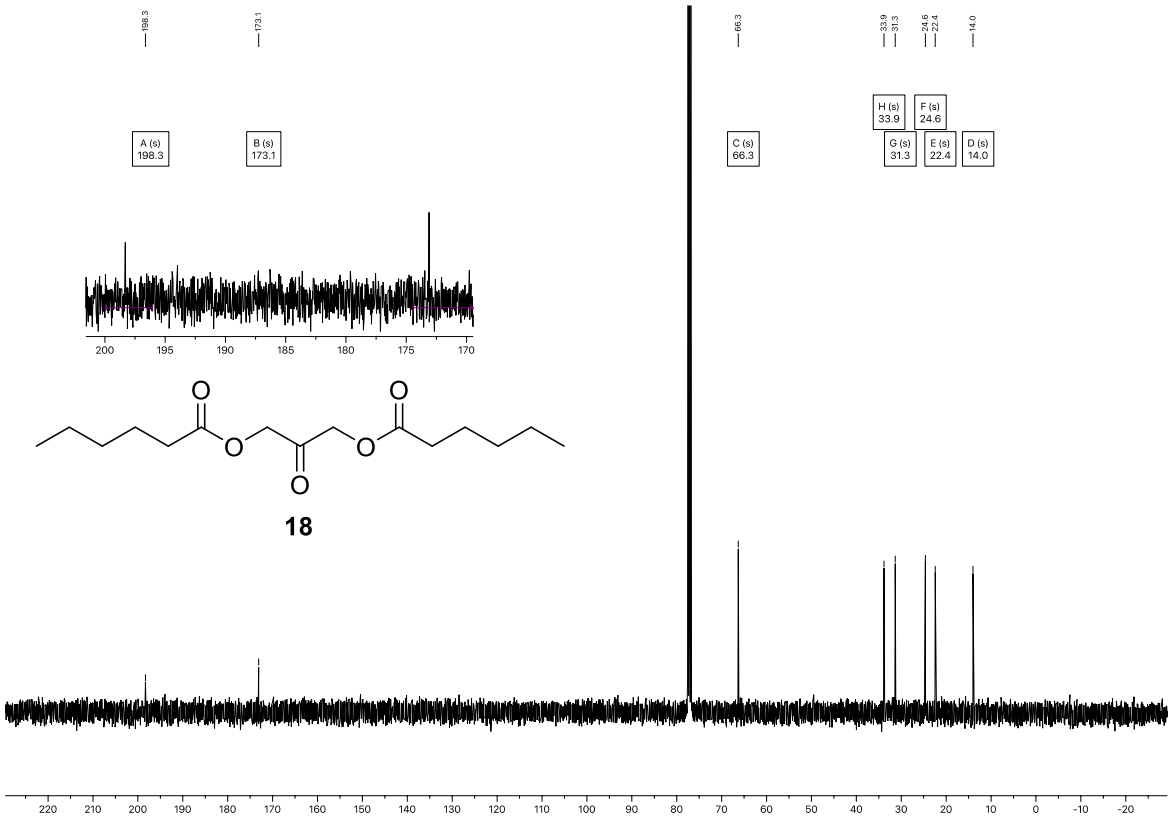

Figure S77: ^{13}C NMR spectrum of compound **18** in $CDCl_3$.

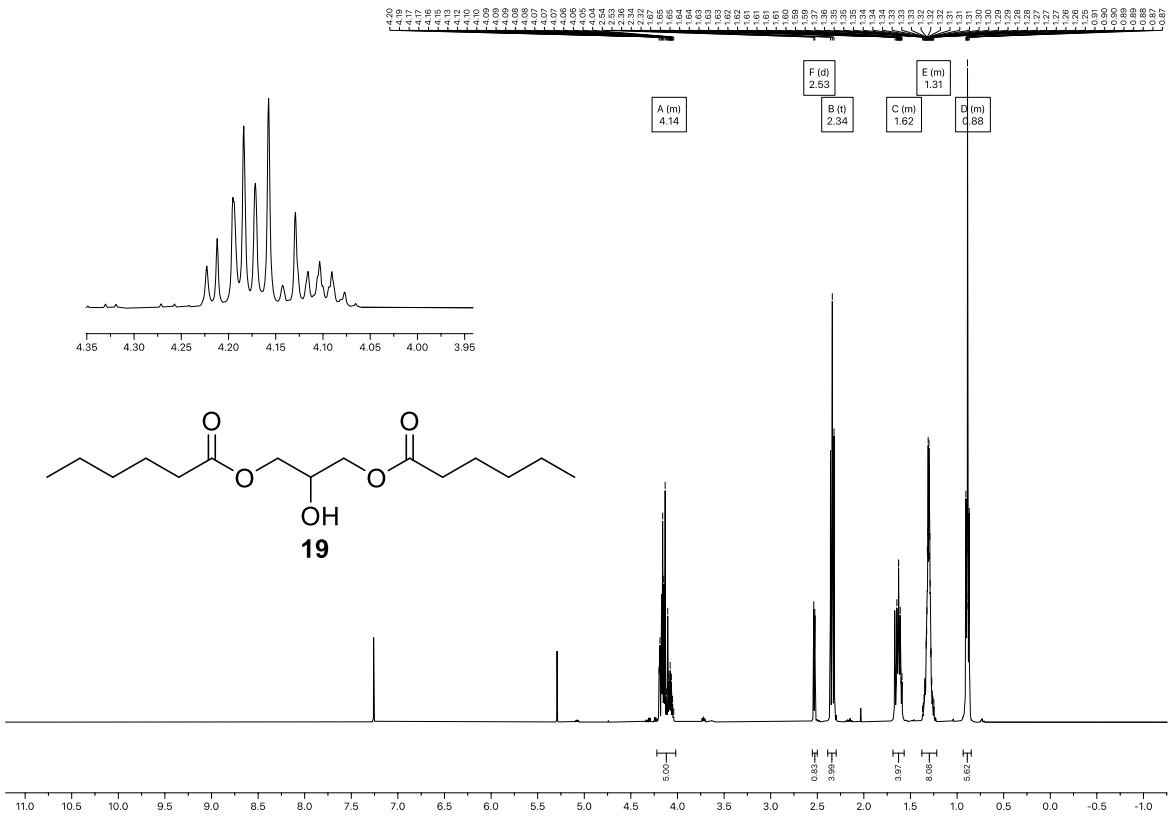

Figure S78: ^{1}H NMR spectrum of compound **19** in $CDCl_3$.

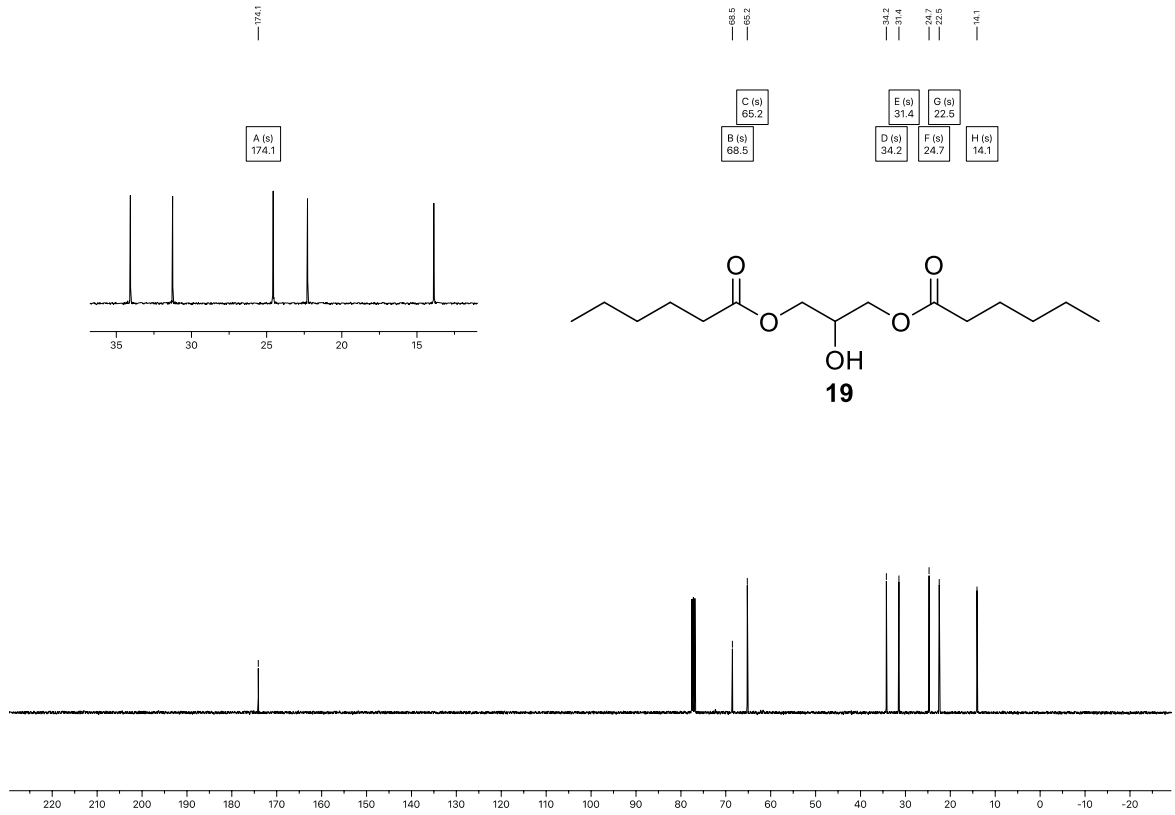

Figure S79: ^{13}C NMR spectrum of compound **19** in $CDCl_3$.

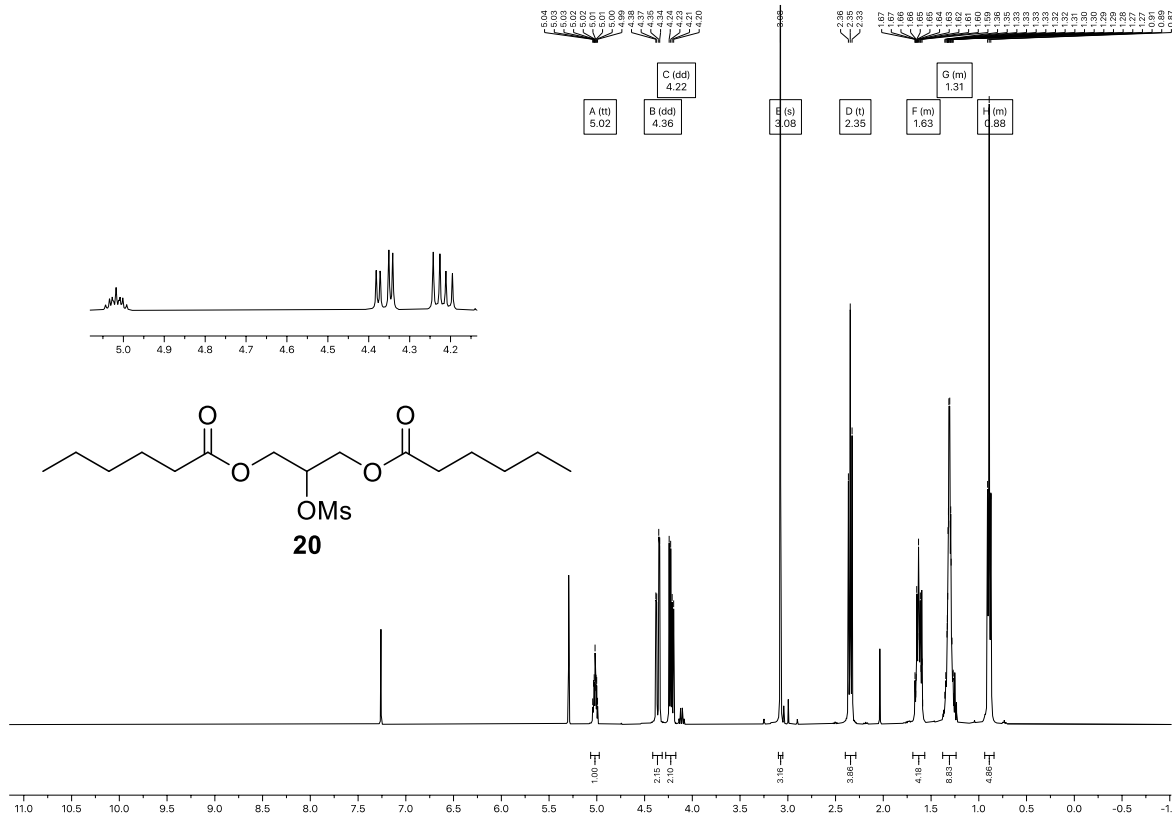

Figure S80: ^{1}H NMR spectrum of compound **20** in $CDCl_3$.

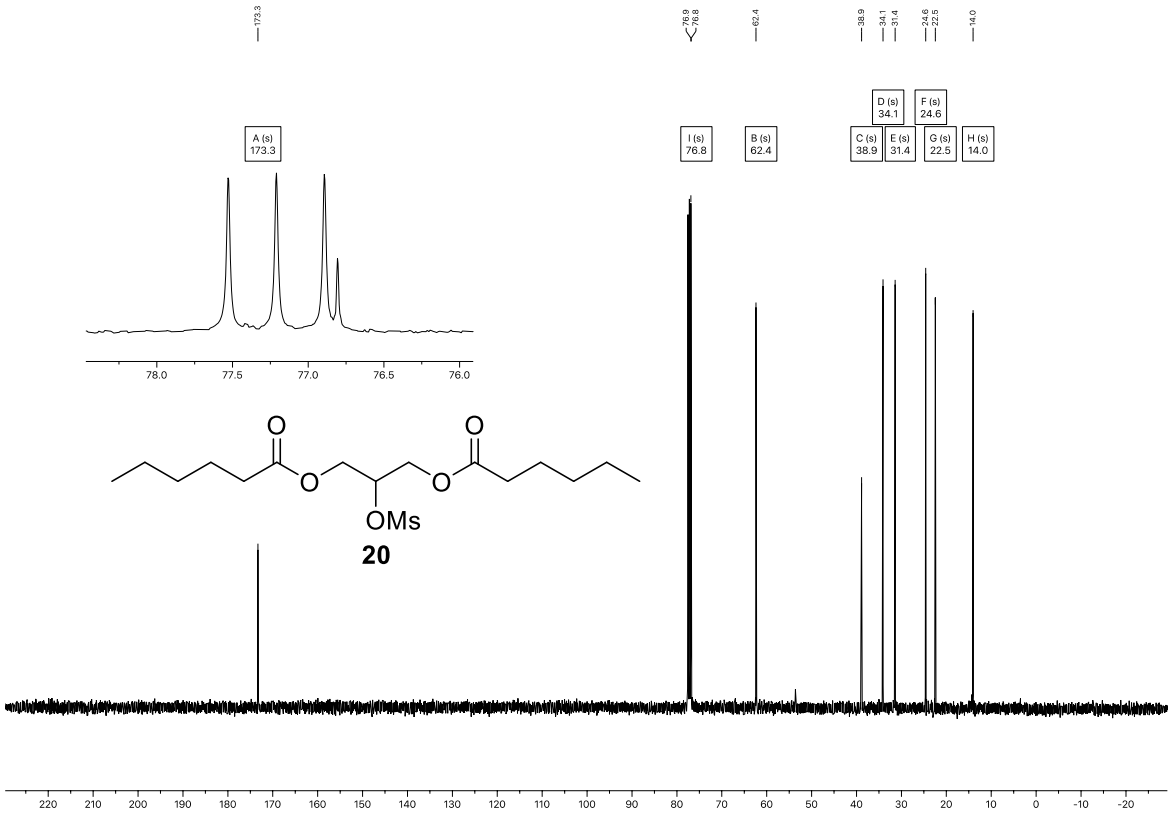

Figure S81: ^{13}C NMR spectrum of compound **20** in $CDCl_3$.

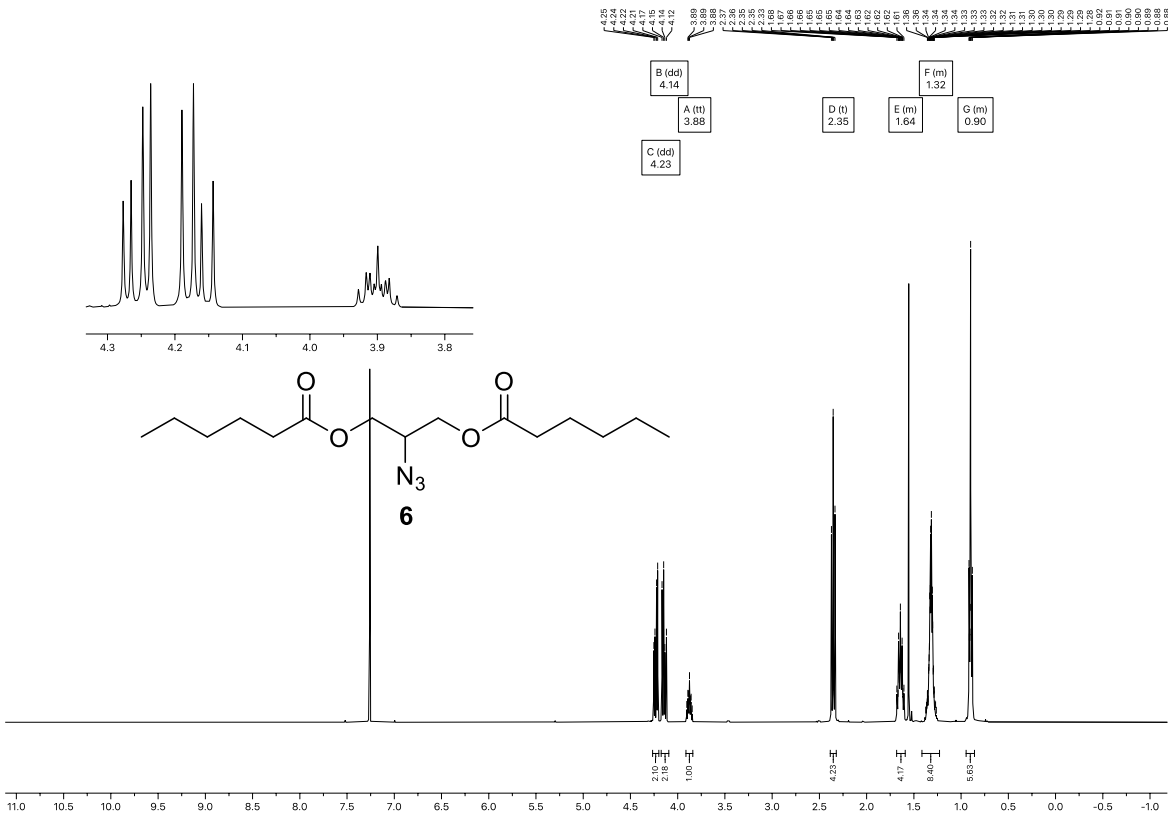

Figure S82: ^{1}H NMR spectrum of compound **6** in $CDCl_3$.

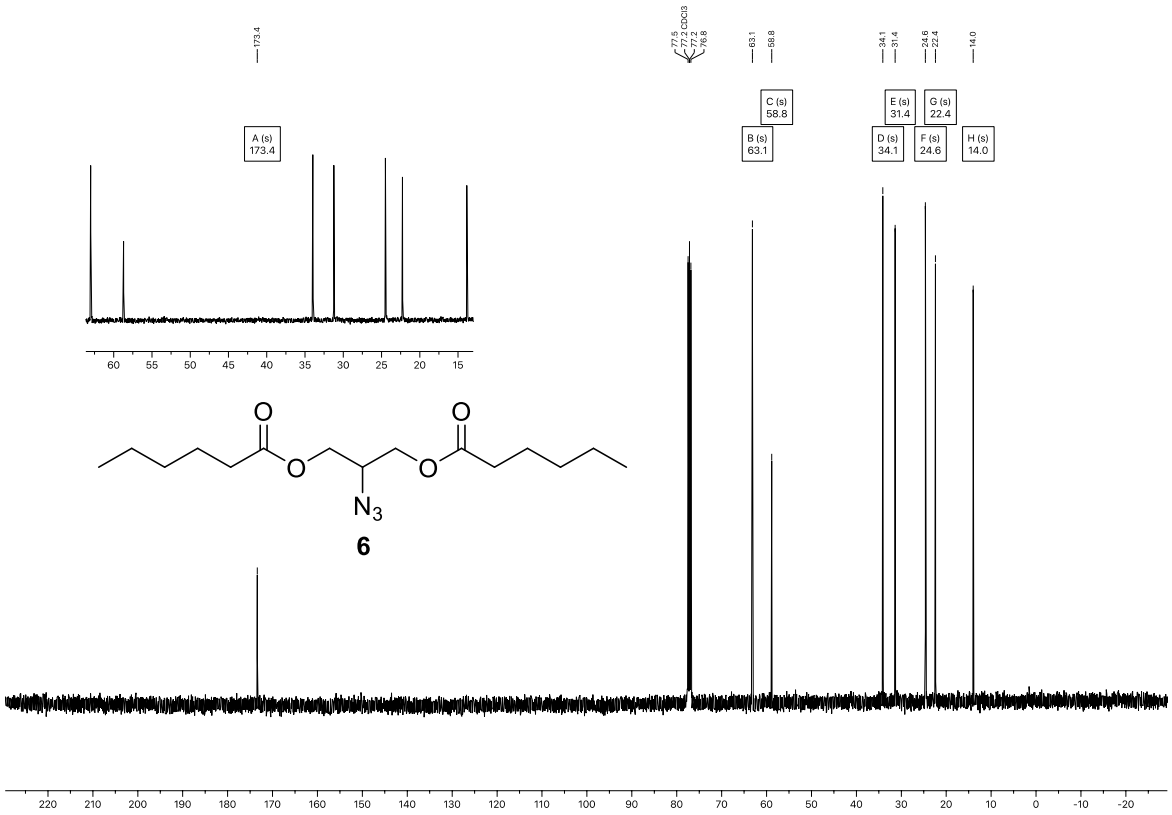

Figure S83: ^{13}C NMR spectrum of compound **6** in $CDCl_3$.

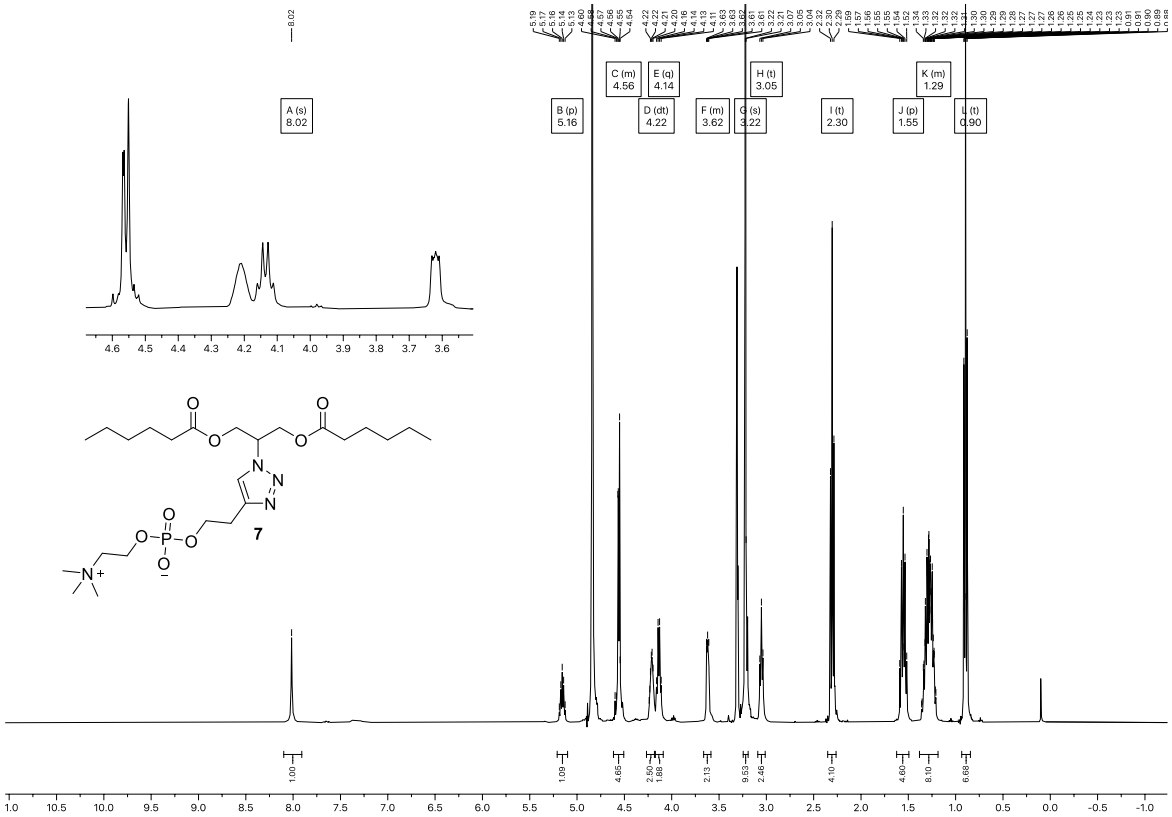

Figure S84: ^{1}H NMR spectrum of compound **7** in CD_3OD.

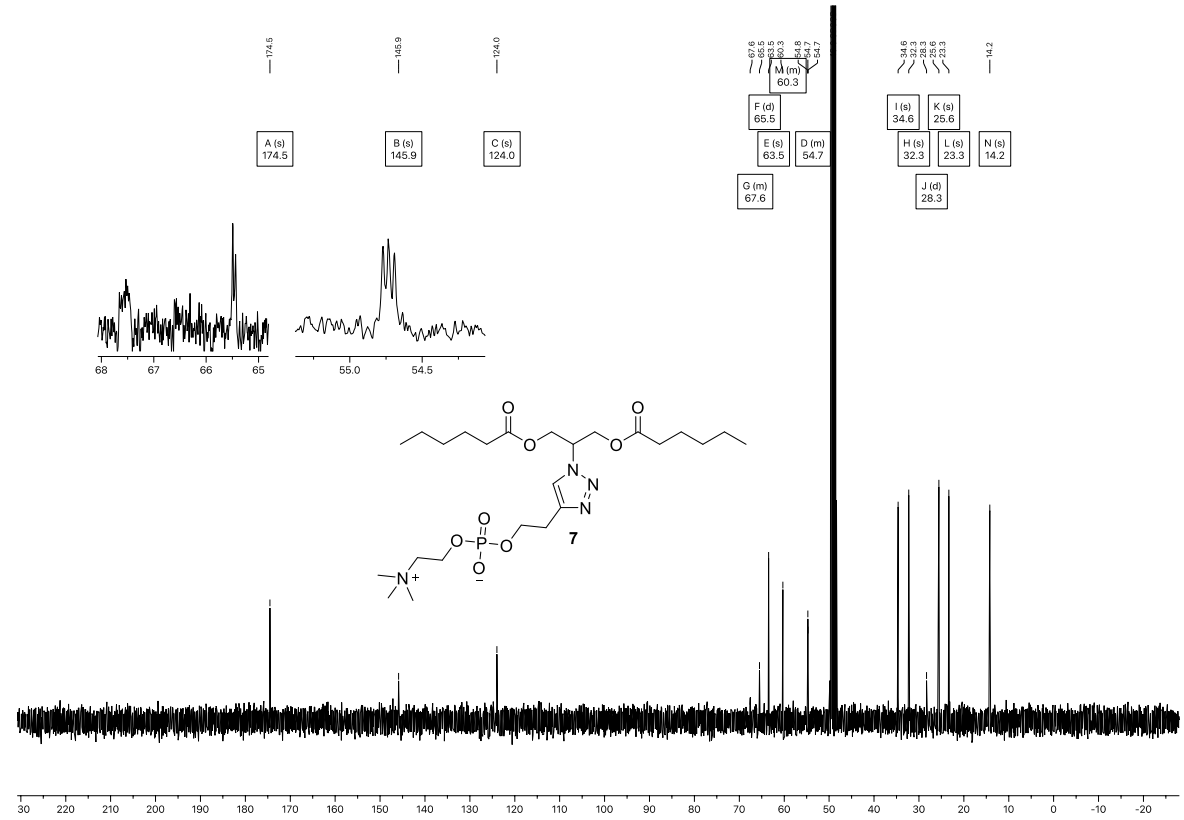

Figure S85: ^{13}C NMR spectrum of compound **7** in CD_3OD.

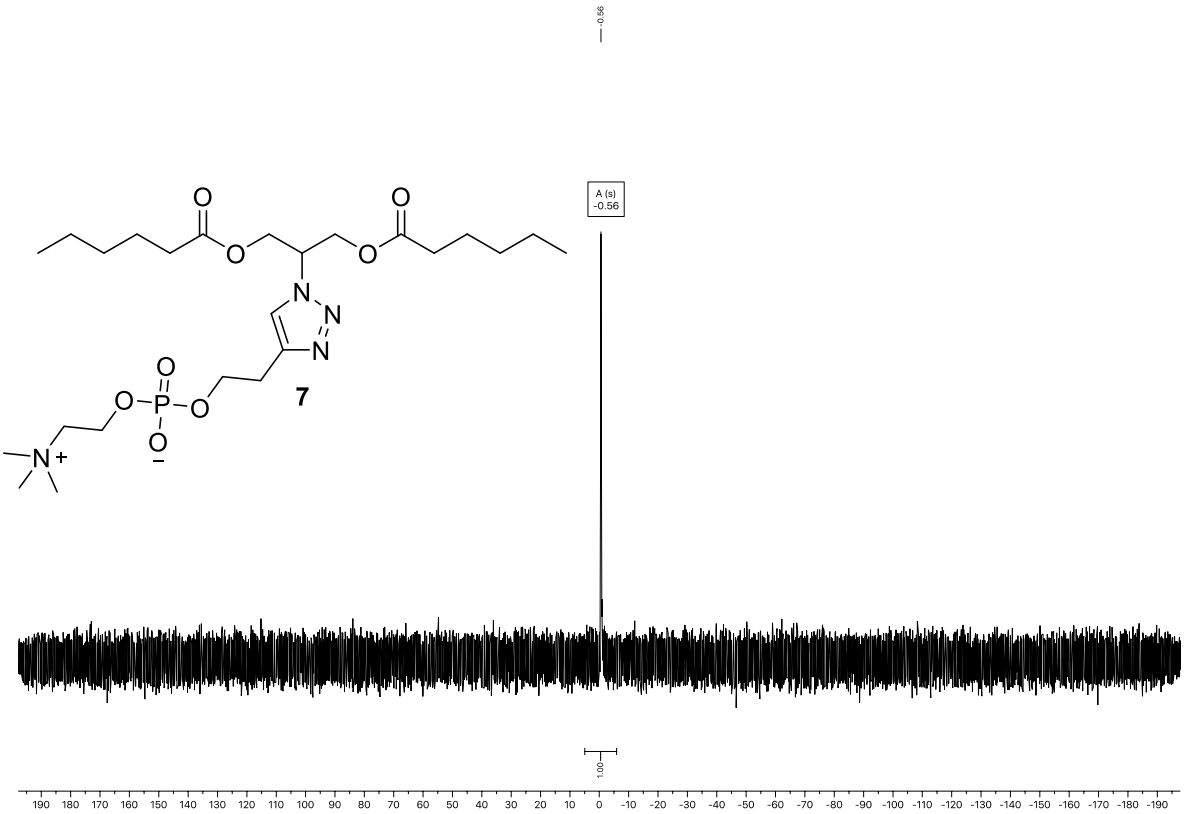

Figure S86: ^{31}P NMR spectrum of compound **7** in CD_3OD.

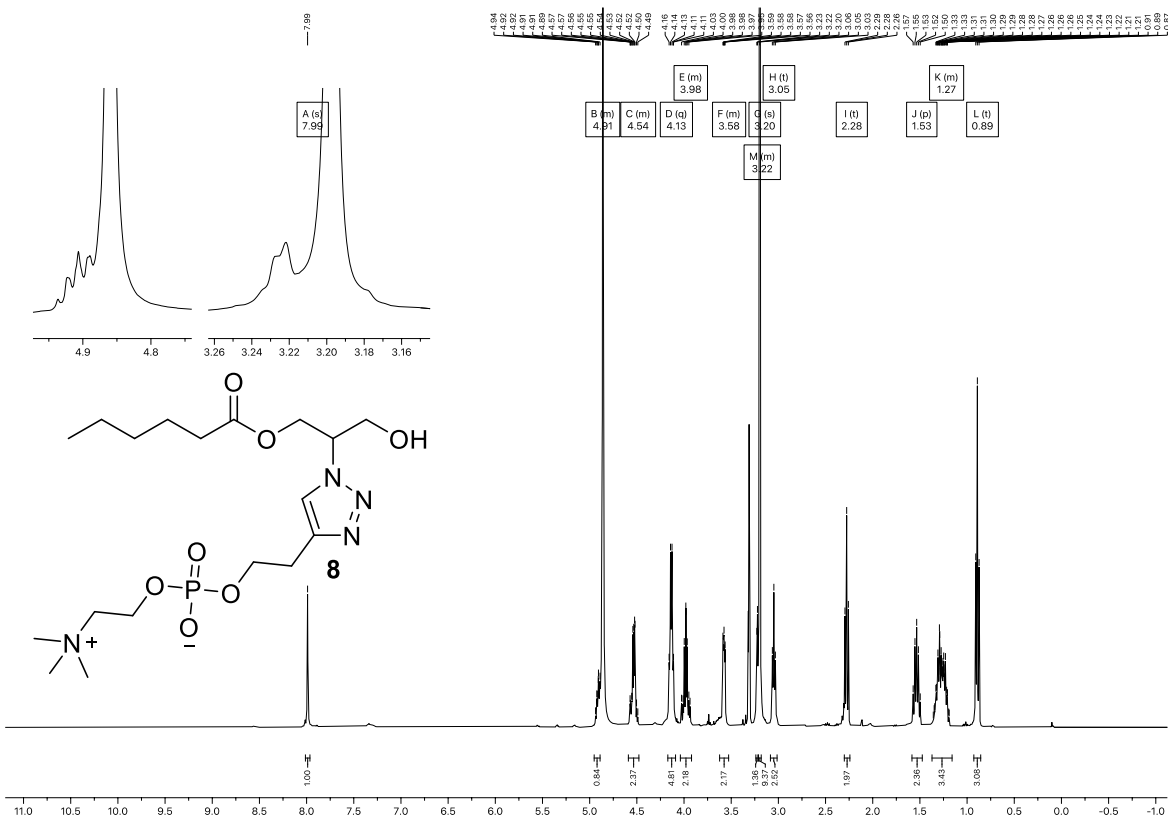

Figure S87: ^{1}H NMR spectrum of compound **8** in CD_3OD.

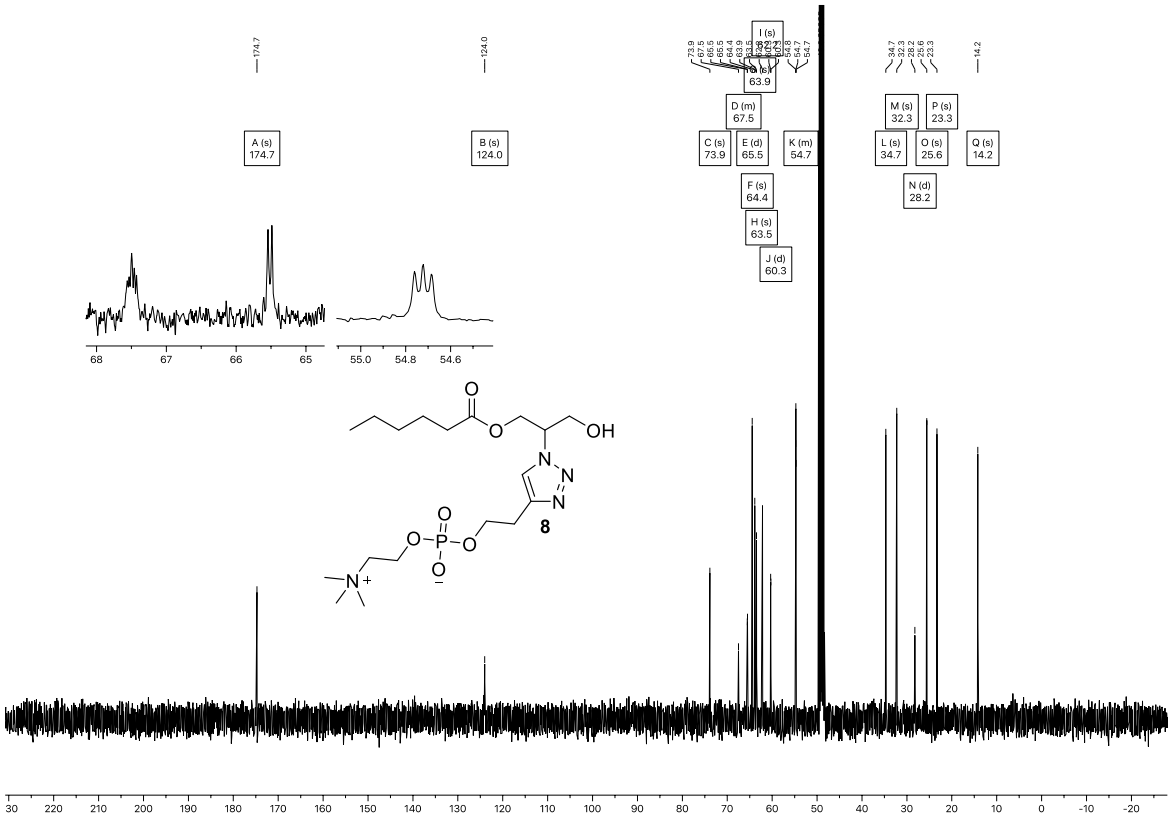

Figure S88: ^{13}C NMR spectrum of compound **8** in CD_3OD.

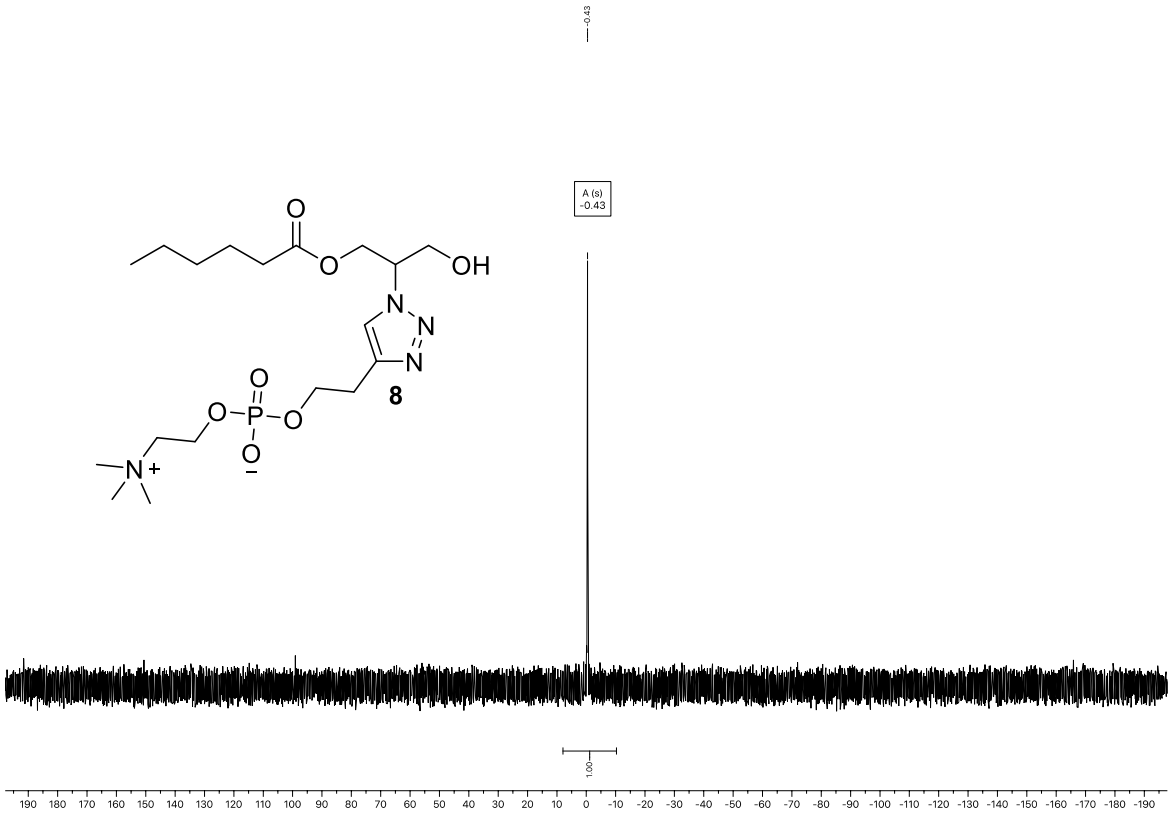

Figure S89: ^{31}P NMR spectrum of compound **8** in CD_3OD.

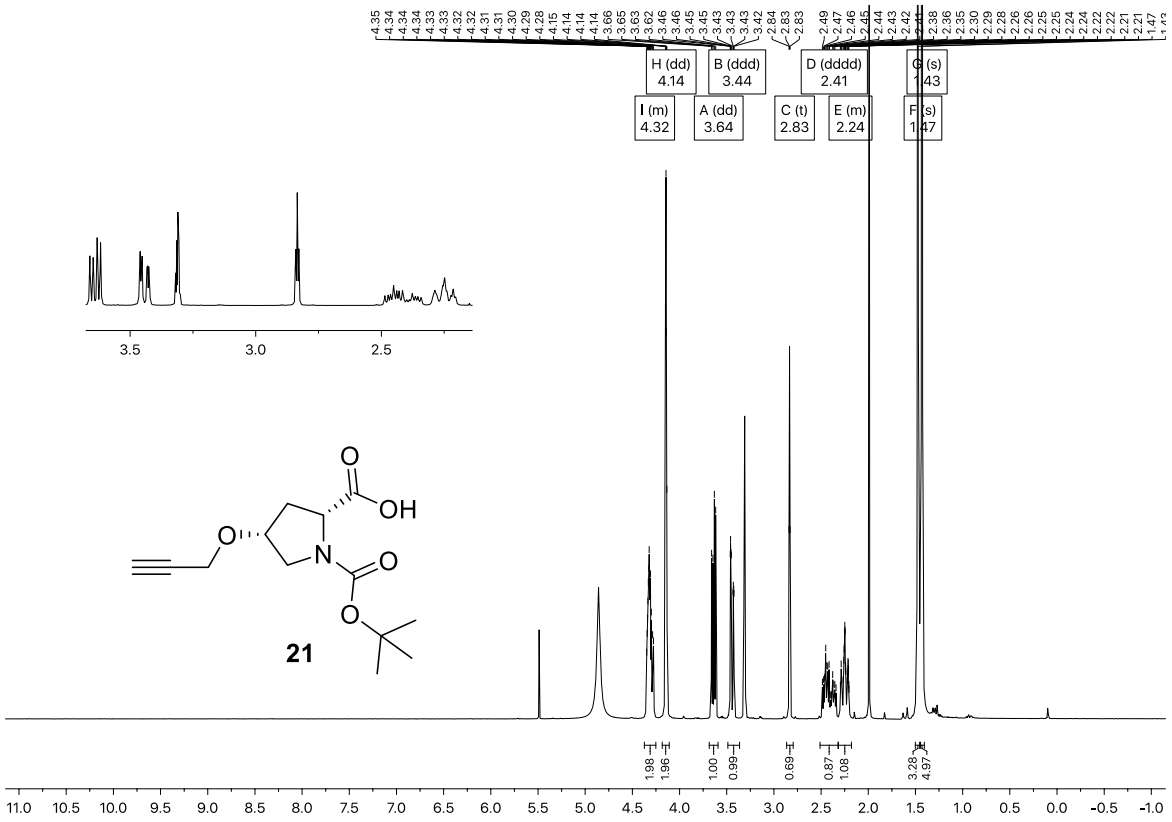

Figure S90: ^{1}H NMR spectrum of compound **21** in $CDCl_3$.

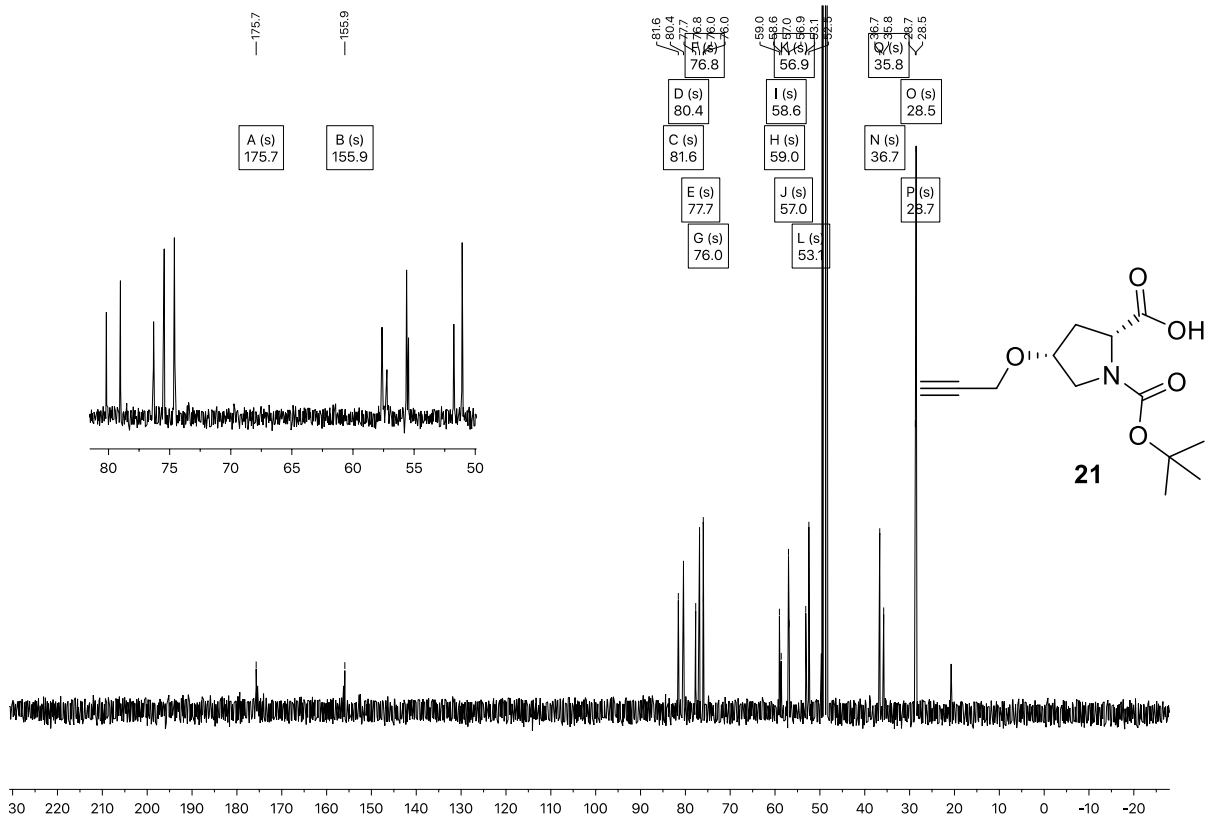

Figure S91: ^{13}C NMR spectrum of compound **21** in $CDCl_3$.

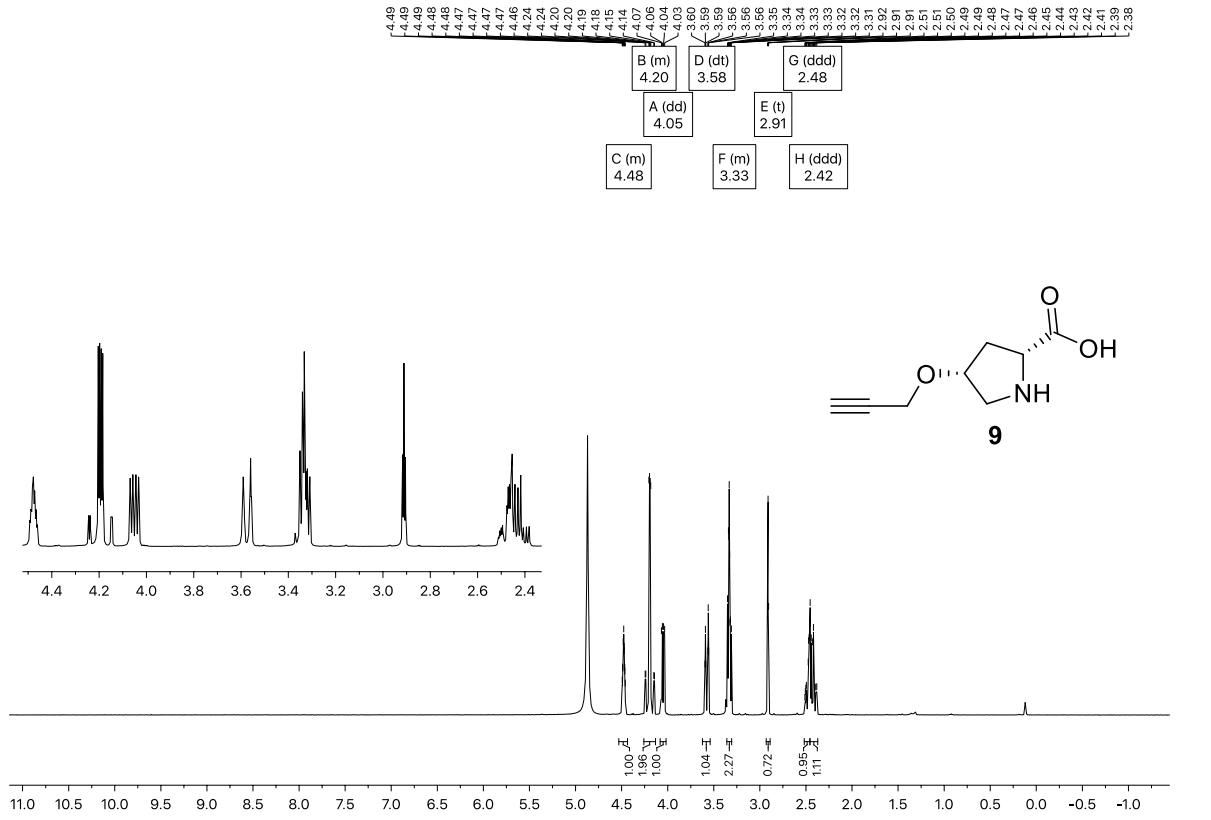

Figure S92: ^{1}H NMR spectrum of compound **9** in CD_3OD.

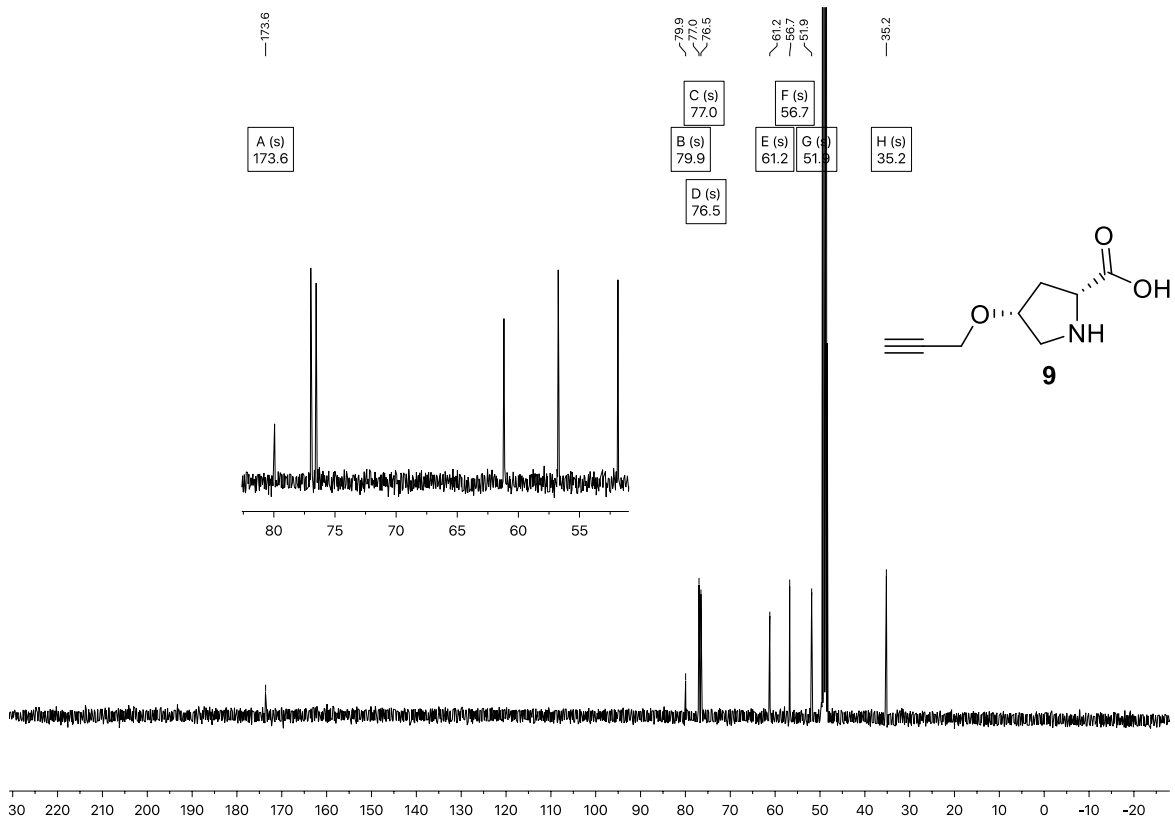

Figure S93: ^{13}C NMR spectrum of compound **9** in CD_3OD.

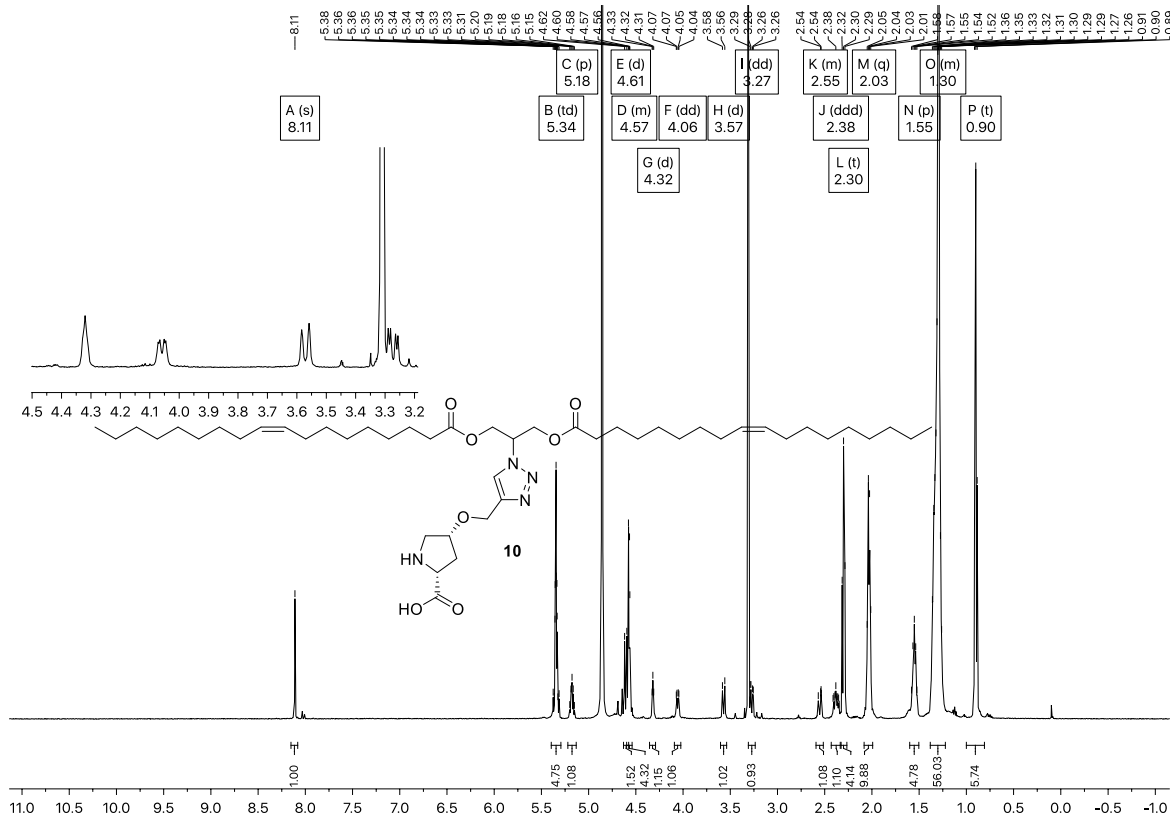

Figure S94: ^{1}H NMR spectrum of compound **10** in CD_3OD.

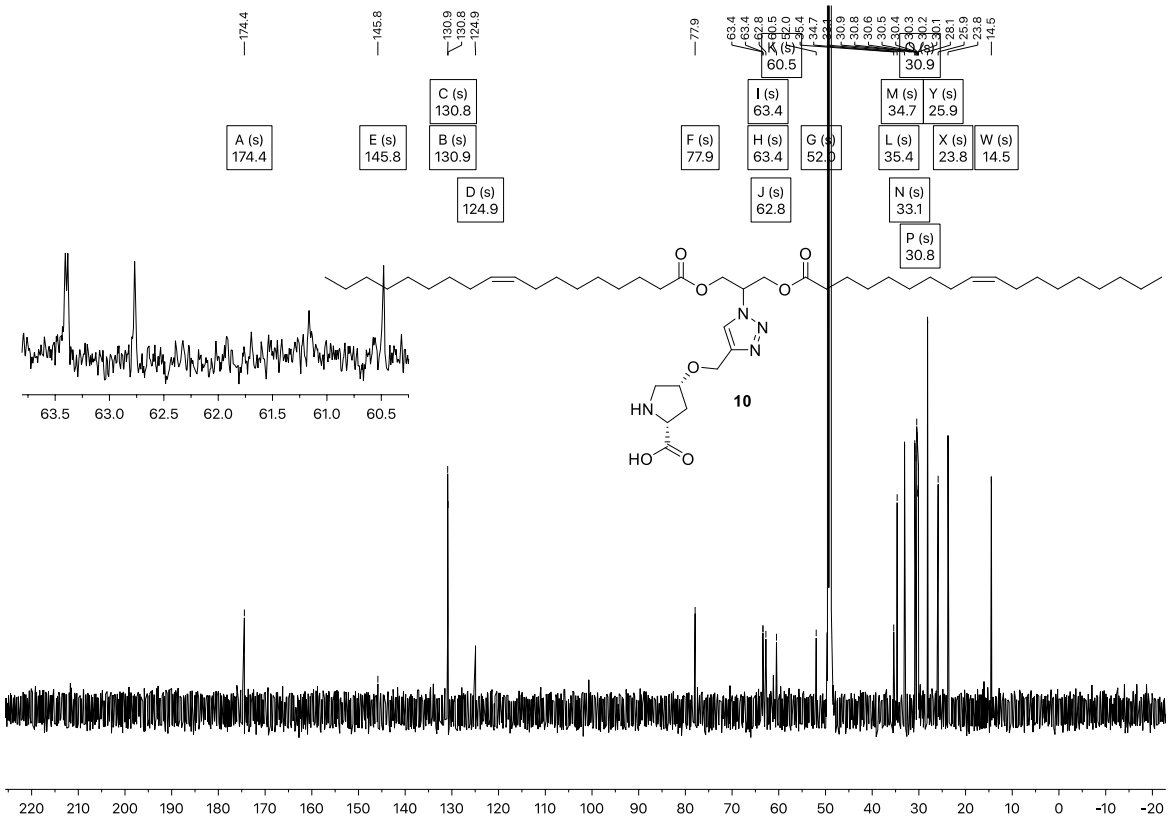

Figure S95: ^{13}C NMR spectrum of compound **10** in CD_3OD.

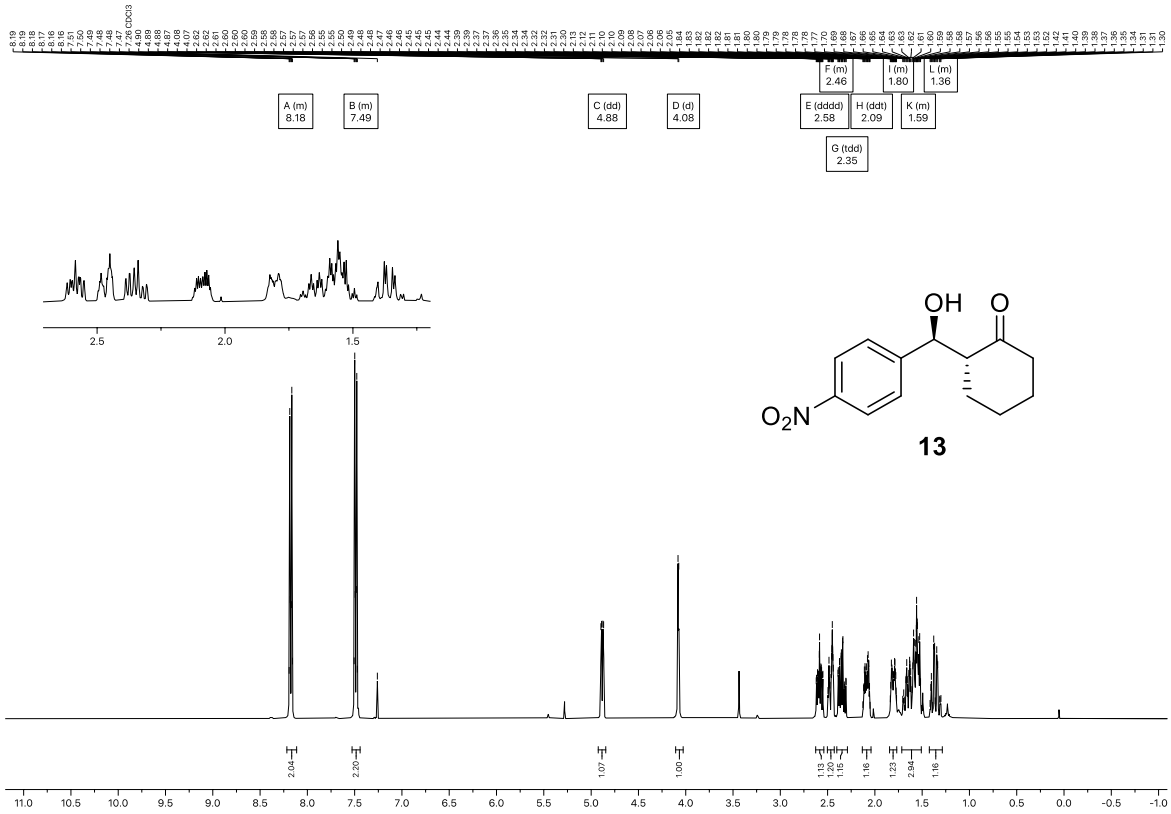

Figure S96: ^{1}H NMR spectrum of compound **13** in $CDCl_3$.

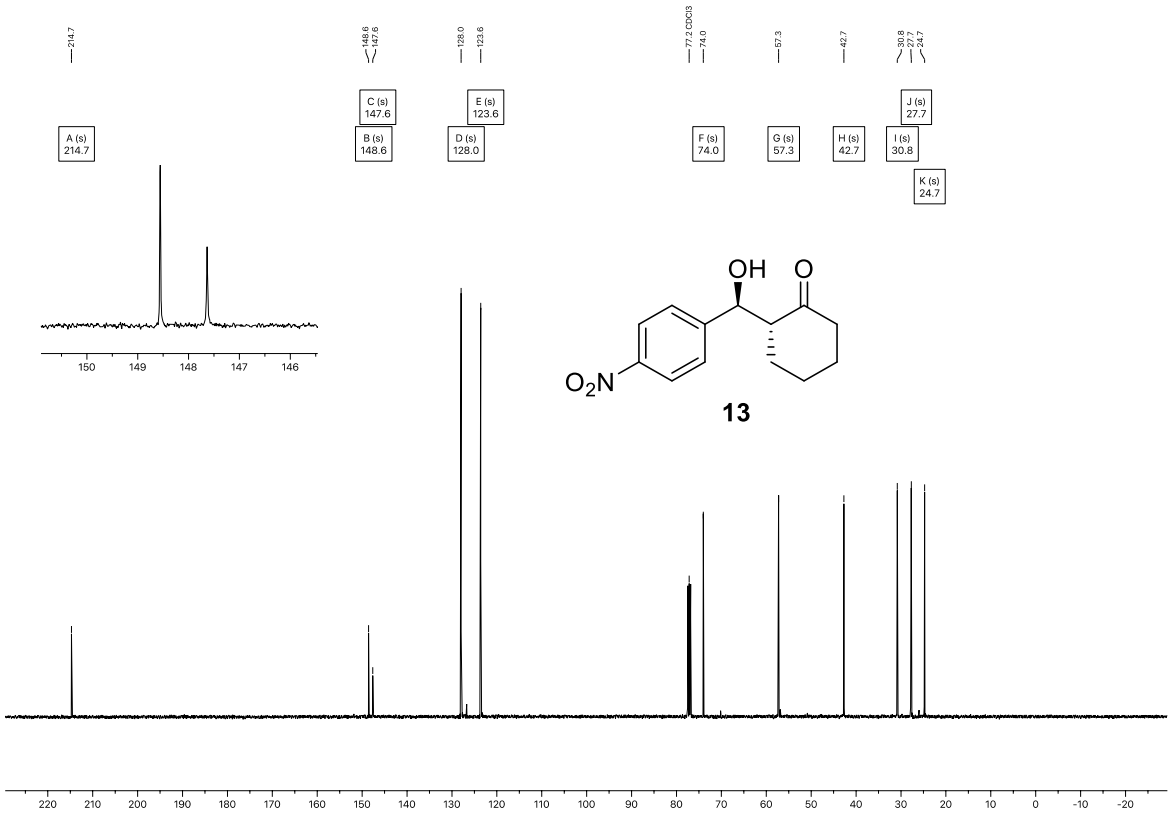

Figure S97: ^{13}C NMR spectrum of compound **13** in $CDCl_3$.

Chiral SFC Traces

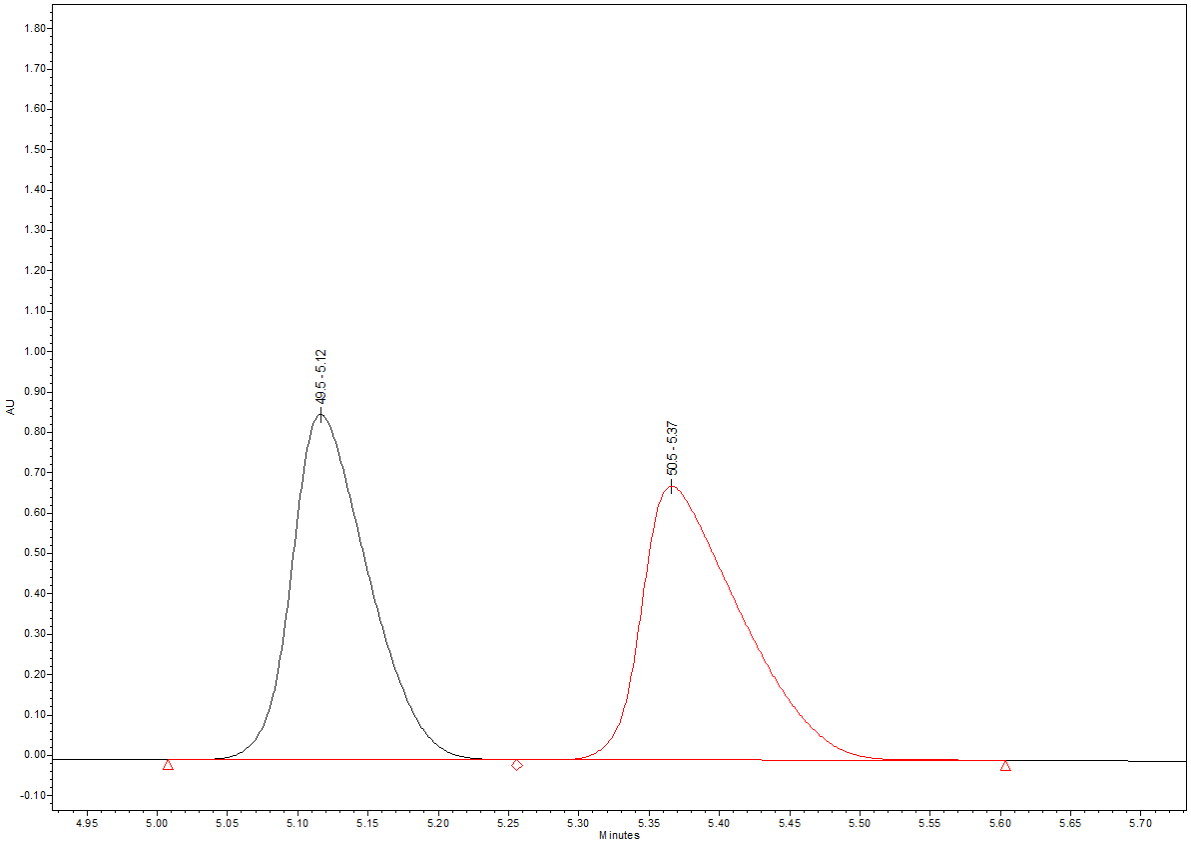

Figure S98: SFC trace of racemic **13**.

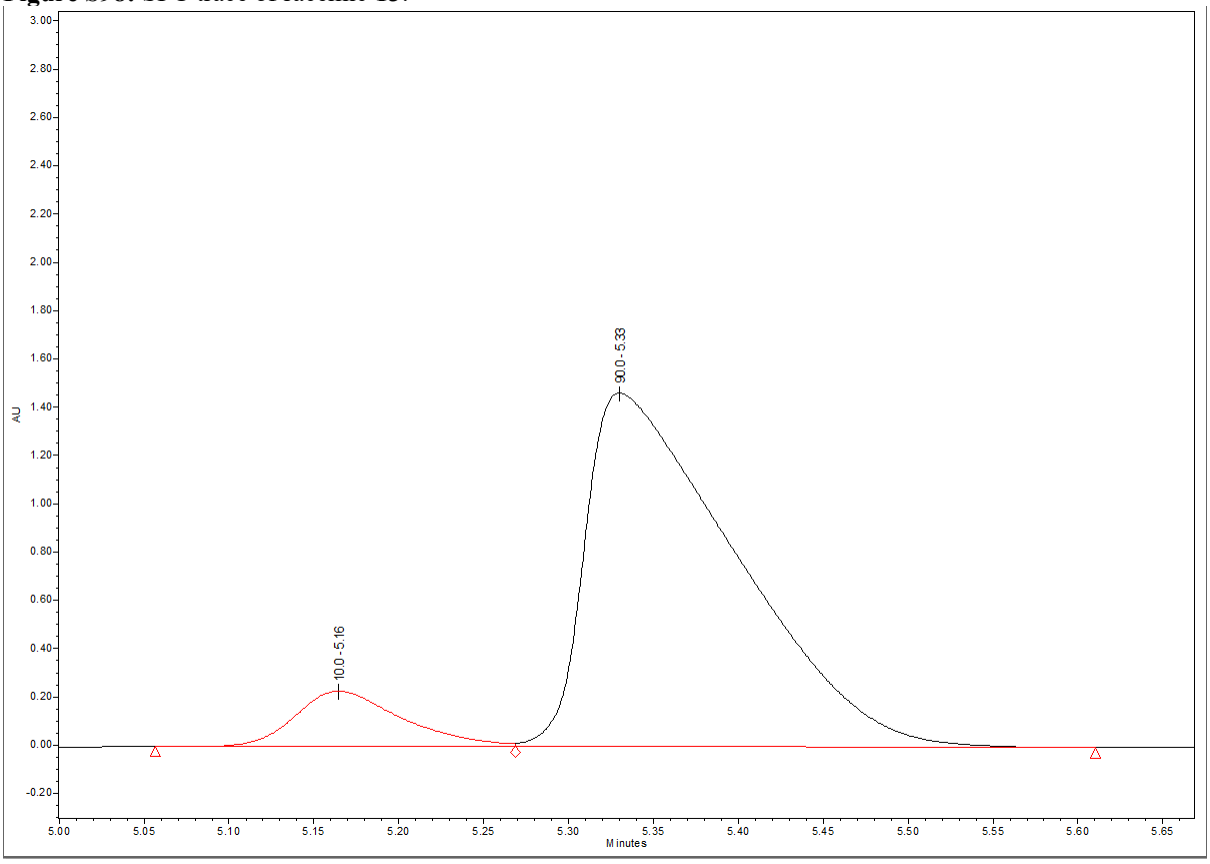

Figure S99: SFC trace of enantioenriched **13** from entry 4 in Fig. 5d.

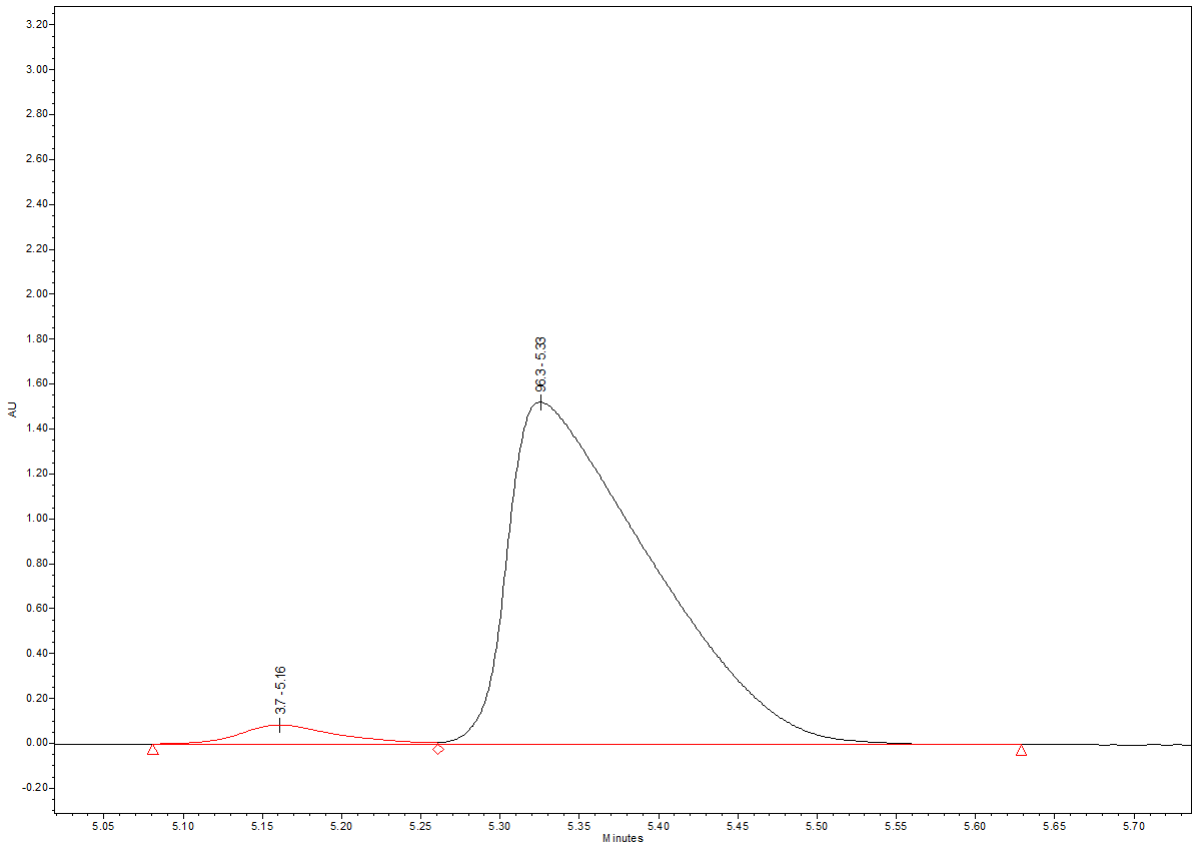

Figure S100: SFC trace of enantioenriched **13** from entry 5 in Fig. 5d.

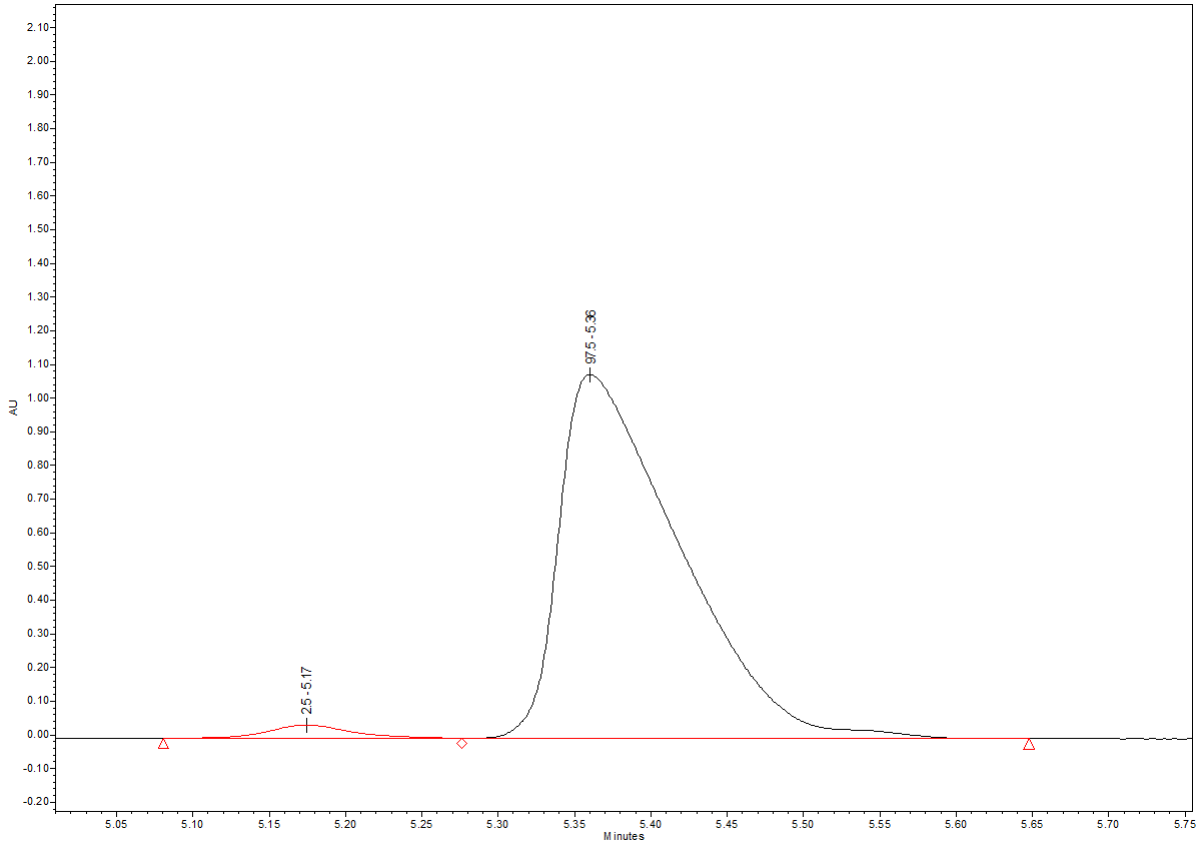

Figure S101: SFC trace of enantioenriched **13** from entry 6 in Fig. 5d.

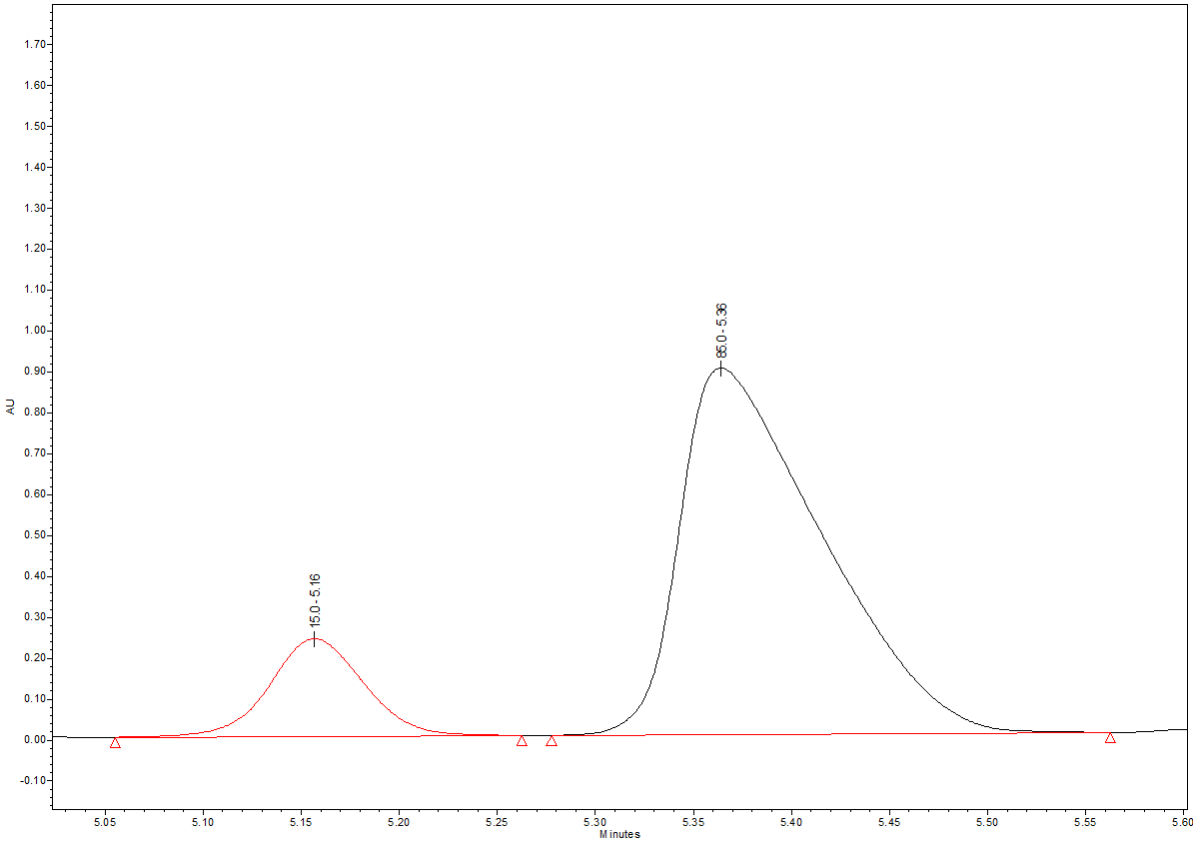

Figure S102: SFC trace of enantioenriched **13** from entry 7 in Fig. 5d.

References

1. Li, S., Bouzidi, L., and Narine, S.S. (2014). Synthesis, crystallization, and melting behavior of metathesis-like triacylglycerol oligomers: Effects of saturation, isomerism, and size. Ind. Eng. Chem. Res. *53*, 14579–14591.
2. Hu, G., and Emrick, T. (2016). Functional Choline Phosphate Polymers. J. Am. Chem. Soc. *138*, 1828–1831.
3. Zeynep, E.Y., Antoine, D., Brice, C., Frank, B., and Christine, J. (2015). Double hydrophilic polyphosphoester containing copolymers as efficient templating agents for calcium carbonate microparticles. J. Mater. Chem. B *3*, 7227–7236.
4. Liu, L., Lee, M.E., Kang, P., and Choi, M.G. (2015). Revisit to Synthesis of Allyl- and Propargyl-Phosphorylcholines: Crystal Structure of Allyl-Phosphorylcholine. Phosphorus, Sulfur Silicon Relat. Elem. *190*, 1525–1534.
5. Wang, Y., Aleiwi, B.A., Wang, Q., and Kurosu, M. (2012). Selective Esterifications of Primary Alcohols in a Water-Containing Solvent. Org. Lett. *14*, 4910–4913.
6. van Oers, M.C.M., Veldmate, W.S., van Hest, J.C.M., and Rutjes, F.P.J.T. (2015). Aqueous asymmetric aldol reactions in polymersome membranes. Polym. Chem. *6*, 5358–5361.
7. Northfield, S.E., Mountford, S.J., Wielens, J., Liu, M., Zhang, L., Herzog, H., Holliday, N.D., Scanlon, M.J., Parker, M.W., Chalmers, D.K., et al. (2015). Propargyloxyproline Regio- and Stereoisomers for Click-Conjugation of Peptides: Synthesis and Application in Linear and Cyclic Peptides. Aust. J. Chem. *68*, 1365–1372.
8. Wang, J., Liang, Y.L., and Qu, J. (2009). Boiling water-catalyzed neutral and selective N-Boc deprotection. Chem. Commun., 5144–5146.
9. Luo, S., Xu, H., Li, J., Zhang, L., and Cheng, J.-P. (2007). A Simple Primary−Tertiary Diamine−Brønsted Acid Catalyst for Asymmetric Direct Aldol Reactions of Linear Aliphatic Ketones. J. Am. Chem. Soc. *129*, 3074–3075.
10. An, Z., Guo, Y., Zhao, L., Li, Z., and He, J. (2014). L-Proline-Grafted Mesoporous Silica with Alternating Hydrophobic and Hydrophilic Blocks to Promote Direct Asymmetric Aldol and Knoevenagel–Michael Cascade Reactions. ACS Catal. *4*, 2566–2576.
11. Loughlin, W.A., Jenkins, I.D., Karis, N.D., and Healy, P.C. (2017). Discovery of new nanomolar inhibitors of GPa: Extension of 2-oxo-1,2-dihydropyridinyl-3-yl amide-based GPa inhibitors. Eur. J. Med. Chem. *127*, 341–356.
12. Michaels, H.A., and Zhu, L. (2011). N , N , N -Tris[(1-benzyl-1 H -1,2,3-triazol-4-yl)methyl]amine (TBTA). In Encyclopedia of Reagents for Organic Synthesis (John Wiley & Sons, Ltd), pp. 1–7.
13. Chattopadhyay, A., and London, E. (1984). Fluorimetric determination of critical micelle concentration avoiding interference from detergent charge. Anal. Biochem. *139*, 408–412.
14. Post, E.A.J., Bissette, A.J., and Fletcher, S.P. (2018). Self-reproducing micelles coupled to a secondary catalyst. Chem. Commun. *54*, 8777–8780.
15. Post, E.A.J., and Fletcher, S.P. (2019). Controlling the Kinetics of Self-Reproducing Micelles by Catalyst Compartmentalization in a Biphasic System. J. Org. Chem. *84*, 2741–2755.
16. Da Costa, G., Mouret, L., Chevance, S., Le Rumeur, E., and Bondon, A. (2007). NMR of molecules interacting with lipids in small unilamellar vesicles. Eur. Biophys. J. *36*, 933–942.